DOCKET NO. 72-26

DIABLO CANYON

INDEPENDENT SPENT FUEL STORAGE INSTALLATION

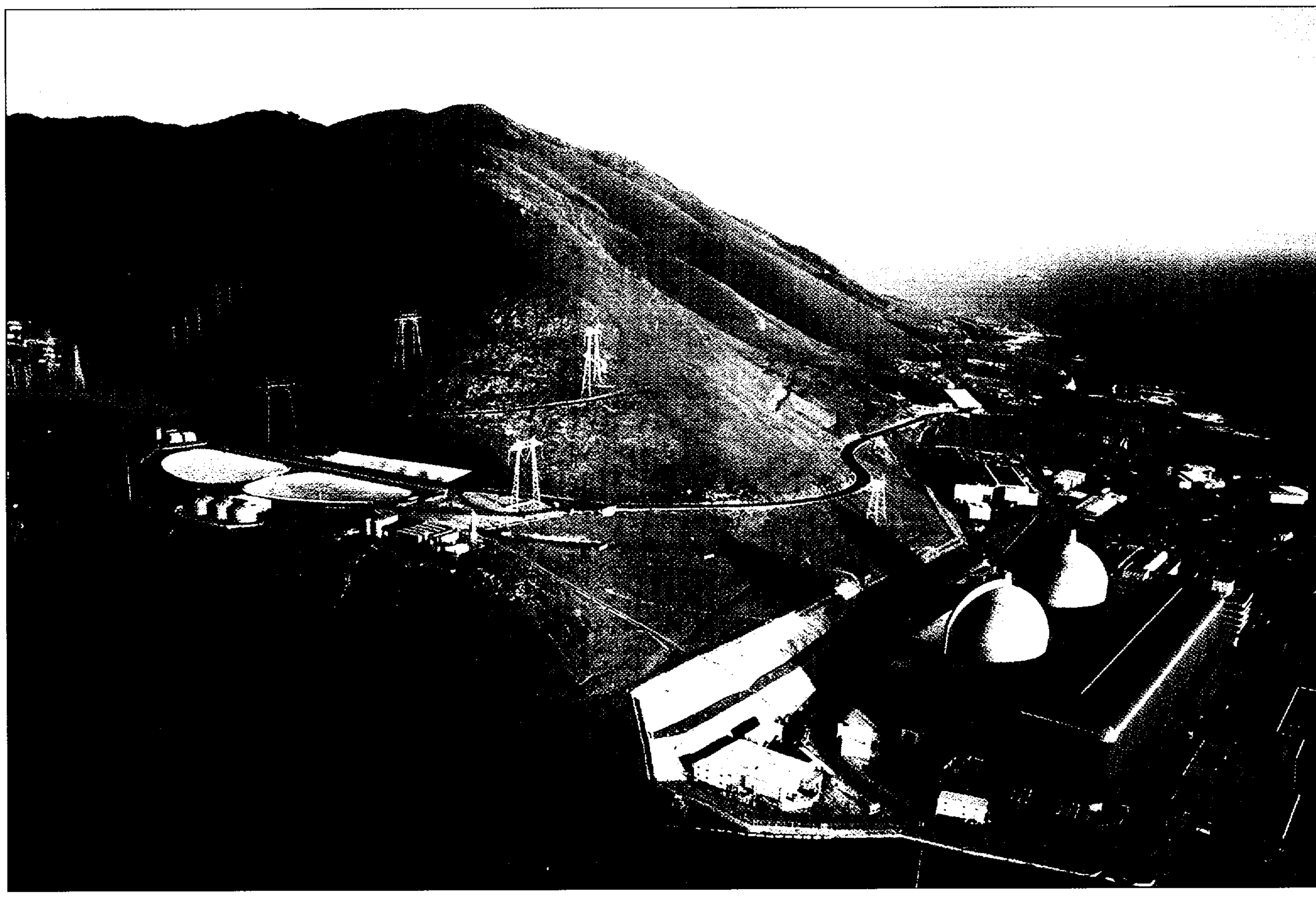

SAFETY ANALYSIS REPORT

PG&E

PACIFIC GAS AND ELECTRIC COMPANY

DIABLO CANYON ISFSI
SAFETY ANALYSIS REPORT

LIST OF CURRENT PAGES

Page No.	Rev.
CONTENTS	
i	
ii	
iii	
GLOSSARY	
1	
2	
3	
4	
5	
6	
7	
8	
CHAPTER 1	
i	
ii	
1.1-1	
1.1-2	
1.1-3	
1.1-4	
1.1-5	
1.2-1	
1.2-2	
1.3-1	
1.3-2	
1.4-1	
1.5-1	
Table 1.1-1	
Table 1.1-2	
CHAPTER 2	
i	
ii	
iii	
iv	
v	
vi	
vii	
viii	
2.1-1	
2.1-2	
2.1-3	
2.1-4	
2.1-5	
2.1-6	
2.2-1	
2.2-2	
2.2-3	
2.2-4	
2.2-5	
2.2-6	
2.2-7	
2.2-8	
2.2-9	
2.2-10	
2.3-1	
2.3-2	
2.3-3	
2.4-1	
2.4-2	
2.4-3	
2.5-1	
2.5-2	
2.5-3	
2.6-1	
2.6-2	
2.6-3	
2.6-4	
2.6-5	
2.6-6	
2.6-7	
2.6-8	
2.6-9	
2.6-10	
2.6-11	
2.6-12	
2.6-13	
2.6-14	
2.6-15	
2.6-16	
2.6-17	
2.6-18	
2.6-19	
2.6-20	
2.6-21	
2.6-22	
2.6-23	
2.6-24	
2.6-25	
2.6-26	
2.6-27	
2.6-28	
2.6-29	
2.6-30	
2.6-31	
2.6-32	
2.6-33	
2.6-34	
2.6-35	
2.6-36	
2.6-37	
2.6-38	
2.6-39	
2.6-40	
2.6-41	
2.6-42	
2.6-43	
2.6-44	
2.6-45	
2.6-46	
2.6-47	
2.6-48	
2.6-49	
2.6-50	
2.6-51	
2.6-52	
2.6-53	

DIABLO CANYON ISFSI
SAFETY ANALYSIS REPORT

LIST OF CURRENT PAGES

LIST OF CURRENT PAGES

Page No.	Rev.
3.3-7	
3.3-8	
3.3-9	
3.3-10	
3.3-11	
3.3-12	
3.3-13	
3.3-14	
3.3-15	
3.3-16	
3.3-17	
3.4-1	
Table 3.1-1	
Table 3.1-2	
Table 3.2-1	
Table 3.2-2	
Table 3.4-1, Sheet 1	
Table 3.4-1, Sheet 2	
Table 3.4-2, Sheet 1	
Table 3.4-2, Sheet 2	
Table 3.4-2, Sheet 3	
Table 3.4-2, Sheet 4	
Table 3.4-3	
Table 3.4-4	
Table 3.4-5	
Figure 3.3-1	
Figure 3.3-2	
CHAPTER 4	
i	
ii	
iii	
iv	
v	
4.1-1	
4.1-2	
4.2-1	
4.2-2	
4.2-3	
4.2-4	
4.2-5	
4.2-6	
4.2-7	
4.2-8	
4.2-9	
4.2-10	
4.2-11	
4.2-12	
4.2-13	
4.2-14	
4.2-15	
4.2-16	
4.2-17	
4.2-18	
4.2-19	
4.2-20	
4.2-21	
4.2-22	
4.2-23	
4.2-24	
4.2-25	
4.2-26	
4.2-27	
4.2-28	
4.3-1	
4.3-2	
4.3-3	
4.3-4	
4.3-5	
4.3-6	
4.3-7	
4.3-8	
4.3-9	
4.4-1	
4.4-2	
4.4-3	
4.4-4	
4.4-5	
4.4-6	
4.4-7	
4.4-8	
4.4-9	
4.4-10	
4.4-11	
4.4-12	
4.4-13	
4.4-14	
4.4-15	
4.4-16	
4.5-1	
4.5-2	
4.5-3	
4.5-4	
4.6-1	
4.6-2	
Table 4.2-1	
Table 4.2-2	
Table 4.2-3	
Table 4.2-4	
Table 4.2-5, Sheet 1	
Table 4.2-5, Sheet 2	
Table 4.2-5, Sheet 3	
Table 4.2-5, Sheet 4	
Table 4.2-5, Sheet 5	
Table 4.2-5, Sheet 6	
Table 4.3-1	
Table 4.5-1	
Figure 4.1-1	
Figure 4.2-1	
Figure 4.2-2	
Figure 4.2-3	
Figure 4.2-4	
Figure 4.2-5	
Figure 4.2-6	
Figure 4.2-7	
Figure 4.2-8	
Figure 4.2-9	
Figure 4.2-10	
Figure 4.2-11	
Figure 4.2-12	
Figure 4.3-1	
Figure 4.3-2	

LIST OF CURRENT PAGES

Page No.	Rev.
Figure 4.3-3	
Figure 4.3-4	
Figure 4.3-5	
Figure 4.3-6	
Figure 4.4-1	
Figure 4.4-2	
Figure 4.4-3, Sheet 1	
Figure 4.4-3, Sheet 2	
Figure 4.4-3, Sheet 3	
Figure 4.4-3, Sheet 4	
Figure 4.4-4	
CHAPTER 5	
i	
ii	
iii	
5.1-1	
5.1-2	
5.1-3	
5.1-4	
5.1-5	
5.1-6	
5.1-7	
5.1-8	
5.1-9	
5.1-10	
5.1-11	
5.1-12	
5.2-1	
5.3-1	
5.4-1	
Table 5.1-1	
Figure 5.1-1, Sheet 1	
Figure 5.1-1, Sheet 2	
Figure 5.1-1, Sheet 3	
Figure 5.1-2, Sheet 1	
Figure 5.1-2, Sheet 2	

Page No.	Rev.
CHAPTER 6	
i	
6.1-1	
6.2-1	
6.3-1	
CHAPTER 7	
i	
ii	
iii	
iv	
v	
7.1-1	
7.1-2	
7.1-3	
7.1-4	
7.1-5	
7.2-1	
7.2-2	
7.2-3	
7.2-4	
7.2-5	
7.2-6	
7.2-7	
7.2-8	
7.3-1	
7.3-2	
7.3-3	
7.3-4	
7.3-5	
7.3-6	
7.4-1	
7.4-2	
7.4-3	
7.5-1	
7.5-2	
7.5-3	
7.5-4	
7.6-1	

Page No.	Rev.
7.7-1	
Table 7.2-1	
Table 7.2-2	
Table 7.2-3	
Table 7.2-4	
Table 7.2-5	
Table 7.2-6	
Table 7.2-7	
Table 7.2-8, Sheet 1	
Table 7.2-8, Sheet 2	
Table 7.3-1	
Table 7.3-2	
Table 7.3-3	
Table 7.3-4	
Table 7.4-1, Sheet 1	
Table 7.4-1, Sheet 2	
Table 7.4-1, Sheet 3	
Table 7.4-2, Sheet 1	
Table 7.4-2, Sheet 2	
Table 7.4-3	
Table 7.4-4	
Table 7.5-1	
Table 7.5-2	
Table 7.5-3	
Table 7.5-4	
Figure 7.3-1	
Figure 7.3-2	
Figure 7.3-3	
Figure 7.3-4	
CHAPTER 8	
i	
ii	
iii	
iv	
8.1-1	
8.1-2	
8.1-3	
8.1-4	
8.1-5	

LIST OF CURRENT PAGES

LIST OF CURRENT PAGES

Page No.	Rev.	Page No.	Rev.	Page No.	Rev.
10.2-11					
10.2-12					
10.2-13					
10.2-14					
10.2-15					
Table 10.1-1					
Table 10.2-1					
Table 10.2-2, Sheet 1					
Table 10.2-2, Sheet 2					
Table 10.2-3, Sheet 1					
Table 10.2-3, Sheet 2					
Table 10.2-4					
Table 10.2-5					
Table 10.2-6					
Table 10.2-7					
Table 10.2-8					
Table 10.2-9					
Table 10.2-10					
Figure 10.2-1					
Figure 10.2-2					
Figure 10.2-3					
Figure 10.2-4					
CHAPTER 11					
i					
11-1					
11-2					
APPENDIX A					
A-1					
A-2					
A-3					
A-4					

DIABLO CANYON ISFSI
SAFETY ANALYSIS REPORT

CONTENTS

VOLUME 1

DIABLO CANYON ISFSI
SAFETY ANALYSIS REPORT

CONTENTS

VOLUME 2

DIABLO CANYON ISFSI
SAFETY ANALYSIS REPORT

CONTENTS

VOLUME 2

GLOSSARY

A glossary of most of the terms and acronyms used in this safety analysis report, including their frequently used variations, is presented in this section as an aid to readers and reviewers.

Accident Events means events that are considered to occur infrequently, if ever, during the lifetime of the facility. Natural phenomena, such as earthquakes, tornadoes, floods, and tsunami, are considered to be accident events.

ALARA means as low as is reasonably achievable.

Boral is a generic term to denote an aluminum-boron carbide cermet manufactured in accordance with U.S. Patent No. 4027377. The individual material supplier may use another trade name to refer to the same product.

BPRA means burnable poison rod assembly.

Cask Transporter (or Transporter) is a U-shaped tracked vehicle used for lifting, handling, and onsite transport of loaded overpacks and the transfer cask.

CEDE means committed effective dose equivalent.

CFR means Code of Federal Regulations.

CIMIS means the California Irrigation Management Information System.

CoC means a certificate of compliance issued by the NRC that approves the design of a spent fuel storage cask design in accordance with Subpart L of 10 CFR 72.

Confinement Boundary means the outline formed by the sealed, cylindrical enclosure of the multi-purpose canister (MPC) shell welded to a solid baseplate, a lid welded around the top circumference of the shell wall, the port cover plates welded to the lid, and the closure ring welded to the lid and MPC shell providing the redundant sealing.

Confinement System means the MPC that encloses and confines the spent nuclear fuel and associated nonfuel hardware during storage.

Consolidated Fuel means a fuel assembly that contains more than 264 fuel rods.

Controlled Area (or Owner-Controlled Area) means the area, outside the restricted area but inside the site boundary, for which access can be limited by PG&E.

GLOSSARY

Cooling Time is the time between discharging a spent fuel assembly and associated nonfuel hardware from the reactor (reactor shutdown) and the time the spent fuel assembly and associated nonfuel hardware are loaded into the MPC.

CTF means the cask transfer facility. The CTF is used to transfer an MPC from the transfer cask to an overpack, following transport from the FHB/AB and prior to moving the loaded overpack to the storage pad. The CTF can also be used to transfer an MPC from a loaded overpack to the transfer cask for transport back to the FHB/AB.

Damaged Fuel Assembly is a fuel assembly with known or suspected cladding defects, as determined by review of records, greater than pinhole leaks or hairline cracks; empty fuel rod locations that are not replaced with dummy fuel rods; or those that cannot be handled by normal means. Fuel assemblies that cannot be handled by normal means due to fuel cladding damage are considered fuel debris.

Damaged Fuel Container (or DFC) means a specially designed enclosure for damaged fuel or fuel debris that permits gaseous and liquid media to escape while minimizing dispersal of gross particulates. The DFC features a lifting location that is suitable for remote handling of a loaded or unloaded DFC.

DBE means design-basis earthquake.

DCPP means Diablo Canyon Power Plant.

DCPP FSAR Update means the FSAR for DCPP that is maintained up-to-date in accordance with 10 CFR 51.71(e).

DCSS means dry cask storage system.

DDE means double design earthquake or deep dose equivalent.

DE means design earthquake.

Design Life is the minimum duration for which the component is engineered to perform its intended function as set forth in this SAR, if operated and maintained in accordance with this SAR.

Diablo Canyon ISFSI (or ISFSI) means the total Diablo Canyon storage system and includes the HI-STORM 100 System, transporter, CTF, storage pads, and ancillary equipment.

GLOSSARY

Diablo Canyon ISFSI Technical Specifications (or Diablo Canyon ISFSI TS or DC ISFSI TS) means the Technical Specifications issued as part of the license for PG&E to operate the Diablo Canyon ISFSI.

DOE means the US Department of Energy.

FHB/AB means the DCPP fuel handling building/auxiliary building.

Fracture Toughness is a property that is a measure of the ability of a material to limit crack propagation under a suddenly applied load.

FSAR means final safety analysis report.

Fuel Basket means a honeycombed structural weldment with square openings that can accept a fuel assembly of the type for which it is designed.

Fuel Debris refers to ruptured fuel rods, severed rods, loose fuel pellets, or fuel assemblies with known or suspected defects that cannot be handled by normal means.

HE means Hosgri earthquake.

High Burnup Fuel is a spent fuel assembly with an average burnup greater than 45,000 MWD/MTU.

HI-STORM 100 Overpack (or Loaded Overpack or Storage Cask) means the cask that receives and contains the sealed MPCs (containing spent nuclear fuel and nonfuel hardware) for final storage on the storage pads. It provides the gamma and neutron shielding, ventilation passages, missile protection, and protection against natural phenomena and accidents for the MPC.

HI-STORM 100SA Overpack is a variant of the HI-STORM 100 overpack that is shorter, has a redesigned top lid, and is outfitted with an extended baseplate and gussets to enable the overpack to be anchored to the storage pad. The HI-STORM 100SA overpack is designed for high-seismic applications and is used at the Diablo Canyon ISFSI.

HI-STORM 100 System consists of the Holtec International MPC, HI-STORM 100SA overpack, and HI-TRAC transfer cask. For Diablo Canyon, the HI-STORM 100SA overpack replaces the HI-STORM 100 overpack.

HI-TRAC 125 Transfer Cask (or HI-TRAC Transfer Cask or HI TRAC or Transfer Cask) means the cask used to house the MPC during MPC fuel loading, unloading, drying, sealing, and onsite transfer operations to an overpack. The HI-TRAC shields the loaded MPC

GLOSSARY

allowing loading operations to be performed while limiting radiation exposure to personnel. The HI-TRAC is equipped with a pair of lifting trunnions to lift and downend/upend the HI-TRAC with a loaded MPC. HI-TRAC is an acronym for Holtec International Transfer Cask. The transfer cask used at the Diablo Canyon ISFSI is the standard HI-TRAC 125 with some optional features.

Holtite is a trademarked Holtec International neutron shield material.

IFBA means integral fuel burnable absorber.

Important to Safety (ITS) means a function or condition required to store spent nuclear fuel safely; to prevent damage to spent nuclear fuel during handling and storage; and to provide reasonable assurance that spent nuclear fuel can be received, handled, packaged, stored, and retrieved without undue risk to the health and safety of the public. This definition is used to classify structures, systems, and components of the ISFSI as important to safety (ITS) or not important to safety (NITS).

Independent Spent Fuel Storage Installation (ISFSI) means a facility designed, constructed, and licensed for the interim storage of spent nuclear fuel and other radioactive materials associated with spent fuel storage in accordance with 10 CFR 72. For Diablo Canyon, this term is clarified to mean the total storage system and includes the HI-STORM 100 System, transporter, CTF, storage pads, and ancillary equipment.

Insolation means incident solar radiation.

Intact Fuel Assembly means a fuel assembly without known or suspected cladding defects greater than pinhole leaks and hairline cracks, and which can be handled by normal means. Partial fuel assemblies, that is fuel assemblies from which fuel rods are missing, shall not be classified as intact fuel assemblies unless dummy fuel rods are used to displace an amount of water greater than or equal to that displaced by the original fuel rod(s).

ISFSI Site means the ISFSI storage site and CTF.

ISFSI Storage Site (or Storage Site) means the area contained within the restricted area fence that circumscribes the ISFSI protected area fence and storage pads.

LAR means license amendment request.

LCO means limiting condition for operation.

LDE means lens dose equivalent.

GLOSSARY

License Life means the duration that the HI-STORM 100 System and the Diablo Canyon ISFSI are authorized by virtue of certification by the US NRC.

Lowest Service Temperature (LST) is the minimum metal temperature of a part for the specified service condition.

LPZ means low population zone.

LTSP means long-term seismic program.

Maximum Reactivity means the highest possible k-effective including bias, uncertainties, and calculational statistics evaluated for the worst-case combination of fuel basket manufacturing tolerances.

MCNP means Monte Carlo N-Particle transport computer code.

Moderate Burnup Fuel is a spent fuel assembly with an average burnup less than or equal to 45,000 MWD/MTU.

MPC-24 means the Holtec MPC designed to store up to 24 intact PWR fuel assemblies and associated nonfuel hardware.

MPC-24E means the Holtec MPC designed to store up to 24 PWR fuel assemblies and associated nonfuel hardware, 4 of which can be DFCs containing damaged fuel assemblies in designated fuel basket locations, and the balance being intact fuel assemblies.

MPC-24EF means the Holtec MPC designed to store up to 24 PWR fuel assemblies and associated nonfuel hardware, 4 of which can be DFCs containing damaged fuel assemblies or fuel debris in designated fuel basket locations, and the balance being intact fuel assemblies.

MPC-32 means the Holtec MPC designed to store up to 32 intact PWR fuel assemblies and associated nonfuel hardware.

MSL means mean sea level.

MTU means metric tons of uranium.

Multi-Purpose Canister (MPC) means the sealed canister that consists of a honeycombed fuel basket contained in a cylindrical canister shell that is welded to a baseplate, lid with welded port cover plates, and closure ring. The MPC is the confinement boundary for storage conditions.

GLOSSARY

MWD/MTU means megawatt-days per metric ton of uranium.

Neutron Shielding means a material used to thermalize and capture neutrons emanating from the radioactive spent nuclear fuel.

NFPA means National Fire Protection Association.

Nonfuel Hardware is defined as burnable poison rod assemblies (BPRAs), thimble plug devices (TPDs), control rod assemblies (CRAs), and other similarly designed devices with different names.

NRC means the US Nuclear Regulatory Commission.

NSOC means the DCPP Nuclear Safety Oversight Committee.

NWPA means the Nuclear Waste Policy Act of 1982 and any amendments thereto.

OBE means operating basis earthquake.

PMF means probable maximum flood.

Post-Core Decay time (PCDT) is synonymous with cooling time.

Preferential Fuel Loading is a requirement in the Diablo Canyon ISFSI Technical Specifications applicable to uniform fuel loading whenever fuel assemblies with significantly different post-irradiation cooling times ($\geq$ 1 year) are to be loaded in the same MPC. Fuel assemblies with the longest post-irradiation cooling time are loaded into fuel storage locations at the periphery of the basket. Fuel assemblies with shorter post-irradiation cooling times are placed toward the center of the basket. Regionalized fuel loading meets the intent of preferential fuel loading. The preferential fuel loading requirement is in addition to other fuel loading restrictions in the Diablo Canyon ISFSI Technical Specifications, such as those for nonfuel hardware and damaged fuel containers.

Protected Area (or ISFSI Protected Area) means the area within the security fence that circumscribes the storage pads.

Protected Area Boundary means the security fence that circumscribes the storage pads.

PSRC means the DCPP Plant Staff Review Committee.

PWR means pressurized water reactor.

GLOSSARY

RCCA means rod cluster control assembly.

Reactivity is used synonymously with effective neutron multiplication factor or k-effective.

Regionalized Fuel Loading is a term used to describe an optional fuel loading strategy used in lieu of uniform fuel loading. Regionalized fuel loading allows high-heat-emitting fuel assemblies to be stored in fuel storage locations in the center of the fuel basket provided lower-heat-emitting fuel assemblies are stored in the peripheral fuel storage locations. When choosing regionalized fuel loading, other restrictions in the Diablo Canyon ISFSI Technical Specifications must be considered also, such as those for nonfuel hardware and damaged fuel containers. Regionalized fuel loading meets the intent of preferential fuel loading.

Restricted Area means the area within the second fence circumscribing the storage pads, access to which is limited by PG&E for the purpose of protecting individuals against undue risks from exposure to radiation and radioactive materials.

Restricted Area Fence means the second fence that circumscribes the storage pads. It is located to ensure the dose rate at this boundary will be less than 2 mrem/hr in compliance with 10 CFR 20 requirements for a restricted area boundary.

SAR means Diablo Canyon ISFSI Safety Analysis Report.

SAT means systematic approach to training.

Security Fence is the first fence circumscribing the storage pads.

SDE means shallow dose equivalent.

Service Life means the duration for which the component is reasonably expected to perform its intended function, if operated and maintained in accordance with the provisions of the CoC. Service life may be much longer than the design life because of the conservatism inherent in the codes, standards, and procedures used to design, fabricate, operate, and maintain the component.

SFP means spent fuel pool.

Single Failure Proof Handling System means that the handling system is designed so that all directly-loaded tension and compression members are engineered to satisfy the enhanced safety criteria of paragraphs 5.1.6(1)(a) and (b) of NUREG-0612.

SNF means spent nuclear fuel.

GLOSSARY

SR means surveillance requirement.

SSC means structures, systems, and components.

SSE means safe shutdown earthquake.

STP means standard temperature and pressure conditions.

TEDE means total effective dose equivalent.

Thermosiphon is the term used to describe the buoyancy-driven natural convection circulation of helium within the MPC.

TLD means thermoluminescent dosimeter.

TODE means total organ dose equivalent.

TPD means thimble plug device.

Transport Route means the route used by the transporter for onsite movement of the loaded transfer cask from the FHB/AB to the CTF.

Uniform Fuel Loading is a fuel loading strategy where any authorized fuel assembly may be stored in any fuel storage location, subject to other restrictions in the Diablo Canyon ISFSI Technical Specifications, such as preferential fuel loading, and those restrictions applicable to nonfuel hardware and damaged fuel containers.

USGS means the US Geological Survey.

UTM means Universal Transverse Mecator and is used to define topographic locations in metric coordinates.

Westinghouse LOPAR fuel assemblies have been used at DCPP and are one of the types of spent fuel assemblies that will be stored at the ISFSI.

Westinghouse VANTAGE 5 fuel assemblies have been used at DCPP and are one of the types of spent fuel assemblies that will be stored at the ISFSI.

χ/Q means site-specific atmospheric dispersion factors used in radiological dose calculations for routine and accidental releases.

ZPA means zero period acceleration.

CHAPTER 1

INTRODUCTION AND GENERAL DESCRIPTION

CONTENTS

CHAPTER 1

INTRODUCTION AND GENERAL DESCRIPTION

TABLES

CHAPTER 1

INTRODUCTION AND GENERAL DESCRIPTION

This chapter explains the need for the Diablo Canyon Independent Spent Fuel Storage Installation (ISFSI), and provides general descriptions of the co-located Diablo Canyon Power Plant (DCPP) and the ISFSI. Also, agents and contractors are identified, as well as material incorporated by reference. Some of the information pertaining to DCPP and the ISFSI site was taken from Chapters 1 and 2 of the DCPP Final Safety Analysis Report (FSAR) Update (Reference 1). Information pertaining to the Diablo Canyon ISFSI and its dry cask storage system was taken from the storage system vendor documents cited in SAR Section 1.5.

1.1 INTRODUCTION

DCPP consists of two nuclear generation units located on the California coast approximately 6 miles northwest of Avila Beach, California. The two units are essentially identical pressurized water reactors (PWRs), each rated at a nominal 1,100 megawatts-electric (MWe). The two units share a fuel handling building/auxiliary building (FHB/AB) as well as certain components of auxiliary systems. The reactors, including their nuclear steam supply systems, were furnished by Westinghouse Electric Corporation. Each reactor has a dedicated fuel handling system and spent fuel pool (SFP). Both SFPs share a single 125-ton capacity crane for fuel handling activities. Both units and the plant site are owned and operated by PG&E.

Unit 1 began commercial operation in May 1985 and Unit 2 in March 1986. The operating licenses expire in September 2021 for Unit 1 and April 2025 for Unit 2. In general, the operating and spent fuel storage histories of DCPP Unit 1 and Unit 2 are similar to those of other PWRs. The spent fuel storage racks were initially of low-density design, capable of accommodating only one and one-third cores of spent fuel assemblies. These low-density racks were replaced in the late 1980s with high-density racks that are currently in use.

Each reactor core contains 193 fuel assemblies, and both units are currently operating on 18- to 21-month refueling cycles. Typically, 76 to 96 spent fuel assemblies are permanently discharged from each unit after a refueling. Each unit has operated for 10 fuel cycles and each is presently operating in its 11th cycle. The spent fuel pool (SFP) for each unit presently has sufficient capacity for the storage of 1,324 fuel assemblies. Based on the existing inventory and the expected generation of spent fuel, each SFP can accommodate the concurrent storage of a full core offload of irradiated fuel plus the anticipated quantity of spent fuel generated from prior refueling operations until 2006. After that time, an alternative means of spent fuel storage at DCPP must be provided unless the spent fuel can be shipped offsite.

The Nuclear Waste Policy Act (NWPA) of 1982 mandated that the Department of Energy (DOE) assume responsibility for the permanent disposal of spent nuclear fuel from the United

States commercial nuclear power plants. Pending the availability of a permanent DOE repository, nuclear power plant operators such as PG&E have been given the responsibility under the NWPA to provide for the interim onsite storage of spent fuel until it is accepted by DOE. DOE has not complied with its NWPA mandate to have a repository in operation commencing in 1998, and no interim spent fuel storage facility has been established. Moreover, no such DOE facility is expected to become operational in a timeframe to meet the DCPP spent fuel storage needs. Thus, spent fuel generated by DCPP will need to remain at DCPP until a DOE or other spent fuel storage facility is available. Consequently, additional spent fuel storage capacity is needed at DCPP no later than 2006.

The additional capacity to accommodate discharged spent fuel as proposed herein will allow DCPP to continue to generate electricity after 2006. Any interruption in the availability of this capacity would almost certainly cause a negative impact on the domestic sector power supply in California. Considering the power supplies in California and in the western United States, and uncertainties about future power supplies, loss of power from DCPP could have significant adverse impacts on the population, the infrastructure, and the economy. Expansion of the onsite spent fuel storage capacity at DCPP as planned by PG&E is necessary to avoid these potential, significant negative impacts.

The Diablo Canyon ISFSI will consist of the storage pads, a cask transfer facility (CTF), an onsite cask transporter, and the dry cask storage system. The dry cask storage system that has been selected by PG&E for the Diablo Canyon ISFSI is the Holtec International (Holtec) HI-STORM 100 System. The HI-STORM 100 System is comprised of a multi-purpose canister (MPC), the HI-STORM 100SA storage overpack, and the HI-TRAC transfer cask. The HI-STORM 100 System is certified by the Nuclear Regulatory Commission (NRC) for use by general licensees as well as site-specific licensees, presently with a 24-PWR fuel assembly MPC and storage overpack (see NRC 10 CFR 72 Certificate of Compliance [CoC] No. 1014) (Reference 2).

Holtec has proposed changes to the certified HI-STORM 100 System in License Amendment Request (LAR) 1014-1, which was submitted to the NRC on August 31, 2000 (Reference 3). The proposed changes include a HI-STORM 100SA storage overpack, a higher-capacity MPC-32 design (for storage of 32 PWR spent fuel assemblies), and MPC designs with different fuel storage capabilities (for example, high burnup fuel and certain damaged fuel). As discussed below, several of these proposed changes are desirable for the Diablo Canyon ISFSI. PG&E understands, however, that several of the proposed changes in LAR 1014-1, such as the designs to accommodate high burnup fuel, may involve extensive NRC review. As discussed below, issuance of a revised CoC No. 1014 may not be required to support the plant-specific Diablo Canyon ISFSI license.

The Diablo Canyon ISFSI is designed to hold up to 140 storage casks (138 casks plus 2 spare locations). The physical characteristics of the spent fuel assemblies to be stored are described in Safety Analysis Report (SAR) Section 3.1. Based on the current fuel strategy and the principal use of the MPC-32, the ISFSI with a storage pad capacity of 140 casks will be capable of storing the spent fuel generated by DCPP Units 1 and 2 over the term of the current operating licenses (2021 and 2025, respectively). In addition, to accommodate spent fuel generated during the licensed period, as well as any damaged fuel assemblies, debris, and nonfuel hardware, PG&E may use three other MPC designs from the HI-STORM 100 System: the MPC-24, MPC-24E, and MPC-24EF. All four MPC designs use the same storage overpack and are either licensed by the current CoC No. 1014 or will be licensed by future revisions to CoC No. 1014. These cask designs will accommodate most of the DCPP specific fuel characteristics.

The PG&E license application incorporates these designs in a preferred cask system licensing approach as follows:

(1) The initial Diablo Canyon ISFSI site-specific license incorporates the MPC capabilities as specified in the CoC No. 1014, as proposed to be amended in Holtec LAR 1014-1. The NRC anticipates issuing a final technical review of LAR 1014-1 and a preliminary Safety Evaluation Report (SER) in late December 2001 or early 2002. Rulemaking is expected to be completed in mid-2002. While the MPC capabilities covered by the Holtec CoC No. 1014 and LAR 1014-1 will not completely envelope all of the spent fuel characteristics eventually needed for DCPP fuel, they will cover most of the current SFP inventory and will permit the storage of nearly all spent fuel and associated nonfuel hardware generated during the license term.

(2) MPC designs that may be needed for the balance of the DCPP spent fuel characteristics will be addressed in future revisions to the CoC. As these changes are submitted by Holtec and approved by the NRC, PG&E will amend the Diablo Canyon ISFSI site-specific license to incorporate these changes. The resulting capability will provide PG&E with the flexibility to store onsite all the spent fuel and nonfuel hardware from DCPP Units 1 and 2 generated during the term of its operating licenses.

(3) In a Federal Register Notice dated October 11, 2001 (66 FR 51823), the NRC issued the final rule change regarding greater than class C (GTCC) waste (for example, split pins and thimble tubes). The rule change applies only to the interim storage of GTCC waste generated or used by commercial nuclear power plants. The rule change allows interim storage of reactor-related GTCC wastes under a 10 CFR 72 site-specific license. In accordance with the guidance of ISG 17, PG&E plans to request a modification to its proposed site-specific license at a future date to allow interim storage of GTCC wastes at the Diablo Canyon ISFSI.

(4) Exemption requests pertaining to the Diablo Canyon ISFSI license application are identified in Table 1.1-1.

Licensing of the Diablo Canyon ISFSI also involves NRC review of a number of site-specific issues. They include the site-specific environmental review, geotechnical issues related to the site and natural phenomena, and other site-specific matters. Although the Holtec LAR 1041-1 includes a high-seismic capability for the storage overpack (the HI-STORM 100SA), it does not incorporate some Diablo Canyon specific information (for example, the pad design, the overpack seismic anchorage design, the cask transporter seismic design, and the CTF design). PG&E is submitting information on these items as part of this site-specific application and intends that these issues be reviewed and licensed as part of the PG&E site-specific 10 CFR 72 license.

This SAR refers to a number of dry storage and ancillary components previously licensed under Revision 0 of the HI-STORM 100 System CoC and FSAR (Reference 4). Some of these components are being modified by Holtec International under the provisions of 10 CFR 72.48. Table 1.1-2 lists two components being modified, and the descriptions of the changes, which are discussed in the text, tables, and figures in this SAR. Only these two 10 CFR 72.48 changes have been determined to be germane to the review of the Diablo Canyon ISFSI license application. These changes have been approved under Holtec's design control program and the proprietary Holtec drawings are being provided to the NRC under separate cover (see DIL-01-008, Reference 5). However, Holtec has determined that completion of the 10 CFR 72.48 evaluations will require the approval of Amendment 1 to the HI-STORM 100 CoC, expected in mid-2002. The drawings referenced in Table 1.1-2 are provided for information only to assist the NRC in their review of this license application. They are not submitted for NRC review as a part of this application since the changes will be approved for use by Holtec under 10 CFR 72.48. The changes authorized under these 10 CFR 72.48 evaluations will be reflected in the next HI-STORM 100 System FSAR update in accordance with 10 CFR 72.48.

In accordance with 10 CFR 72.42, the Diablo Canyon ISFSI license is requested for a term of 20 years. If near the end of the initial license, permanent or interim DOE High Level Waste (HLW) facilities are unavailable for acceptance of commercial nuclear spent fuel, PG&E expects to submit an application for ISFSI license renewal pursuant to 10 CFR 72.42(b). To support the operational needs for continued DCPP operation, PG&E requests that the Diablo Canyon ISFSI site-specific license be issued by the end of 2003. The schedule for constructing and operating the Diablo Canyon ISFSI is dependent upon the timely completion of the NRC environmental review process and technical reviews of the site-specific license application. With the submittal of the Diablo Canyon ISFSI license application in December 2001, and based on a review of other applicants licensing schedules, PG&E believes that the review process at the NRC can be completed in approximately 2 years. Assuming no delays in the review process, and NRC issuance of the Diablo Canyon ISFSI license in 2003, PG&E plans to have the Diablo Canyon ISFSI in full operational status with initial placement of fuel in storage casks in 2005. This schedule provides a contingency period to ensure the Diablo Canyon ISFSI operation by 2006.

PG&E emphasizes that meeting the storage needs by 2006 is essential for continued DCPP operation. If the licensing schedule for the Diablo Canyon ISFSI cannot support that need with reasonable assurance, PG&E will need to reevaluate other alternatives for spent fuel storage. PG&E is presently maintaining the option of reracking the SFPs with higher density racks to provide additional storage with full-core-offload capability past 2006. However, the lead-time to implement this alternative is significant. Accordingly, PG&E needs to promptly determine the feasibility of licensing the Diablo Canyon ISFSI on the required schedule, and therefore requests an expedited NRC decision on the feasibility of the licensing approach and schedule outlined above.

Initial site characterization and storage system design activities have been conducted for the Diablo Canyon ISFSI. PG&E does not plan to initiate extensive facility construction activities until the NRC environmental review is completed, permits obtained, and the Diablo Canyon ISFSI license has been issued or the necessary environmental findings made. Thus, Diablo Canyon ISFSI construction work is not expected to begin until 2004 at the earliest. Nonetheless, pending NRC approval of the Diablo Canyon ISFSI license application, PG&E intends to proceed with relatively minor site preparation activities such as infrastructure development and access road work, and is in the process of obtaining the appropriate permits from other agencies for such work.

The Diablo Canyon ISFSI is designed to protect the stored fuel and prevent release of radioactive material under all normal, off-normal, and accident conditions of storage in accordance with all applicable regulatory requirements contained in 10 CFR 72. This SAR, as well as other parts of the Diablo Canyon ISFSI license application, have been prepared in compliance with the requirements of 10 CFR 72 and using the guidance contained in Regulatory Guide 3.62, "Standard Format and Content for the Safety Analysis Report for Onsite Storage of Spent Fuel Storage Casks," (February 1989); and NUREG-1567, "Standard Review Plan for Spent Fuel Dry Storage Facilities," (March 2000).

Additionally, PG&E has submitted a 10 CFR 50 LAR on September 13, 2001, seeking NRC approval to take credit for soluble boron in the spent fuel pools to increase the existing storage capacity and thus maintain spent fuel storage with full core offload capability through approximately 2006 and will submit a 10 CFR 50 LAR in early 2002 to permit cask handling activities in the DCPP fuel handling building/auxiliary building.

PG&E has evaluated the above proposed actions and determined that the proposed actions and mitigating measures do not involve: (a) a significant hazards consideration, (b) a significant change in the types or significant increase in the amounts of any effluents that may be released offsite, or (c) a significant increase in individual or cumulative occupational radiation exposure. This document should allow the NRC to conclude that the proposed actions to implement a spent fuel storage program consisting of a 10 CFR 72 license application and amendments to the DCPP 10 CFR 50 operating license do not adversely impact the public health and safety.

1.2 GENERAL DESCRIPTION OF LOCATION

The DCPP site consists of approximately 750 acres of land located in San Luis Obispo County, California, adjacent to the Pacific Ocean and roughly equidistant from San Francisco and Los Angeles. The site is located directly southeast of Montana de Oro State park, which is located along the coast of California in San Luis Obispo County. This site area is approximately 12 miles west-southwest of the city of San Luis Obispo, the county seat and nearest significant population center.

The nearest residential community is Los Osos, approximately 8 miles north of the plant site. The township of Avila Beach is located along the coast at a distance of approximately 6 miles southeast of the plant site. The city of Morro Bay is located along the coast approximately 10 miles northwest of the plant site. A number of other cities, as well as some unincorporated residential areas, exist along the coast and inland. However, these are at distances greater than 8 miles from the plant site. Only a few individuals reside within 5 miles of the plant site.

Access to the plant site is controlled by security fencing that defines the plant-protected area within the owner-controlled area, which is surrounded by a farm-type fence. The plant site is located near the mouth of Diablo Creek, and a portion of the site is bounded by the Pacific Ocean. All coastal properties located north of Diablo Creek, extending north to the southerly boundary of Montana de Oro State Park and reaching inland approximately 0.5 miles are owned by PG&E. Coastal properties located south of Diablo Creek and reaching inland approximately 0.5 miles are owned by Eureka Energy Company, a wholly owned subsidiary of PG&E. Except for the DCPP site, the 4,500 acres of this owner-controlled area are encumbered by two grazing leases.

PG&E has complete authority to control all activities within the site boundary and this authority extends to the mean high water line along the ocean. On land, there are no activities unrelated to plant operation within the owner-controlled area. The plant site is not traversed by public highway or railroad. Normal access to the site is from the south by private road through the owner-controlled area, which is fenced and posted by PG&E. The offshore area is not under PG&E control and is at times entered by commercial or sports fishing boats.

The plant site occupies a coastal terrace that ranges in elevation from 60 to 150 ft above mean sea level (MSL) and is approximately 1,000 ft wide. Plant grade, determined at the turbine building main floor, is at elevation 85 ft above MSL. The seaward edge of the terrace is a near-vertical cliff. Back from the terrace and extending for several miles inland are the rugged Irish hills, an area of steep, brush-covered hillsides and deep canyons that are part of the San Luis Mountains, which attain an elevation of 1,500 ft within about a mile of the site.

The reactors and ancillary structures are situated on top of bedrock. The coastal areas surrounding the plant are well drained, primarily via Diablo Creek, and groundwater is at a depth of at least 170 ft below the surface of the ISFSI pad. The climate of the site area is typical of that along the central California coast. The winter comprises the rainy season, with more than 80 percent of the average annual rainfall of approximately 16 inches. The average annual temperature of the site area is about 55°F, with a variation between approximately 32°F minimum and 97°F maximum, which reflects the strong marine influence.

The ISFSI is located within the PG&E owner-controlled area at DCPP. Figure 2.1-1 shows the location of the plant and ISFSI sites on a map of western San Luis Obispo County. Figure 2.1-2 shows a plan drawing of the ISFSI site. A more detailed description of the ISFSI site is provided in SAR Section 2.1.

1.3 GENERAL STORAGE SYSTEM DESCRIPTION

The Diablo Canyon ISFSI includes the following major structures, systems, and components (SSCs): the storage pads, CTF, onsite transporter, and dry cask storage system. The dry cask storage system selected by PG&E is the Holtec International HI-STORM 100 System, which has been certified by the NRC for use by general licensees as well as site-specific licensees (Reference 2). The HI-STORM 100 System is comprised of the MPC, the HI-STORM 100 storage overpack, and the HI-TRAC transfer cask; the design and operation of these components are described in detail in the HI-STORM 100 System FSAR. In addition, Holtec International has proposed a number of changes to the generically-certified HI-STORM 100 System in its LAR 1014-1, which has been submitted to the NRC for review and approval. A general description of major structures, systems, and components is provided herein. More detailed descriptions of the HI-STORM 100 System are contained in Section 4.2 of this SAR and in the Holtec International documents cited in References 2 through 4 of SAR Section 1.5. Likewise, more details on the storage pads, CTF, and transporter are provided in Sections 4.2 through 4.4 of this SAR.

Figure 4.2-7 shows a cut-away view of the MPC and the storage overpack. The MPC, shown partially withdrawn from the overpack, provides the confinement boundary for the spent fuel and associated nonfuel hardware. It is an integrally-welded pressure vessel that holds up to 24 or 32 DCPP spent fuel assemblies and meets the stress limits of the ASME Boiler and Pressure Vessel Code, Section III, Subsection NB. The MPCs are welded cylindrical structures consisting of a honeycomb fuel basket, a baseplate, canister shell, a lid, and a closure ring. The honeycomb fuel basket uses geometric spacing and Boral neutron absorbers for criticality control. The MPC is made entirely of stainless steel, except for the neutron absorbers and an aluminum seal washer in the vent and drain ports.

A loaded MPC is stored within the HI-STORM 100SA overpack in an anchored vertical orientation. The overpack provides gamma and neutron shielding, ventilation passages, and protects the MPC from missiles and natural phenomena. It is a rugged, heavy-walled cylindrical container. The main structural function of the storage overpack is provided by carbon steel, and the main shielding function is provided by unreinforced concrete. The overpack concrete is enclosed by cylindrical steel shells, a thick steel baseplate, and a top plate. The overpack lid has appropriate concrete shielding attached to its top to provide neutron and gamma attenuation in the vertical direction. Inlets at the bottom and corresponding outlets at the top of the overpack allow air to circulate naturally to cool the MPC. The inner shell of the overpack has channels attached to its inner diameter to guide the MPC during insertion/removal, provide a flexible medium to absorb impact loads, and to allow cooling airflow to circulate through the overpack.

The transfer cask provides an internal, cylindrical cavity of sufficient size to house an MPC during loading, unloading, and movement of the MPC from the SFP to the overpack. It provides gamma and neutron shielding and protects the MPC from missiles and natural phenomena. The structural function of the transfer cask is provided by the carbon steel shell, top lid, and pool lid. Neutron and gamma shielding are provided by water and lead, respectively. Figure 4.2-8 shows the transfer cask. The MPC access hole through the transfer cask top lid allows the lowering/raising of the MPC between the transfer cask and the overpack. The pool lid is bolted to the bottom flange of the transfer cask and is used during MPC fuel loading and sealing operations. In addition to providing shielding in the axial direction, the pool lid incorporates a seal that is designed to hold borated water in the transfer cask inner cavity, thereby preventing contamination of the exterior of the MPC by contaminated SFP water.

A transporter is used to move the transfer cask/MPC assembly from outside the FHB/AB to the CTF, which is adjacent to the ISFSI storage pads. After the MPC is placed in the overpack at the CTF, the transporter is again used to move the loaded overpack to the storage pads. The transporter is a U-shaped tracked vehicle consisting of the vehicle main frame, hydraulic lifting towers, an overhead beam system that connects between the lifting towers, a cask restraint system, the drive and control systems, and a series of cask lifting attachments. The transporter design permits the transfer cask/MPC assembly to be handled vertically or horizontally, and the loaded overpack vertically. Figure 4.3-1 shows the transporter with the transfer cask in the horizontal orientation.

As shown in Figure 4.1-1, the CTF is located about 100 ft from the storage pads. The CTF has a lifting platform designed to position an overpack below grade to facilitate the transfer of a loaded MPC from the HI-TRAC transfer cask to the overpack. Figure 4.4-3 shows the CTF.

The loaded overpacks are stored on a series of concrete storage pads within a protected area separate from that of DCPP. Each storage pad is designed to accommodate up to 20 loaded overpacks in a 4-by-5 array as shown in Figure 4.1-1. Ultimately, seven such pads may be built to accommodate a full offload of Units 1 and 2 reactor cores and their SFPs at the end of their existing operating licenses. Each loaded overpack is approximately 11 ft in diameter, 20 ft high, and weighs about 360,000 pounds. There is approximately 6 ft, surface-to-surface distance between the overpacks. The series of 7 storage pads will cover an area approximately 500 ft by 105 ft. The protected area has applicable barrier, access, and surveillance controls meeting 10 CFR 73.55 for an ISFSI co-located with a nuclear power plant.

The preparation and loading of the MPCs take place in the FHB/AB. These activities, plus the full summary of activities culminating in the storage of MPCs on the storage pads, are described in Sections 4.4 and 5.1.

The important-to-safety SSCs of the ISFSI are identified in Section 4.5.

1.4 IDENTIFICATION OF AGENTS AND CONTRACTORS

Engineering, site preparation, and construction of the ISFSI storage pads and CTF will be performed by PG&E, using specialty contractors as necessary.

Holtec International will provide the spent fuel storage system, consisting of the HI-STORM 100SA overpack, the MPC, and the HI-TRAC transfer cask; the transporter; and design criteria for the ISFSI storage pads, and CTF.

PG&E will be responsible for the operation of the ISFSI.

All of these activities involving important-to-safety structures, systems, and components are subject to NRC-approved QA programs as discussed in Chapter 11.0 and in the Holtec references cited in Section 1.5.

1.5 MATERIAL INCORPORATED BY REFERENCE

1. Diablo Canyon Power Plant Units 1 & 2 Final Safety Analysis Report Update, Revision 14, November 2001.

2. 10 CFR 72 Certificate of Compliance No. 1014 for the HI-STORM 100 System, Holtec International, Revision 0, May 2000.

3. License Amendment Request 1014-1, Holtec International, Revision 2, July 2001, including Supplements 1 through 4 dated August 17, 2001; October 5, 2001; October 12, 2001; and October 19, 2001; respectively.

4. Final Safety Analysis Report for the HI-STORM 100 System, Holtec International Report No. HI-2002444, Revision 0, July 2000.

5. Submittal of Holtec Proprietary Design Drawing Packages, PG&E Letter to the NRC DIL-01-008, dated December 21, 2001

6. License Application, Attachment B, Units 1 and 2 Diablo Canyon Power Plant, Emergency Plan, 2001.

7. License Application, Attachment C, Proposed Technical Specifications, 2001.

8. License Application, Attachment D, Training Program, 2001.

9. License Application, Attachment E, Quality Assurance Program, 2001.

10. License Application, Attachment F, Preliminary Decommissioning Plan, 2001.

TABLE 1.1-1

DIABLO CANYON ISFSI LICENSE APPLICATION
EXEMPTION REQUESTS

Code of Federal Regulations Reference	Exemption Request
10 CFR 72.72(d)	PG&E is requesting an exemption from storing spent fuel and high-level radioactive waste records in duplicate. Refer to Diablo Canyon ISFSI SAR, Section 9.4.2.
10 CFR 72.124(c)	On November 12, 1997, the NRC granted PG&E an exemption from the requirements of 10 CFR 74 concerning criticality monitors. PG&E is requesting an exemption from the 10 CFR 72.124(c) criticality monitoring requirements by requesting an extension of the NRC's November 12, 1997, exemption for the FHB/AB to envelop the activities associated with the Diablo Canyon ISFSI SAR. Reference Diablo Canyon ISFSI SAR, Section 4.2.3.3.5 and the 10 CFR 50 LAR in support of ISFSI licensing.
10 CFR 73.55	PG&E is requesting an exemption from four 10 CFR 73.55 requirements, as described in the Security Program license amendment request (LAR) 01-09. Refer to PG&E letter DCL-01-127, dated December 21, 2001.

TABLE 1.1-2

10 CFR 72.48 CHANGES TO THE HI-STORM 100 SYSTEM
GERMANE TO THE DIABLO CANYON ISFSI LICENSE APPLICATION

AFFECTED COMPONENT	HI-STORM FSAR DRAWING NO.	NEW HOLTEC DRAWING NO.	DESCRIPTION OF CHANGES	STATUS OF 72.48 EVALUATION
HI-TRAC 125 Transfer Cask with Pool Lid	1880	3438	Created dual purpose lid ("D") version of HI-TRAC 125. Removed pocket trunnions, added upper and lower gussets for securing transfer cask to adjacent structures.	Requires NRC approval of HI-STORM Amendment 1 to complete
HI-TRAC 125 Transfer Lid	1928	3437	Created mating device ancillary to allow removal of the transfer cask pool lid and transfer of the MPC to the overpack without the need for the transfer lid.	Requires NRC approval of HI-STORM Amendment 1 to complete

DIABLO CANYON ISFSI
SAFETY ANALYSIS REPORT

CHAPTER 2

SITE CHARACTERISTICS

CONTENTS

CHAPTER 2

SITE CHARACTERISTICS

CONTENTS (Continued)

CHAPTER 2

SITE CHARACTERISTICS

TABLES

CHAPTER 2

SITE CHARACTERISTICS

FIGURES

SITE CHARACTERISTICS

FIGURES (Continued)

CHAPTER 2

SITE CHARACTERISTICS

FIGURES (Continued)

CHAPTER 2

SITE CHARACTERISTICS

FIGURES (Continued)

CHAPTER 2

SITE CHARACTERISTICS

FIGURES (Continued)

CHAPTER 2

SITE CHARACTERISTICS

This chapter provides information on the location of the Diablo Canyon ISFSI and descriptions of the geographical, demographical, meteorological, hydrological, seismological, and geological characteristics of the storage site and the surrounding vicinity. Some of the provided information is taken from Chapters 1 and 2 of the DCPP FSAR Update.

2.1 GEOGRAPHY AND DEMOGRAPHY OF SITE SELECTED

A description of the geography and demography of the Diablo Canyon area is contained in the DCPP FSAR Update. This information generally applies to the Diablo Canyon ISFSI, as described below.

2.1.1 SITE LOCATION

The general area surrounding the Diablo Canyon Power Plant and the ISFSI is shown in Figure 2.1-1. The ISFSI will be located within the PG&E owner-controlled area at Diablo Canyon, which consists of approximately 750 acres of land located in San Luis Obispo County, California, adjacent to the Pacific Ocean and roughly equidistant from San Francisco and Los Angeles. The boundary of this area is used for the analyses required in accordance with 10 CFR 72.104 and 72.106. This area is located along the coast of California in San Luis Obispo County directly southeast of Montana de Oro State Park and is approximately 12 miles west-southwest of the city of San Luis Obispo, the county seat and the nearest significant population center.

The nearest residential community is Los Osos, approximately 8 miles north of the ISFSI site. This community is located in a mountainous area adjacent to Montana de Oro State Park. The township of Avila Beach is located down the coast approximately 6 miles southeast of the ISFSI site. The city of Morro Bay is located up the coast approximately 10 miles northwest of the site. A number of other cities, as well as some unincorporated residential areas, exist along the coast and inland. However, these communities are greater than 8 miles from the ISFSI site. Only a few individuals reside within 5 miles of the site.

The DCPP facilities and the ISFSI site are located near the mouth of Diablo Creek, and a portion of the power plant site is bounded by the Pacific Ocean. Approximately 165 acres of the owner-controlled area are located north of Diablo Creek. The remaining 595 acres are located adjacent to and south of Diablo Creek. The entire acreage is owned by PG&E.

The ISFSI is located at latitude 35°12'52" North and longitude 120°51'00" West. The Universal Transverse Mercator (UTM) coordinates of the ISFSI are 695,689 meters East and 3,898,723 meters North. Figure 2.1-1 shows the location of the Diablo Canyon plant and ISFSI sites, on a map of western San Luis Obispo County. Figure 2.1-2 shows a plan drawing of the ISFSI site.

2.1.2 SITE DESCRIPTION

A security fence that defines the ISFSI protected area within the owner-controlled area, which is surrounded by a farm-type fence, controls access to the ISFSI site. PG&E owns all coastal properties north of Diablo Creek, to the southerly boundary of Montana de Oro State Park and inland a distance of 0.5 to 1.75 miles. Similarly, PG&E owns all coastal properties south of Diablo Creek for approximately 8 miles and inland approximately 1.75 miles. Except for the DCPP and ISFSI sites, all of the acreage north and south of DCPP and the ISFSI are encumbered by two grazing leases. In accordance with an agreement in principle reached in 2000 with the Central Coast Regional Water Quality Control Board, land north of DCPP, consisting of 2,013 acres of watersheds draining to approximately 5.7 miles of coastline, will be preserved by a conservation easement for ecological purposes. The primary goal is protection of marine resources from Fields Cove to Coon Creek through watershed and habitat protection of all the lands draining to that coastline. In addition, PG&E will protect 547 acres draining to Coon Creek through Best Management Practices for as long as PG&E operates the plant or holds the property, whichever is longer.

The Diablo Canyon owner-controlled area occupies a coastal terrace and adjacent uplands that range in elevation from 60 to 1,400 ft above mean sea level (MSL). The DCPP facilities, other than the intake and discharge structures, occupy an area between 60 and 150 ft MSL and approximately 1,000 ft wide. The ISFSI is located approximately 0.22 miles northeast of the Unit 1 containment (ISFSI/containment center-to-center) at an elevation of approximately 310 ft MSL (Figure 2.1-2). The seaward edge of the terrace is a near-vertical cliff. Back from the terrace and extending for several miles inland are the rugged Irish hills, an area of steep, brush-covered hillsides and deep canyons that are part of the San Luis Mountains. The coastal areas surrounding the ISFSI are well drained, primarily via Diablo Creek, and the water table is typically low.

The ISFSI is located between hillsides and is situated directly on bedrock at the site area. The topography of the site and the limited rainfall preclude any possibility of flooding. Even in the event of a probable maximum flood (PMF) and hypothetical plugging of the 10 ft diameter drainage pipe located below the two nearby switchyards, no flooding of the ISFSI is expected to occur since the roadway located north of Diablo Creek will serve as a bypass for flood waters. Water levels will flow below the elevation of the ISFSI.

The climate of the site area is typical of that along the central California coast and reflects a strong maritime influence. The rainy season is in the winter, producing more than 80 percent of the average annual rainfall of approximately 16 inches. The average annual temperature of the site area is about 55°F.

PG&E has full authority to control all activities within the ISFSI site and owner-controlled area boundaries; this authority extends to the mean high water line along the ocean coastline. The mineral rights within the 165-acre PG&E portion of the site are owned by PG&E; there is no information suggesting that the land contains commercially valuable minerals. On land, there are no activities unrelated to the ISFSI or power plant operation within the site exclusion area. The owner-controlled area is not traversed by public highway or railroad. Normal access to the ISFSI and DCPP sites is from the south by a 6.5-mile long private road through the owner-controlled area, which is fenced and posted by PG&E. The private road is connected to a local public roadway, Avila Beach Drive, which runs along the shoreline of San Luis Obispo Bay. A US Coast Guard station is located adjacent to the security gate, inside the owner-controlled area. The major access to the area is via US Highway 101, which passes about 9 miles east of the ISFSI site and is accessible at approximately 15 miles to the southeast of the site.

2.1.3 POPULATION DISTRIBUTION AND TRENDS

The population distribution and projections for areas around the ISFSI site are based on the 2000 census and on estimates prepared by the California Department of Finance. As described in Section 2.1.2, the ISFSI site is located approximately 0.22 miles northeast of the Unit 1 containment. The population data presented in this section for the ISFSI are based on distances from the Unit 1 containment rather than distances from the ISFSI site. The 0.22-mile offset to the ISFSI, however, is considered to have negligible effect on the population estimates at various distances and directions from the ISFSI.

The population data are provided for areas within a 50-mile radius of the ISFSI. Population distributions are provided for areas within specific radii and sectors, and include the 2000 census data as well as projections for the years 2010 and 2025.

The area within 50 miles of the ISFSI includes most of San Luis Obispo County, some portions of Santa Barbara County, and a small area of Monterey County. Approximately 55 percent of the area within the radius is on land, with the balance being the Pacific Ocean. In general, the portion of California that lies within 50 miles of the ISFSI is relatively sparsely populated, having approximately 424,000 residents in 2000.

The 2000 census population of this region is very close to that projected in the original FSAR for DCPP, and subsequent projections by the Department of Finance are similarly close to earlier projections. Table 2.1-1 shows population trends of the State of California and of San Luis Obispo and Santa Barbara Counties. Table 2.1-2 shows the growth since 1960 of the principal cities within 50 miles of the ISFSI site. Table 2.1-3 lists communities within 50 miles of the ISFSI site having a population of 1,000 or more, provides the distance and direction from the ISFSI site, and shows the 2000 population.

2.1.3.1 Population Within 10 Miles

In 1980, approximately 16,760 persons resided within 10 miles of the ISFSI site. The 1990 census counted approximately 22,200 residents within the same 10 miles. The 2000 census counted approximately 23,700 residents within the same 10 miles. As in 1980, the nearest residence is approximately 1.5 miles north-northwest of the ISFSI site and is occupied by two persons. There are 4 permanently inhabited dwellings, with approximately

14 residents, within 5 miles of the ISFSI. The population within a 6-mile radius, the low population zone (LPZ) as used in the emergency plan, is estimated to be 100.

Figure 2.1-3 shows the 2000 population within a 10-mile radius, wherein the area is divided into 22.5° sectors and part circles with radii of 1, 2, 3, 4, 5, and 10 miles. Figures 2.1-4 and 2.1-5 show projected population distributions for 2010 and 2025, respectively, and are based primarily on population projections published by the California Department of Finance. The distributions are based on the assumption that the land usage will not change in character during the next 25 years, and that population growth within 10 miles will be proportional to growth in San Luis Obispo County as a whole.

2.1.3.2 Population Between 10 and 50 miles

Figure 2.1-6 shows the 2000 population distribution between 10 and 50 miles within the sectors of 22.5°, with part circles of radii of 10, 20, 30, 40, and 50 miles. Figures 2.1-7 and 2.1-8 show projected distributions for 2010 and 2025, respectively, and are based primarily on population projections published by the Department of Finance and interviews with area government officials. In 2000, some 82 percent of those persons within 50 miles of the ISFSI site resided in the population centers listed in Table 2.1-3.

2.1.3.3 Transient Population

In addition to the resident population presented in the tables and population distribution charts, there is a seasonal influx of vacation and weekend visitors, especially during the summer months. This influx is heaviest south along the coast from Avila Beach to south of Oceano.

During August, the month of heaviest influx, the maximum overnight transient population in motels and state parks in this area is approximately 100,000 persons. However, there are no significant seasonal or diurnal shifts in population or population distribution within the LPZ. Table 2.1-4 lists transient population for recreation areas within 50 miles of the site for the periods of record listed.

Within the LPZ, the maximum-recorded number of persons at any single time is estimated to be 5,000. This figure is provided by the State Department of Parks and Recreation and corresponds to the maximum daytime use of Montana de Oro State Park. Overnight use is considerably less, with an estimated maximum of 400. Evacuation of these numbers of persons from the park in the event of a radiation release could be accomplished as provided for in the emergency plan, with a reasonable probability that no injury would result.

2.1.3.4 Public Facilities and Institutions

Several elementary schools are located within 10 miles of the ISFSI site, near Los Osos and Avila Beach. These schools serve the local communities and do not draw from outlying areas. California Polytechnic State University is 12 miles north-northeast of the ISFSI site and has an enrollment of approximately 17,000. Cuesta College is located 10 miles northeast of the site and has an enrollment of approximately 10,000.

Montana de Oro State Park is located north of the site. Its area of principal use is along the beach, between 4 and 5 miles north-northwest of the site. The total number of visitor days during a 12-month period over the previous 5 years averages 600,000.

2.1.4 USE OF NEARBY LAND AND WATERS

The San Luis Range, reaching a height of 1,800 ft, dominates the region between the site and US Route 101. This upland country is used to a limited extent for grazing beef cattle and, to a very minor extent, dairy cattle. There are also wild and domestic goats, deer, and other wildlife in the vicinity of the plant site. The terrain east of US Route 101, lying in the mostly inaccessible Santa Lucia Mountains, is sparsely populated with little development. A large portion of this area is included within the Los Padres National Forest.

2.1.4.1 Agriculture

San Luis Obispo County has relatively little level land, except for a few small coastal valleys such as the Santa Maria and San Luis Valleys, and some land along the county's northern border in the Salinas Valley and Carrizo Plain areas. Farming is a significant land use in the county. Principal crops include wine grapes, vegetables, nurseries, fruits, nuts, and grain. There are several vineyards and wineries located in the county. The county's leading agricultural product is wine grapes, valued at approximately $74,000,000 in 1998. The total farm acreage in the county is approximately 1,200,000. The county contains a total of 2,128,640 acres.

2.1.4.2 Dairy

The only dairy activity is 12 miles northeast of the site at California Polytechnic State University, located in the city of San Luis Obispo, which produces 1,200 gallons of milk per day. Some replacement heifers and dry cows are sometimes pastured on property adjacent to the site.

2.1.4.3 Fisheries

The ISFSI site is located between two fishing harbors that support commercial and sport fishing activities. Port San Luis Harbor is located in Avila Beach, approximately 6 miles down coast of the ISFSI site. Morro Bay Harbor is located approximately 10 miles up coast of the site. In 1994 the combined sport catch totaled approximately 342,000 rockfish and 6,000 fish of other species, from a total of 16 fishing vessels.

Commercial landings are calculated by poundage of landings by port. In 1994, at Port San Luis and Morro Bay Harbors, the landings were estimated to be as follows: 2,474,000 pounds of rockfish, 5,405,000 pounds of other fish species, 1,300 pounds of abalone, 2,694,000 pounds of squid, 534,000 pounds of crab, 418,000 pounds of shrimp, and 4,400 pounds of urchins.

There has been a dramatic decrease since 1970 in the abalone catch, with approximately 621,000 pounds taken in 1966 and 200,000 pounds taken in 1970, due primarily to severe restrictions imposed by the California Department of Fish and Game. Some data suggest that the southern movement of the Southern California sea otter may have had an impact on the red abalone population.

2.1.4.4 Water use

There are two public water supply groundwater basins within 10 miles of the site. Avila Beach County Water and Sewer District and San Miguelito Mutual Water and Sewer Company provide water to the Avila Beach and Avila Valley area. The property owners to the north and south of the ISFSI site capture surface water from small intermittent streams and springs for minimal domestic use. PG&E's lessee captures water 2 to 4 miles south of the ISFSI site from streams and springs between Pecho Canyon and Rattlesnake Canyon. Property owned by PG&E captures water from Crowbar Canyon, 1 mile north of the plant site. In addition, an ocean water desalinization plant was built and has been in operation at DCPP since 1985.

2.1.4.5 Land Usage Within 5 Miles

The only agricultural activities indicated by county records are cattle grazing in much of the area surrounding the site, and a farm in the east-southeast sector, producing legumes and cereal grass such as grains. The farm is located along the site access road on the coastal plateau, starting approximately 2 miles from the plant and extending to 4.5 miles from the ISFSI. There is also a household garden greater than 500 square ft in the east sector. These activities are being conducted on land leased from PG&E.

2.1.4.6 Other Nearby Usage

The community of Avila Beach lies approximately 6 miles east-southeast of the plant, immediately adjacent to the owner-controlled area. Port San Luis Harbor is located directly opposite the security entrance that controls entry into the Diablo Canyon owner-controlled area via the private access road. A small public beach is located next to the harbor area and is used frequently by the public for access to the harbor waters for recreation purposes.

A tanker-loading pier owned by UNOCAL Oil Company is located in Port San Luis Harbor directly adjacent to the small beach area. Prior to 1999, there were also several UNOCAL oil storage tanks located on the hills immediately southeast of Avila Beach. Approximately 1 to 2 local tankers per month offloaded oil for storage in these tanks until the late 1990s. The tanks were removed in 1998 as a part of an effort by UNOCAL to clean up soil contamination due to oil leaks from piping beneath Avila Beach.

2.2 NEARBY INDUSTRIAL, TRANSPORTATION, AND MILITARY FACILITIES

2.2.1 OFFSITE POTENTIAL HAZARDS

2.2.1.1 Description of Location and Routes

Industry in the vicinity of the Diablo Canyon ISFSI site is mainly light and of a local nature, serving the needs of agriculture in the area. Food processing and refining of crude oil are the major industries in the area, although the numbers employed are not large. Less than 8 percent of the work force in San Luis Obispo County is engaged in manufacturing. The largest industrial complex is Vandenberg Air Force Base, located approximately 35 miles south-southeast of the DCPP site in Santa Barbara County.

Port San Luis Harbor and the Point San Luis Lighthouse property are located approximately 6 miles south-southeast of the DCPP site. The Point San Luis Lighthouse is located on a 30-acre parcel of land. Until 1990, the US Coast Guard owned the lighthouse property. In 1990 the Port San Luis Harbor District, owners and operators of the Port San Luis Harbor, were granted ownership of the lighthouse and the 30 acres, except for approximately 3 acres of land, in 3 parcels, which the Coast Guard retained as owners in order to operate and maintain the modern light station and navigating equipment located on those 3 acres.

Located approximately 6 miles east-southeast of the DCPP site is the Port San Luis tanker-loading pier. The pier is located on property that is owned by the Port San Luis Harbor District and leased by UNOCAL, which built and owns the pier. However, this pier is no longer active as tanker traffic into Port San Luis has been discontinued.

US Highway 101 is the main arterial road serving the coastal region in this portion of California. It passes approximately 9 miles east of the site, separated from it by the Irish Hills. US Highway 1 passes approximately 10 miles to the north and carries moderate traffic between San Luis Obispo and the coast. The nearest public access from a US highway is by county roads in Clark Valley, 5 miles north, and See Canyon, 5 miles east. Access to the site is by Avila Beach Drive, a county road, to the entrance of the PG&E private road system.

The Southern Pacific Transportation Company provides rail service to the county by a route that essentially parallels US Highway 101. It passes approximately 9 miles east of the site, separated from it by the Irish Hills. There is no spur track into the DCPP site.

Coastal shipping lanes are approximately 20 miles offshore. Prior to 1998, there were local tankers coming into and out of Estero Bay, which is north of the DCPP site. There is no further tanker traffic in either Port San Luis or Estero Bay. The local tanker terminal at Estero Bay closed in 1994, and Avila Pier ceased operation in 1998. Petroleum products and crude oil are no longer stored at Avila Beach since the storage tanks there were removed in 1999. However, some petroleum products and crude oil continue to be stored at Estero Bay, approximately 10 miles from the DCPP site.

The San Luis Obispo County Airport is located 12 miles east of the DCPP site. The airport serves approximately 52 scheduled landings and departures per day of commercial commuter flights, provided primarily by turbo-prop aircraft that seat no more than 41 people with a gross weight of no more than 30,000 pounds. The airport also serves approximately 10,000 total landings and departures of private aircraft per month. These consist mostly of aircraft that seat no more than 8 people, with an average gross weight of less than 12,500 pounds. Although there are no specific air traffic restrictions over DCPP, most air traffic into and out of the San Luis Obispo Airport does not approach within 5 miles of the ISFSI site because of the mountainous terrain.

There is a federal flight corridor (V-27) approximately 5 miles east of the ISFSI that is used for aircraft flying between Santa Barbara and Big Sur areas, with an estimated 20 flights per day. The majority of the aircraft using this route is above 10,000 ft. Sometimes this corridor is used also for traffic in to San Luis Obispo Airport and, in this case, has traffic that passes as close as 1 mile of the ISFSI site at an elevation of 3,000 ft. However, this portion of the route is normally only used for aircraft to align for instrument landing. The more commonly used approach route for visual landings passes 8 miles from the Diablo Canyon ISFSI site on the far side of the San Luis Range.

There is also a military training route (VR-249), which runs parallel to the site and its center is approximately 2 miles off shore. This training route is not frequently used. (Estimated at less then 50 flights per year). Its use requires a minimum of 5 miles visibility, and the flights are to maintain their altitude between 1,500 ft and a ceiling of 3,000 ft. Most aircraft using this route are military helicopters.

There is a municipal airport near Oceano, located 15 miles east-southeast of the DCPP site, which accommodates only small (12,500 pounds or less) private planes. The traffic at this airport is estimated to be no more than 2,200 flights per month. The Camp San Luis Obispo airfield is located 8 miles northeast of the DCPP site, but is now shown as helicopter use only.

The peak Vandenberg Air Force Base employment is approximately 4,400 people, including 3,200 military and 1,200 civilian personnel. Missiles fired to the Western Pacific Missile Range are not directed north or northwest, and are thus away from the DCPP site. Missile launch sites are approximately 36 miles south of DCPP. Polar orbit launches are in a southerly direction. Vandenberg Air Force Base is a designated alternate landing site for the space shuttles, but has not been used for that purpose to date. The landing approach is normally west to east, and does not bring the shuttles within 30 miles of the ISFSI site.

The nearest US Army installation is the Hunter-Liggett Military Reservation located in Monterey County, approximately 45 miles north of the DCPP site. The California National Guard (CNG) maintains Camp Roberts, located on the border of Monterey County and San Luis Obispo County, southeast of the Hunter-Liggett Military Reservation and approximately 30 miles north of the DCPP site. The CNG also maintains Camp San Luis Obispo, located in San Luis Obispo County, approximately 10 miles northeast of the DCPP site. In addition, as noted earlier, a US Coast Guard Light station is located in Avila Beach on property commonly known as the Point San Luis Lighthouse property.

No significant amounts of any hazardous products are commercially manufactured, stored, or transported within 5 miles of the DCPP site. Within 6 to 10 miles of the site, up to 1998, 1 to 2 local tankers per month offloaded oil for storage at Avila Beach. However, such shipments no longer occur and oil is no longer transported through or stored at Avila Beach. Due to very limited industry within San Luis Obispo County and the distances involved, any hazardous products or materials commercially manufactured, stored, or transported in the areas between 5 and 10 miles from the site are not considered to be a significant hazard to the ISFSI.

2.2.1.2 Hazards from Facilities and Ground Transportation

The ISFSI is located in a remote, sparsely populated, undeveloped area. The ISFSI site is in a canyon, which is east and above DCPP Units 1 and 2, and is directly protected on two sides by hillsides. There are no industrial facilities (other than DCPP), public transportation routes, or military bases within 5 miles of the ISFSI. Therefore, activities related to such facilities do not occur near the ISFSI and, thus, do not pose any hazard to the ISFSI.

Local shipping tankers may come within 10 miles of the DCPP site, but will remain outside of a 5-mile range. Coastal shipping lanes are approximately 20 miles offshore. Therefore, shipping does not pose a hazard to the ISFSI.

No commercial explosive or combustible materials are stored within 5 miles of the site, and no natural gas or other pipelines pass within 5 miles of the site. Therefore, there is no potential hazard to the ISFSI from any explosions or fires involving such materials.

Since there are no rail lines or public transportation routes within 5 miles of the ISFSI location, no credible explosions involving truck or rail transportation events need to be considered, pursuant to Regulatory Guide 1.91 (Reference 1). Similarly, explosions involving shipping events offshore at the DCPP site are unlikely. Although the shortest distance from the ISFSI location to the ocean is approximately 1/2-mile, there is no shipping traffic within 5 miles of this location. Therefore, consistent with the guidance of Regulatory Guide 1.91, explosions involving shipping events are not considered credible accidents for the ISFSI.

2.2.1.3 Hazards from Air Crashes

Aircraft crashes were assessed in accordance with the guidance of NUREG-0800, Section 3.5.1.6, Aircraft Hazards (Reference 2). Although this guidance applies to power reactor sites, the analysis of aircraft crash probabilities on the site is not dependent on the nature of the site other than size of the facility involved and, thus, the guidance of NUREG-0800 can be applied to the Diablo Canyon ISFSI site.

As specified in NUREG-0800, the probability of aircraft crashes is considered to be negligibly low by inspection and does not require further analysis if the three criteria specified in Item II.1 of Section 3.5.1.6 are met. In particular, Criterion 1 of Section 3.5.1.6 specifies that the plant-to-airport distance, D, must be greater than 10 statute miles, and the projected annual number of operations must be less than $1000D^2$. San Luis Obispo Airport is at a distance of 12 miles, with annual flight totals of approximately 139,000, which is less than $1000(12)^2$ or 144,000. The airport at Oceano is 15 miles away, with flight totals of no more than approximately 26,400 per year, which is less than $1000(15)^2$ or 225,000. Vandenberg Air Force Base is 35 miles away and flight totals there are not expected to be more than $1000(35)^2$ or 1,225,000 per year (or more than 3300 each day). Therefore, Criterion 1 is met.

Criterion 2 specifies that the facility must be at least 5 statute miles from the edge of military training routes. There is a military training flight corridor (VR-249) that is within approximately 2 miles of the Diablo Canyon ISFSI site. This route is evaluated below.

Criterion 3 specifies that the facility must be at least 2 statute miles beyond the nearest edge of a federal airway, holding pattern, or approach pattern. There is a federal airway (V-27) whose edge is within approximately 1 mile east of the ISFSI site. As a result, this route is evaluated below.

Evaluation of Airways

For situations where federal airways or aviation corridors pass through the vicinity of the ISFSI site, the probability per year of an aircraft crashing into the site (P_{fa}) is estimated in accordance with NUREG-0800. The probability depends on factors such as altitude, frequency, and width of the corridor and corresponding distribution of past accidents. Per NUREG-0800, the following expression is used to calculate the probability:

$$P_{fa} = C \times N \times A/w$$

Where:

C = Inflight crash rate per mile for aircraft using airway

w = Width of airway (plus twice the distance from the airway edge to the site when the site is outside the airway) in miles

N = Number of flights per year along airway

A = Effective area of the site in square miles

For the ISFSI site, the effective area is calculated based on the location of the site between rolling hills and the resulting limited angle of access by an aircraft in a crash situation.

Conservatively, the site area is taken as twice its approximate area of 100,000 square ft or 7.2×10^{-3} square miles.

Based on this requirement, the following analyses are performed:

For local traffic on V-27:

V-27 use for local aircraft is usually limited to a vector intercept to setup for instrument landings at San Luis Obispo Airport. As stated above, there are approximately 52 scheduled commercial aircraft landings and takeoffs per day. In addition, there are approximately 10,000 total landings and takeoffs of private aircraft per month. Since the use of V-27 is normally limited to the setup for instrument landings from the south, conservatively, it is estimated that 50 percent of the commercial and private traffic is coming from the south and 10 percent of the commercial aircraft are using this route for setup for landing. For the private aircraft usage, because of limited instrument landing capability and qualification, conservatively only about 5 percent would be on this route. As a result, N would be equal to approximately 1975 flights per year. Per NUREG-0800, C is provided as 4×10^{-10}. Per federal guidelines, the width of the airway is 8 miles and the center is approximately 5 miles from the site. As a result, (w) is conservatively taken to equal 10 miles.

$$P1_{fa} = CxNxa/w = (4 \times 10^{-10}) \times (1975) \times (7 \times 10^{-3})/(10) = 5.53 \times 10^{-10}$$

For commercial traffic flying on V-27 and not landing locally:

V-27 is a federal flight route from the Santa Barbara area northwest to the Big Sur area. Most of the aircraft on this route are normally flying at altitudes above 10,000 ft, with some smaller aircraft at elevations as low as 3,500 ft. Per the FAA Standards Office, the number of aircraft on this route is conservatively estimated at 20 per day or 7,300 per year. Using the same data as above and adjusting for the number of flights:

$$P2_{fa} = CxNxa/w = (4 \times 10^{-10}) \times (7300) \times (7 \times 10^{-3})/(10) = 2.04 \times 10^{-9}$$

For military aircraft flying on VR-249:

VR-249 is a military training route, which requires 5 miles visibility and the aircraft are to be at greater than 1,500 ft and less than 3,000 ft. The route is used very infrequently and is estimated to have approximately 50 flights a year, which are mostly helicopters. Conservatively, N is taken to be 100 flights. The center of the route is approximately 2 miles off shore; therefore, (w) is conservatively set at 1 mile in this calculation.

$$P3_{fa} = CxNxa/w = (4 \times 10^{-10}) \times (100) \times (7 \times 10^{-3})/(1) = 2.8 \times 10^{-10}$$

Summary of aircraft hazards

As stated above, and with the exception of the vector approach from V-27, the landing patterns and distance to the local airports would not significantly increase the probability of a crash at the ISFSI site. In addition, there are no designated airspaces or holding patterns, which are within the limits of Criterion 2 of NUREG-0800. As result, the total aircraft hazard probability at the Diablo Canyon ISFSI site is equal to the sum of the individual probabilities calculated above.

$$\text{Total} = P1_{fa} + P2_{fa} + P3_{fa} = (5.53 \times 10^{-10}) + (2.04 \times 10^{-9}) + (2.8 \times 10^{-10}) = 2.87 \times 10^{-9}$$

Based on the above calculation, the total aircraft hazard probability is determined to be approximately 2.87×10^{-9}, which is considerably less than the threshold of 1×10^{-7} specified in NUREG-0800 as a credible event requiring further analysis. Therefore, aircraft impacts are not considered a design basis event for the ISFSI.

PG&E is aware the NRC is considering revising security regulations which may affect aircraft hazard requirements relating to aircraft hazards. Following adoption of any new security regulations by the NRC, PG&E will comply with any such revised requirements as appropriate.

2.2.2 ONSITE POTENTIAL HAZARDS

2.2.2.1 Structures and Facilities

At the DCPP site, including the ISFSI storage site, there are no cooling towers or stacks with a potential for collapse. Therefore, such hazards need not be considered for any potential effects on the ISFSI.

There are 500-kV transmission lines that run in close proximity of the ISFSI storage site and on the hill above it (Figure 2.2-1). A 500-kV transmission line drop is postulated as a result of a transmission tower collapse or transmission line hardware failure near the ISFSI storage site and the cask transfer facility (CTF), as discussed on Section 8.2.8. The worst-case fault condition for a cask is that which places a cask in the conduction path for the largest current. This condition is the line drop of a single conductor of one phase with resulting single line-to-ground fault current and voltage-induced arc at the point of contact.

It is concluded that the postulated transmission line break will not cause the affected cask components to exceed either normal or accident condition temperature limits and that localized material damage at the point of arc on the shell of the overpack and transfer cask water jacket is bounded by accident conditions discussed in Sections 8.2.2 (tornado missile) and 8.2.11 (loss of shielding, HI-TRAC transfer cask water jacket). As a result of the considerations, it is apparent that the postulated transmission line break does not adversely affect the thermal performance of either system.

In addition to the 500-kV lines, the towers that support these lines were evaluated for any potential effect (Figure 2.2-1). They have been evaluated, and although the towers could fail as a result of a severe wind event, there would be no separation of the towers from their foundations, and the towers on the hillside would not have credible contact with the ISFSI storage site. However, the towers, which are located near the ISFSI storage site could, in these events, collapse and strike either the MPC while at the CTF or the loaded overpacks stored on the pads. As a result, as discussed in Section 8.2.16, this impact potential has been evaluated, and it does not adversely affect the MPC or the loaded overpacks.

2.2.2.2 Hazards from Fires

The ISFSI or the fuel storage systems have no credible exposure to fires caused by offsite transportation accidents, pipelines, or manufacturing facilities because of the distance to these transportation routes and the lack of facilities in the proximity of the site. However, there are onsite sources that were evaluated.

Fires are classified as human-induced or natural phenomena design events in accordance with ANSI/ANS 57.9, Design Events III and IV (Reference 3). To identify sources and to establish a conservative design basis for onsite exposure, a walkdown was performed of the CTF, ISFSI storage site, and the complete transportation route from the FHB/AB to the CTF and ISFSI storage site. Based on that walkdown, the following fire events are postulated:

(1) Onsite transporter fuel tank fire

(2) Other onsite vehicle fuel tank fires

(3) Combustion of other local stationary fuel tanks

(4) Combustion of other local combustible materials

(5) Fire in the surrounding vegetation

The potential for fire is addressed for both the HI-STORM 100 overpack and the HI-TRAC transfer cask. Locations where the potential for fire is addressed include the ISFSI storage pad; the area immediately surrounding the ISFSI storage pad, including the CTF; and along the transport route between DCPP and the ISFSI storage pad. These design-bases fires and their evaluations are detailed in Section 8.2.5.

For the evaluation of the onsite transporter and other onsite vehicle fuel tank fires (Events 1 and 2), it is postulated that the fuel tank is ruptured, spilling all the contained fuel, and the fuel is ignited. The fuel tank capacity of the onsite transporter is limited to a maximum of 50 gallons of fuel. The maximum fuel tank capacity for other onsite vehicles in proximity to the transport route and the ISFSI storage pads is assumed to be 30 gallons. Any transient sources of fuel in larger volumes, such as tanker trucks, will be administratively controlled to provide a sufficient distance from the ISFSI storage pads (at all times), the CTF (while transferring an MPC), and the transport route during the cask transport. As discussed in Section 8.2.5, the results of analyses indicate that neither the storage cask nor the transfer cask undergoes any structural degradation and that only a small amount of shielding material (concrete and water) is damaged or lost. This analysis bounds the 30-gallon onsite vehicle fuel tank fire (Event 2).

All onsite stationary fuel tanks (Event 3) are at least 100 ft from the nearest storage cask, the transport route, and the CTF (Figure 2.2-1). Therefore, there is at least a 100-ft clearance between combustible fuel tanks and the nearest cask in transport, at the CTF, or on the ISFSI storage pads. These existing stationary tanks have been evaluated, but due to their distances to the transport route or the storage pads, the total energy received by the storage cask or the transporter is insignificant compared to the design basis fire event.

No combustible materials will be stored within the security fence around the ISFSI storage pads at any time. In addition, prior to any cask operation involving fuel transport, a walkdown of the general area and transportation route will be performed to assure all local combustible materials (Event 4), including all transient combustibles, are controlled in accordance with administrative procedures.

The native vegetation surrounding the ISFSI storage pad is primarily grass, with no significant brush and no trees. Maintenance programs will prevent uncontrolled growth of the surrounding vegetation. As discussed in Section 8.2.5, a conservative fire model was established for evaluation of grass fires, which has demonstrated that grass fires are bounded by the 50-gallon transporter fuel tank fire evaluation.

In summary, as discussed in Section 8.2.5, the potential effects of any of these postulated fires have been found to be insignificant or acceptable. The physical layout of the Diablo Canyon ISFSI and the administrative controls on fuel sources ensure that the general design criteria related to fire protection specified in 10 CFR 72.122(c) are met (Reference 4).

2.2.2.3 Onsite Explosion Hazards

The storage site has no credible exposure to explosion caused by transportation accidents, pipelines, or manufacturing facilities because of the distance to these transportation routes and the lack of facilities in the proximity of the site. However, there are potential onsite hazards that must be evaluated.

Explosions are classified as human-induced or natural phenomena design events in accordance with ANSI/ANS 57.9 Design Events III and IV. To determine the potential explosive hazards, which could affect the ISFSI or the fuel transportation system, a walkdown of the ISFSI storage area and the transportation route from the FHB/AB was completed. The following explosion sources and event categories have been identified and evaluated in Section 8.2.6:

(1) Detonation of a transporter or an onsite vehicle fuel tank

(2) Detonation of a propane bottle transported past the ISFSI storage pad

(3) Detonation of an acetylene bottle transported past the ISFSI storage pad

(4) Detonation of large stationary fuel tanks in the vicinity of the transport route

(5) Detonation of mineral oil from the Unit 2 main bank transformers

(6) Explosive decompression of a compressed gas cylinder

(7) Detonation of the bulk hydrogen storage facility

(8) Detonation of acetylene bottles stored on the east side of the cold machine shop

Figure 2.2-1 shows the location of the stationary potential sources (sources 4, 5, 7, and 8). Events 1, 2, 3, and 6 are assumed to occur in the vicinity of the ISFSI storage pads, CTF, or transport route and potentially affect both the loaded overpack and the transfer cask. The assumed distance between the source of detonation and the nearest loaded overpack is 50 ft. This is based on: (a) no gasoline-powered vehicles being allowed within the ISFSI protected area, and (b) the minimum distance between the storage casks and the north side of the ISFSI protected area fence (where the road is) being 50 ft. Detonation sources in the vicinity of the CTF or transporter during fuel transportation or storage operations will be controlled by administrative procedures to provide sufficient distance. Events 4 through 8 occur in the vicinity of the transport route and affect only the transfer cask.

In all of the above evaluations, the effect on the loaded overpacks or transport cask is minimal, and there will be no loss of function. For Events 1 through 3, the size of the fuel tanks, number of cylinders, how they are transported, when they are transported, and the physical distance to the storage pads, CTF, or transporter are controlled by administrative procedures. For Event 4, the distance of the existing fuel tanks from the transportation route precludes any effect on the transportation of the spent fuel to the storage pads or CTF. Event 5 involves the mineral oil in the Unit 2 main bank transformers. The detonation of this oil is normally not considered credible because of its flash point. However, there is some potential for an electrical short or other ignition source to be the cause of ignition. As a result, this was evaluated as discussed in Section 8.2.6 and found to be risk insignificant based on Regulatory Guide 1.91 acceptance criteria. Event 6 concerns decompression of gas cylinders and the possible missile damage to the transfer cask and overpack. The evaluation performed in Section 8.2.6 shows that there would be no significant damage or loss of function by this event. Event 7 involves the transportation of the transfer cask past a potential hydrogen explosion hazard (Figure 2.2-1). Section 8.2.6 discusses the evaluation that was performed for this event. The evaluation shows that the probability of a detonation at the moment the transporter is in the vicinity is so small that it is not credible per the guidelines of Regulatory

Guide 1.91. Event 8 was evaluated, as discussed in Section 8.2.6, where it is shown that the number of acetylene bottles that would have to be stored on the east side of the cold machine shop and detonate to degrade the structural integrity of the transfer cask far exceeds the available bottle storage space.

The Cask Transportation Evaluation Program will be developed, implemented, and maintained to ensure that no additional hazards are introduced either at the storage pads, CTF, or on the transportation route during onsite transport of the loaded overpacks or transfer cask. That program will include limitation on hazards and will require a transportation route walkdown prior to any movement of the transporter with nuclear fuel between the FHB/AB and the CTF, and between the CTF and the storage pads. The walkdown will require the evaluation or removal of any identified hazards prior to the movement of the transporter. The program will also control all movement of vehicles or activities during onsite transport that could have an adverse effect on the loaded overpacks or transfer cask.

2.2.2.4 Chemical Hazards

A walkdown of all chemical hazards was performed in the ISFSI storage pad and CTF areas, and along the transportation route. Chemical hazards were identified that could have an effect on the ISFSI or the transportation system. To ensure minimum potential for chemical hazards, the administrative program provided to control fire and explosive hazards will also include identification, control, and evaluation of hazardous chemicals.

2.2.3 SUMMARY

In summary, there are no credible accident scenarios involving any offsite industrial, transportation, or military facilities in the area around the DCPP site that will have any significant adverse impact on the ISFSI. In addition, there are no potential onsite fires, explosions, or chemical hazards that would have a significant impact on the ISFSI.

2.2.4 REFERENCES

1. Regulatory Guide 1.91, Evaluations of Explosions Postulated to Occur on Transportation Routes near Nuclear Power Plants, US Nuclear Regulatory Commission, February 1978.

2. Standard Review Plan for the Review of Safety Analysis Reports for Nuclear Power Plants, USNRC, NUREG-0800, July 1981.

3. ANSI/ANS 57.9, 1992, Design Criteria for an Independent Spent Fuel Storage Installation (Dry Storage Type), American National Standards Institute.

4. 10 CFR 72, Licensing Requirements for the Independent Storage of Spent Nuclear Fuel and High-Level Radioactive Waste.

2.3 METEOROLOGY

The meteorology of the Diablo Canyon area is described in Section 2.3 of the DCPP FSAR Update. Information in the FSAR Update includes discussion of the regional climatology, local meteorology, topographical information, onsite meteorological measurement program, and diffusion estimates for the Diablo Canyon owner-controlled area, which includes the ISFSI site. Relevant tables and figures supporting the discussion are included in the FSAR Update.

Meteorological conditions for the ISFSI site are expected to be the same as for DCPP since the ISFSI site is located approximately 0.22 miles and slightly uphill from the DCPP facilities. No significant changes in climate or meteorological characteristics can occur within such a short distance and, thus, existing meteorological measurements for DCPP are expected to be equally applicable to the ISFSI. Diffusion estimates at the ISFSI site are provided in Section 2.3.4.

The FSAR Update is maintained up to date by PG&E through periodic revisions made in accordance with 10 CFR 50.71(e). Hence, the information contained in the FSAR Update is current, and no further revision is necessary for applicability to the ISFSI. Therefore, in accordance with the guidance of Regulatory Guide 3.62, material from Section 2.3 of the FSAR Update is incorporated herein by reference in support of the ISFSI license application. The following paragraphs provide a brief summary of various discussions from Section 2.3 of the FSAR Update.

2.3.1 REGIONAL CLIMATOLOGY

The climate of the area is typical of the central California coastal region and is characterized by small diurnal and seasonal temperature variations and scanty summer precipitation. The prevailing wind direction is from the northwest, and the annual average wind speed is about 10 mph. In the dry season, which extends from May through September, the Pacific high-pressure area is located off the California coast, and the Pacific storm track is located far to the north. Moderate to strong sea breezes are common during the afternoon hours of this season while, at night, weak offshore drainage winds (land breezes) are prevalent. There is a high frequency of fog and low stratus clouds during the dry season, associated with a strong low-level temperature inversion.

The mountains that extend in a general northwest-to-southeast direction along the coastline affect the general circulation patterns. This range of mountains is indented by numerous canyons and valleys, each of which has its own land-sea breeze regime. As the air flows along this barrier, it is dispersed inland by the valleys and canyons that indent the coastal range. Once the air enters these valleys and canyons, it is controlled by the local terrain features.

The annual mean number of days with severe weather conditions, such as tornadoes and ice storms at west coast sites, is zero. Thunderstorms and hail are also rare phenomena, the average occurrence being less than 3 days per year. The maximum-recorded precipitation in the San Luis Obispo region is 3.28 inches in 1 hour at the DCPP site, and 5.98 inches in 24 hours at San Luis Obispo. The 24-hour maximum and the 1-hour maximum occurred on March 4, 1978.

The maximum-recorded annual precipitation at San Luis Obispo was 54.53 inches during 1969. The average annual precipitation at San Luis Obispo is 21.53 inches. There are no fastest mile wind speed records in the general area of Diablo Canyon; surface peak gusts at 46 mph have been reported at Santa Maria, California, and peak gusts of 84 mph have been recorded at the 250 ft level at the Diablo Canyon site.

2.3.2 LOCAL METEOROLOGY

The average annual temperature at the ISFSI site is approximately 55°F (based on measurements made at the DCPP primary meteorological tower). Generally, the warmest mean monthly temperature occurs in October, and the coldest mean monthly temperature occurs in December. The highest hourly temperature, as recorded at one of the recording stations, is 97°F in October 1987, and Diablo Canyon experienced below-freezing temperatures in December 1990 for several hours. Essentially no snow or ice occurs at the ISFSI site.

Solar radiation data considered representative of the Diablo Canyon ISFSI site is collected by the California Irrigation Management Information System (CIMIS), Department of Water Resources, at the California Polytechnic State University in San Luis Obispo, California. The CIMIS collection site is about 12 miles northeast of the Diablo Canyon ISFSI site. For a period of record between May 1, 1986 and December 31, 1999, the maximum measured incident solar radiation (insolation) values at the CIMIS site were 766 g-cal/cm^2 per day for a 24-hour period and 754 g-cal/cm^2 per day for a 12-hour period, both on June 1, 1989. The daily (24-hour) average for the period of record was 430 g-cal/cm^2 per day. For the Diablo Canyon ISFSI site, the insolation values would likely be lower than the CIMIS values because of more frequent fog in the ISFSI area.

The average annual precipitation in the area is approximately 16 inches. The highest monthly total recorded between 1967 and 1981 was 11.26 inches. The greatest amount of precipitation received in a 24-hour period was 3.28 inches. These maxima were recorded in January 1969 and March 1978, respectively. The maximum hourly amount recorded in the Diablo Canyon area during the same period is 2.35 inches.

The highest recorded peak wind gust at the primary meteorological tower is 84 mph, and the maximum-recorded hourly mean wind speed is 54 mph. Persistence analysis of wind directions in the Diablo Canyon area shows that, despite the prevalence of the marine inversion and the northwesterly wind flow gradient along the California coast, the long-term accumulation of emissions in any particular geographical area downwind is virtually impossible. Pollutants injected into the marine inversion layer of the coastal wind regime are transported and dispersed by a complex array of land-sea breeze regimes that exist all along the coast wherever canyons or valleys indent the coastal range.

Topographical influences on both short-term and long-term diffusion estimates are pronounced in that the ridge lines east of the ISFSI location extend at least to the average height of the marine inversion base. The implications of this barrier are:

(1) Any material released that is diverted along the coastline will be diluted and dispersed by the natural valleys and canyons, which indent the coastline.

(2) Any material released that is transported over the ridgeline will be distributed through a deep layer because of the enhanced vertical mixing due to topographic features.

2.3.3 ONSITE METEOROLOGICAL MEASUREMENT PROGRAM

The current onsite meteorological monitoring system supporting DCPP operation will serve as the onsite meteorological measurement program for the ISFSI. The system consists of two independent subsystems that measure meteorological conditions and process the information into useable data. The measurement subsystems consist of a primary meteorological tower and a backup meteorological tower. The program has been designed and continually updated to conform with Regulatory Guide 1.23.

A supplemental meteorological measurement system is also located in the vicinity of DCPP. The supplemental system consists of two Doppler acoustic sounders and six tower sites. Data from the supplemental system are used for emergency response purposes to access the location and movement of any radioactive plume.

2.3.4 DIFFUSION ESTIMATES

For ISFSI dose calculations required by 10 CFR 72.104, (normal operations and anticipated occurrences), site boundary χ/Q values range from 9.2×10^{-8} to 3.4×10^{-6} sec/m^3 and nearest residence χ/Q values range from 2.0×10^{-8} to 4.2×10^{-7} sec/m^3. These values are taken from Table 11.6-13 of the DCPP FSAR Update and have been determined to be applicable to the ISFSI site. They will be used, as appropriate, for dose calculations related to normal operations and anticipated occurrences.

Compliance with 10 CFR 72.106 requires calculation of design basis accident doses at the controlled area boundary (site boundary for the Diablo Canyon ISFSI), which is about 400 meters from the ISFSI at its closest point. Based on information from the DCPP FSAR Update, Section 2.3.4 and Table 2.3-41, a χ/Q of 4.5×10^{-4} sec/m^3 has been determined to be a conservative estimate applicable to the ISFSI site and will be used for accident dose calculations.

2.4 SURFACE HYDROLOGY

Hydrologic information pertaining to the Diablo Canyon area in general has been documented in the DCPP FSAR Update. Much of this information pertains also to the ISFSI location since the hydrologic characteristics in the Diablo Canyon area do not vary significantly in the general vicinity of the ISFSI and power plant facilities. Specific features relevant to hydrologic engineering at the ISFSI location are described in this section, with reference to supporting information in the FSAR Update where appropriate.

2.4.1 HYDROLOGIC DESCRIPTION

The topography and an outline of the drainage basin in the region surrounding the ISFSI site are shown in Figure 2.4-1. This map is reproduced from the US Geological Survey (USGS) Port San Luis and Pismo Beach 7.5-minute topographic quadrangles. The basin drains to Diablo Creek, which discharges into the Pacific Ocean. Figure 2.4-2 shows the Diablo Creek drainage basin to a larger scale. The basin encompasses approximately 5 square miles and is bounded by ridges reaching a maximum elevation of 1,819 ft above mean sea level (MSL) at Saddle Peak, located approximately 2 miles to the east of the ISFSI.

The hydrologic characteristics of the ISFSI site are influenced by the Pacific Ocean on the west and by local storm runoff collected from the basin drained by Diablo Creek. The maximum and minimum flows in Diablo Creek are highly variable. Average flows tend to be nearer the minimum flow value of 0.44 cfs. Maximum flows reflect short-term conditions associated with storm events. Usually within 1 or 2 days following a storm, flows return to normal. Flows during the wet season (October-April) vary daily and monthly. Dry season flows are sustained by groundwater seepage and are more consistent from day to day, tapering off over time. There is no other creek or river within the site area or the drainage basin.

Water is supplied to DCPP from three sources: Diablo Creek, two site wells, and an ocean water desalinization plant that has been used since 1985. The Diablo Creek collection point is located upstream and to the east of the 500-kV switchyard.

2.4.2 FLOODS

The DCPP FSAR Update addresses flood considerations pertinent to the power plant facilities at Diablo Canyon. The following discussion identifies flood considerations from the FSAR Update that are pertinent to the ISFSI location. Topography and ISFSI site structures limit flood design considerations to local floods from Diablo Creek. The canyon confining Diablo Creek will remain intact and is more than sufficient to channel any conceivable flood without any hazard to the ISFSI. Channel blockage from any landslides downstream of the ISFSI location and to an extent sufficient to flood the ISFSI area is not possible because of the topographic location and elevation of the ISFSI.

There are no dams or natural features in Diablo Creek that would hinder or retain runoff for a significant period of time. At the ISFSI, runoff can be efficiently drained by the adjacent natural and constructed drainage features.

If the culverts and drainage out of the ISFSI area become plugged during periods of high precipitation, water may locally and temporarily pond. Drainage in the vicinity of the ISFSI is shown in Figure 2.4-3. No significant ponding should occur since, due to the open terrain and location, any additional runoff into the ISFSI area will drain away from the facility toward Diablo Creek or the ocean. No adverse impact is expected on ISFSI operation or spent fuel confinement.

Two water reservoirs constructed in rock and located in the vicinity of the ISFSI maintain redundant water supplies in support of operation of Units 1 and 2. If the reservoirs were to overflow due to an unlikely accumulation of runoff from high precipitation, the local topography would cause water to drain toward the creek and ocean. No adverse impact on the ISFSI would be expected from overflow of the reservoirs.

2.4.3 PROBABLE MAXIMUM FLOOD (PMF) ON STREAMS AND RIVERS

Diablo Creek is the only significant channel for the drainage basin within which the ISFSI is located. This drainage basin includes approximately 5.2 square miles. The potential PMF upstream of the location of the power plant facilities was found to have a peak discharge of approximately 6,900 cfs, with a total volume of approximately 4,300 acre-ft for a 24-hour storm.

As documented in the DCPP FSAR Update, the drainage capacity of Diablo Creek through this area is more than sufficient to efficiently channel the PMF volume directly into the Pacific Ocean with no retention time. This volume of water discharged from the Diablo Creek basin will not cause any local flooding around the power plant or overtop the switchyards, even if the 10-ft diameter culvert passing under the switchyards were to temporarily plug. If the culvert were plugged, any water impounded east of the 500-kV switchyard would be discharged along Diablo Creek Road (elevation of approximately 250 ft MSL opposite the ISFSI) and through the stilling basin located between the switchyards. The floodwaters would pass through the diversion scheme with adequate freeboard near each switchyard, on the opposite side of the canyon, and below the elevation of the ISFSI (310 ft MSL). The water released would not cause any flooding of the ISFSI.

2.4.4 POTENTIAL DAM FAILURES (SEISMICALLY INDUCED)

There are no dams in the watershed area. Outside the watershed area, any seismic-induced failure of dams would not affect the ISFSI.

2.4.5 PROBABLE MAXIMUM SURGE AND SEICHE FLOODING

Due to the elevation of the ISFSI, there is no credible scenario that would create any flooding from a maximum surge or seiche.

2.4.6 PROBABLE MAXIMUM TSUNAMI FLOODING

Due to the elevation of the ISFSI, a maximum tsunami would not cause any flooding to the ISFSI.

2.4.7 ICE FLOODING

Flooding due to ice melt events is not credible because of the mild climate and infrequency of freezing temperatures in the region.

2.4.8 FLOOD PROTECTION REQUIREMENTS

No cooling water canals, reservoirs, rivers or streams are used in operation of the ISFSI. There are no channel diversions in the region that can alter any water flow patterns so as to affect the ISFSI. Hence, low flow conditions need not be considered.

Based on these considerations, there are no credible hydrological scenarios that can adversely affect the ISFSI. Thus, specialized hydrological engineering considerations and flood protection requirements for the ISFSI facilities are not necessary. Only typical grading and drainage provisions for storm runoff are needed.

2.4.9 ENVIRONMENTAL ACCEPTANCE OF EFFLUENTS

SAR Section 3.3.1.7.2 indicates that there are no radioactive wastes created by the HI-STORM 100 System while in storage at the storage pads, transport to or from the CTF, or at the CTF.

Environmental Report Sections 2.5, 4.1, and 4.2 address the environmental effects of potential effluents from the ISFSI. It is concluded that surface runoff from the ISFSI has no radioactive contamination and will not adversely affect the surrounding ecosystem.

Diablo Creek is the only source of surface water other than ocean water used at DCPP for support of power plant operation. No water is used to support ISFSI operation. Potable water used to support ISFSI administration is provided by existing systems at DCPP. Such support of ISFSI administrative activities will be provided according to plant procedures. No other significant surface or groundwater sources exist or are used in this area. There is no public use of any surface waters or groundwater from the Diablo Canyon site. Therefore, no detailed analysis of acceptance of effluents by surface waters or groundwater due to ISFSI operation is relevant.

2.5 SUBSURFACE HYDROLOGY

This section is based on information provided in the DCPP FSAR Update and recent geotechnical investigations performed to characterize the ISFSI, CTF, and transport route.

2.5.1 GROUNDWATER IN DCPP AREA

Groundwater in the DCPP area is found in the narrow, relatively thin gravel alluvium along Diablo Creek, in fractures in the bedrock of the Obispo Formation, and along the contact that marks the top of bedrock and the base of some of the extensive terrace deposits that flank the coast. Two seeps and a small spring were encountered during excavations for the power plant.

The main groundwater table beneath the coastal terrace north and south of the power plant is controlled by sea level at the coastline and gradually rises beneath the hills southeast of the power plant. Hence, this water table beneath the power plant and the ISFSI is about the elevation of Diablo Creek, sloping upward from sea level at the coast to 200 ft above the 500-kV switchyard.

Groundwater in the alluvium of Diablo Creek is documented from the makeup water wells. Makeup water wells No. 1 and No. 2 with collar elevations at 232 ft above mean sea level (MSL) and 329 ft MSL, respectively, produce water from the alluvium in Diablo Creek and from fractured sandstone and dolomite of the Obispo formation. The water table varies, depending on the month of the year, but is generally controlled by flows in the alluvium near elevation 200 ft MSL.

Groundwater above the base of the thick terrace deposits is recorded in several places. On the terrace north of Diablo Creek, monitoring wells MW-1 through MW-4 (collar elevations range between 115 and 210 ft MSL) at the closed waste holding pond showed water levels in 1985 at elevations between 64 and 127.5 ft MSL. In parking lot 7, south of DCPP, two piezometers in 1996 and 1997, recorded groundwater at a depth of 40 to 77 ft and recording a perched water table near the top of the wave-cut bedrock platform. Groundwater seeps also issue from a perched water table on the marine terrace platform (about 30 ft MSL) in Patton Cove. Local perched water tables also occur within the Obispo Formation above the marine bedrock platforms. These perched water tables occur on impermeable strata, such as clay beds, within the Obispo Formation. An example is the small spring that issues from the hillslope above and east of Patton Cove at elevation about 600 ft MSL. A few areas of dense vegetation indicative of seeps also issue from bedrock along the lower canyon walls of Diablo Creek below the raw water reservoir.

2.5.2 GROUNDWATER AT ISFSI

As discussed above, groundwater beneath the ISFSI site is controlled by the elevation of water in Diablo Creek that is at about elevation 100 ft MSL opposite the ISFSI. This is at least 190 ft below the ISFSI pads, which are at elevation 310 ft MSL.

Clay beds beneath the ISFSI could impede groundwater infiltration and form temporary perched water tables during the rainy season. In all but one of the 15 borings drilled at and near the ISFSI site, no evidence of a perched water table was found during drilling. Typically the clay beds in the core were moist, but not saturated, indicating no perched water at the time of drilling. However when boring 01-F was being drilled on the slope above the ISFSI a rainstorm soaked the Diablo Canyon area in the night. The next morning clear water was observed issuing from the borehole that was 29 ft deep, but the flow stopped and was at 6.5 ft deep by the time the drilling was started; analysis of the boring shows a very thin clay on bedding at 6.8 ft but other clay beds are deeper than 29 ft. These data confirm that temporary perched water can accumulate locally in the slope above less permeable beds (Reference 1, Data Report B). In addition the dense vegetation, indicative of moist rock, is 20 to 30 ft above Diablo Creek in the lower canyon wall north of the ISFSI. This and other seeps are evident in the upper canyon wall north of the ISFSI site mark perched water seeping out above impermeable beds.

2.5.3 GROUNDWATER AT CTF

Groundwater levels below the CTF are near the elevation of Diablo Creek, at elevation 100 ft MSL, as described in Section 2.5.2. This is at least 190 ft below the CTF, which is at elevation 310 ft MSL.

2.5.4 GROUNDWATER ALONG TRANSPORT ROUTE

The main groundwater levels beneath the transport route are controlled by the elevation of water in Diablo Creek (25 to 75 ft MSL) near DCPP and the ISFSI and by sea level along the coastal terrace. Estimated groundwater levels beneath the transport route are as follows:

Plant View and Shore Cliff Roads - The route crosses the lower marine terraces and the regional groundwater table probably is slightly above sea level and is more than 50 to 100 ft below the roadway. In places, a perched groundwater table occurs, locally above the contact between the bedrock and the overlying marine terrace. This perched water is 30 to over 50 ft below the roadway.

Reservoir Road - The route generally follows the hillside where the road has been cut into dolomite and sandstone bedrock of the Obispo Formation. The strata dips into the hillslope away from the road. The regional groundwater in this area lies near the same elevation (about 100 ft MSL) as beneath the ISFSI site (Section 2.5.2), some 50 to 140 ft below the roadway. The clay beds in the sandstone bedrock may become temporary groundwater barriers that slow the percolation of water through the fractured rock of the slope, but these beds dip into the slope away from the road and no seeps indicative of perched water are known along this part of the slope.

2.5.5 GROUNDWATER SUMMARY

Based on available information, groundwater quality or quantity is not expected to be affected by construction or operation of the ISFSI, CTF, or access road. Construction and operation of the ISFSI does not involve the use of groundwater, and there is no public use of onsite groundwater. The occurrence of temporary perched water over clay beds in the dolomite and sandstone bedrock that underlie the slopes above the ISFSI and the transport route has no adverse effects on the ISFSI or the transport route because any potential effect will be mitigated by drains in the proposed cutslopes above the ISFSI, or other means as described in Section 4.2.1.1.9.

2.5.6 REFERENCES

1. Geologic Data Reports A through K, William Lettis & Associates, December 2001.

2.6 GEOLOGY AND SEISMOLOGY

The Diablo Canyon Independent Spent Fuel Storage Installation (ISFSI) will be located directly inland from the power plant on a graded bedrock hillslope adjacent to the DCPP raw water reservoir (Figure 2.6-1). It was desirable to select a site having bedrock properties and earthquake response characteristics comparable to those of the bedrock beneath the Diablo Canyon power block, such that existing DCPP design-basis ground motions could be used in the design of the ISFSI.

In this section, the geologic and seismologic conditions in the region are described and evaluated. Detailed information is provided regarding the earthquake vibratory ground motions, foundation characteristics, and slope stability at the ISFSI and CTF sites. Information regarding foundation characteristics and slope stability also is provided for the transport route between the power block and the CTF. The information is in compliance with the criteria in Appendix A of 10 CFR 100, and 10 CFR 72.102, and meets the format and content recommendations of Regulatory Guide 3.62. Several commercial technical computer software programs were used to assist in the analyses performed for Section 2.6.

An external, independent Seismic Hazards Review Board advised on the studies carried out for this section of the licensing submittal. A letter summarizing the conclusions of the consulting board is provided in Reference 1, as are the names and affiliations of the project team responsible for preparation of this section.

Definitions

For the purposes of Section 2.6, the following definitions and boundaries were used to describe the ISFSI study area and plant site region, as illustrated on Figure 2.6-1 (definitions of other terms used in this report are in the glossary at the front of the report):

- plant site region: the area of the Irish Hills and vicinity within a 10-mile radius of the Diablo Canyon ISFSI
- plant site area: the area within the DCPP boundary
- ISFSI study area: the area extending along the nose of the ridge behind the power plant and encompassing the ISFSI site and CTF site

Conclusions

Geologic, seismologic, and geotechnical investigations for the ISFSI yielded the following conclusions:

- The ISFSI will be founded on bedrock that is part of the same continuous, thick sequence of sandstone and dolomite beds upon which the DCPP power block is sited.

The shear wave velocity characteristics of the rock at the ISFSI and CTF sites are within the same range as those at the power block. Additionally, the ISFSI and CTF sites are approximately the same distance from the Hosgri fault zone, the controlling earthquake source for the DCPP. Thus, the foundation conditions and ground-motion response characteristics are the same as those at the DCPP (discussed in Section 2.6.1.10).

- Because the ground-motion response characteristics at the ISFSI are the same as those at the DCPP, the DCPP earthquake ground motions are appropriate for use in the licensing of the ISFSI, in accordance with 10 CFR 72.102(f) (discussed in Section 2.6.2).

- Because ISFSI pad sliding, slope stability, and the stability of the transporter are affected by longer-period ground motions than those characterized by the DCPP ground motions, response spectra having a longer-period component were developed. The longer-period component conservatively incorporates the near-fault effects of fault rupture directivity and fling. These spectra, referred to as the ISFSI long-period ground motions (ILP), and associated time histories, were used to analyze elements that may be affected by longer-period ground motions (discussed in Section 2.6.2.5).

- Several minor bedrock faults were observed at the ISFSI and CTF sites. These minor faults are not capable; hence, there is no potential for surface faulting at the ISFSI or CTF sites (discussed in Section 2.6.3).

- The sandstone and dolomite bedrock, including zones of friable rock, that underlies the ISFSI and CTF sites area is stable, and has sufficient capacity to support the loads imposed by the ISFSI pads and casks and the CTF without settlement or differential movement (discussed in Section 2.6.4).

- There are no active landslides or other evidence of existing ground instability at the ISFSI and CTF sites, or on the hillslope above the ISFSI site (discussed in Section 2.6.1.12).

- The stability of the hillslope and the slopes associated with the pads, CTF, and transport route under static and seismic conditions was analyzed using conservative assumptions regarding slope geometry, material properties, seismic inputs, and analytical procedures (discussed in Section 2.6.5). The analyses show that the slopes have ample factors of safety under static conditions. The cutslope above the ISFSI site may experience local wedge movements or small displacements if exposed to the design-basis earthquakes. Mitigation measures to address these movements are described in Sections 4.2.1.1.9.1 and 4.2.1.1.9.2.

- The transport route follows existing paved roads, except for a portion of the route that will be constructed to avoid a landslide at Patton Cove along the coast. The route will have foundation conditions satisfactory for the transporter (discussed in Section 4.3.3). Small debris flows could potentially close portions of the road during or immediately following severe weather (discussed in Section 2.6.5.4). Because the transport route will not be used during severe weather, the flows will not be a hazard to the transporter.

2.6.1 GEOLOGIC, SEISMOLOGIC AND GEOTECHNICAL INVESTIGATIONS

Extensive geologic, seismologic and geotechnical investigations were performed to characterize the ISFSI and CTF sites. These investigations included compilation and review of pre-existing information developed for construction of the power plant, the raw water reservoir, and the 230-kV and 500-kV switchyards, as well as extensive detailed investigations performed in the ISFSI study area. These investigations are described in References 2 and 3. The investigations focused on collecting information to address four primary objectives:

- to evaluate foundation properties beneath the ISFSI pads, the CTF facility, and the transport route

- to evaluate the stability of the proposed cutslopes and existing hillslope above the ISFSI pads and along the transport route

- to identify and characterize bedrock faults at the site

- to compare bedrock conditions at the ISFSI site with bedrock conditions beneath the DCPP power block for the purpose of characterizing earthquake ground motions

Investigations in the plant site area included interpretation of aerial photography, review of existing data and literature, and field reconnaissance. In particular, borehole and trench data collected in the 1960s and 1970s for the power plant were compiled, reviewed, and used to evaluate stratigraphic conditions beneath the power block and between the power block and the ISFSI site.

Investigations in the ISFSI study area and along the transport route were conducted to develop detailed information on the lithology, structure, geometry, and physical properties of bedrock beneath the ISFSI and CTF sites, and beneath the transport route. Investigations of the ISFSI and CTF site geology included 17 borings at 14 locations, 22 trenches and test pits, a seismic refraction survey, down-hole geophysics and televiewer surveys, petrographic analysis of rock samples, laboratory analysis of soil and rock properties, and detailed surface mapping (Reference 3). These data were used to develop a detailed geologic map of the plant site area, the ISFSI study area and transport route, and 12 geologic cross sections to illustrate the subsurface distribution of bedrock lithology and structure (Reference 2, Attachment 16).

2.6.1.1 Existing Geologic, Seismologic, and Geotechnical Information

Existing geologic, seismologic, and geotechnical information includes that collected for licensing the operating DCPP, construction of the raw water reservoir, and construction of the 230-kV and 500-kV switchyards. Regional and site-specific geologic, seismologic and geotechnical investigations at the DCPP site are documented in Sections 2.5.1 and 2.5.2 of the DCPP Final Safety Analysis Report (FSAR) Update, submitted in support of continued operation of Units 1 and 2 (Reference 4). In response to License Condition Item 2.C.(7) of the Unit 1 Operating License DPR-80, issued in 1980, PG&E was required to reevaluate the seismic design bases for the DCPP. This reevaluation became known as the Long Term Seismic Program (LTSP). The program was conducted between 1985 and 1991. In June 1991, the Nuclear Regulatory Commission (NRC) issued Supplement Number 34 to the Diablo Canyon Safety Evaluation Report (Reference 5), in which the NRC concluded that PG&E had satisfied License Condition Item 2.C.(7). The LTSP evaluations are docketed in the LTSP Final Report (Reference 6) and the Addendum to the Final Report (Reference 7). The information presented herein summarizes and refers to the DCPP FSAR Update and LTSP reports.

Existing regional and site-specific geologic, seismologic and geotechnical information for the ISFSI is discussed in the following docketed references:

Regional physiography:	DCPP FSAR Update, Section 2.5.1.1.1
Geologic setting:	DCPP FSAR Update, Section 2.5.1.1.2.1 LTSP Final Report, Chapter 2
Tectonic features:	DCPP FSAR Update, Sections 2.5.1.1.2.2 and 2.5.1.1.2.3 LTSP Final Report, Chapter 2
Geologic history:	DCPP FSAR Update, Section 2.5.1.1.3 LTSP Final Report, Chapter 2
Regional geologic structure and stratigraphy:	DCPP FSAR Update, Sections 2.5.1.1.4 and 2.5.1.1.5 LTSP Final Report, Chapter 2
Geologic structure and stratigraphy of the plant site area:	DCPP FSAR Update, Section 2.5.1.2 LTSP Final Report, Chapter 2
Slope stability of the plant site area:	Slope Stability Report

Earthquake history and association of earthquakes with geologic structures:	DCPP FSAR Update, Sections 2.5.2.5 and 2.5.2.6 LTSP Final Report, Chapter 2
Maximum earthquakes affecting the plant site area:	DCPP FSAR Update, Section 2.5.2.9 LTSP Final Report, Chapter 3
Earthquake ground accelerations and response spectra:	DCPP FSAR Update, 2.5.2.10 and 3.71 LTSP Final Report, Chapter 4

The ISFSI is sited on a bedrock slope that was previously used as a source of fill materials for construction of the 500-kV and 230-kV switchyards. The first geologic and geotechnical studies in the area were performed by Harding Miller Lawson & Associates (HML) (Reference 8). The study was conducted prior to the borrow excavation to obtain information regarding the excavatability and suitability of the site materials for switchyard fills. Their investigations included borings, test pits, and refraction surveys. The depth of their explorations, however, was limited to the depth of the planned (and as-built) borrow excavation, and did not extend below the present post-excavation site elevations. All the material investigated by HML was removed during the borrow excavation and used for construction of the switchyard fills.

In addition, an assessment of slope stability near the DCPP was performed following the heavy winter storms of 1996-1997 (Reference 9). This report includes a map of landslides in the plant site area, and a slope stability analysis of the natural hillslope and cutslope between the power plant and the ISFSI.

2.6.1.2 Detailed ISFSI Study Area Investigations

Additional detailed geologic, seismic, and geotechnical studies were performed in the ISFSI study area. References 2 and 3 further describe the method, technical approach, and results of the detailed studies. The following field, office, and laboratory investigations were performed:

Activity	Documented in
Interpretation of 1968 aerial photography, by PG&E Geosciences Department (Geosciences) and William Lettis & Associates, Inc. (WLA)	Reference 2, Attachment 16
Evaluation of previous geologic investigations in the power plant area, including borings by HML and others, by Geosciences and WLA	Reference 2, Attachment 16
Detailed geologic mapping of structures and lithology, by Geosciences and WLA	Reference 2, Attachment 16

Activity	Documented in
Analysis of rock mass strength, by Geosciences and WLA	Reference 2, Attachment 16
Evaluation of rock fractures, by Geosciences and WLA	Reference 2, Attachment 16
Analysis of potential rock slope stability, by Geosciences, WLA, and Geomatrix Consultants	Reference 2, Attachments 17, 18, 20, 21, 23
Geologic mapping of the power plant site and ISFSI study area, by WLA	Reference 3, Data Report A
Drilling and logging of 17 exploratory diamond-core borings at 14 locations at and near the ISFSI and CTF sites, by WLA	Reference 3, Data Report B
Implementation of two surface seismic refraction lines to measure compressional wave and shear wave velocities of shallow bedrock across the ISFSI site, by GeoVision	Reference 3, Data Report C
Suspension logging of compression and shear wave velocities from boreholes 98BA-1, -3 and -4, by GeoVision	Reference 3, Data Report C
Excavation and logging of 22 exploratory trenches at 14 locations to expose bedrock structures and lithology at the ISFSI site, by WLA	Reference 3, Data Report D
Natural gamma and caliper logging of borings 00BA-1 and -2, and optical televiewer imaging of all borings drilled in 2000 and 2001, by NORCAL Geophysical Consultants	Reference 3, Data Report E
Compilation of discontinuity data, by WLA	Reference 3, Data Report F
Soil testing of clay beds, by Cooper Testing Laboratories	Reference 3, Data Report G
Characterization of rock mass strength, by WLA	Reference 3, Data Report H
Rock strength testing of representative core samples, by GeoTest Unlimited	Reference 3, Data Report I
Petrographic analyses and x-ray diffraction testing of rock samples, by Spectrum Petrographics, Inc.	Reference 3, Data Report J
X-ray diffraction testing and petrographic analysis of clay beds, by Schwein/Christensen Laboratories, Inc.	Reference 3, Data Report K

2.6.1.3 General Description of the ISFSI Study Area

The location and topography of the ISFSI and CTF sites and the transport route are shown in Figures 2.6-1, 2.6-2, and 2.6-3. Detailed investigations of the seismotectonic setting performed for the LTSP (LTSP Final Report, Chapter 2) show that the plant site area lies along the active tectonic boundary between the Pacific and North American plates in coastal Central California. It is located within the San Andreas fault system, about 48 miles west of the main San Andreas fault, and about 3 miles east of the offshore Hosgri fault zone. Current tectonic activity in the region is dominated by active strike-slip faulting along the Hosgri fault zone, and reverse faulting within the Los Osos/Santa Maria domain. The plant site area is on a structural subblock of the San Luis Range (the Irish Hills subblock, Figure 2.6-4), bordered on the northeast and southwest by the Los Osos and southwestern boundary zone reverse faults, respectively, and on the west by the Hosgri fault zone (LTSP Final Report, Chapter 2, Figure 2-50). Since the end of the early Quaternary, the Irish Hills subblock has been slowly elevated along these bounding faults. Detailed mapping and paleoseismic investigations performed for the LTSP (LTSP Final Report) and the DCPP FSAR Update, Section 2.5.1 show that no capable faults are present within the plant site area.

Within the Irish Hills structural subblock, the principal geologic structure is the northwest-trending Pismo syncline (termed the San Luis-Pismo syncline in the DCPP FSAR Update, Section 2.5.1.1.5.2). This 20-mile-long regional structure deforms rocks of the Miocene Monterey and Obispo formations, and the Pliocene Pismo Formation. Fold deformation occurred primarily during the Pliocene, and ceased sometime in the late Pliocene or early Quaternary. Detailed mapping of Quaternary marine terraces across the axis and flanks of the syncline during the LTSP (LTSP Final Report, Plates 10 and 12) documents the absence of fold deformation and associated faulting within the Irish Hills structural subblock for at least the past 500,000 to 1,000,000 years (LTSP Final Report, page 2-34).

The plant site area is situated on the eroded southwestern limb of the Pismo syncline (Figure 2.6-4), within Miocene bedrock of the Obispo Formation (Figure 2.6-5). This regional structure has subsidiary folds that are hundreds to 10,000 ft long and hundreds of feet wide (DCPP FSAR Update, Section 2.5.1.1.5.2, p. 2.5-19, -20). One of these structures, a small northwest-trending syncline, is located directly northeast of the power block (DCPP FSAR Update, Section 2.5.1.2.4.2, p. 2.5-32, -33, Figure 2.5-8). This is the same small syncline that extends across the western part of the ISFSI site (Figures 2.6-5, 2.6-6, and 2.6-7).

Along the coast, the Obispo and Monterey formations have been eroded and incised by former high stands of sea level, leaving a preserved sequence of marine terraces and terrace remnants (Figures 2.6-2 and 2.6-7). The foundation for the power block was excavated into rock below the lower two marine terraces, which are approximately 80,000 and 120,000 years old, respectively (LTSP Final Report, Chapter 2). The power block is founded on competent sandstone and siltstone of the Obispo Formation, the same stratigraphic unit that underlies the ISFSI site.

The ISFSI will be on a prominent ridge directly south of the raw water reservoir and east of the DCPP (Figures 2.6-7 and 2.6-8). The ridge area was used formerly as a borrow source to derive fill material for construction of the 230-kV and 500-kV switchyards. The borrow excavation, completed in 1971, removed up to 100 ft of material from the ISFSI site area and extended deep into bedrock (Figures -2.6-2, 2.6-3, and 2.6-9 through 2.6-12). As a result, the ISFSI and CTF facilities will be founded on bedrock, and the foundation stability and seismic response will be controlled by the bedrock properties. The borrow area cutslope is 900 by 600 ft in plan view, and 300 ft high. The slope of the cut face varies between 2.5:1 and 4:1 (22 to 14 degrees). The former borrow activity at the site stripped surficial soil and weathered rock from the hillside above the ISFSI site, leaving a bedrock slope covered with a veneer of rock rubble. The proposed cutslopes south of the ISFSI pads will be cut entirely in bedrock.

The ISFSI site will be accessed via the transport route, which will follow existing paved roads, except where the road is routed inland from Patton Cove. The transport route starts at the power block, and ends at the ISFSI (Figures 2.6-1, 2.6-3, and 2.6-7).

2.6.1.4 Stratigraphy

2.6.1.4.1 Plant Site Area Stratigraphy

The plant site area is underlain by bedrock of the early and middle Miocene Obispo Formation, and middle Miocene diabase intrusions (References 10 and 6, Chapter 2). Geologic studies for the original DCPP FSAR Update classified bedrock at the power plant site as strata from the middle and late Miocene Monterey Formation. Subsequent studies published by the U.S. Geological Survey (Reference 10), and conducted during the LTSP (LTSP Final Report, Chapter 2) and this ISFSI study reclassified most of the bedrock in the plant site area as part of the Obispo Formation.

Hall and others (Reference 10) divided the Obispo Formation into two members: a fine-grained, massively bedded, resistant zeolitized tuff (mapped as Tor), and a thick sequence of interbedded marine sandstone, siltstone, and dolomite (mapped as Tof) (Figures 2.6-6 and 2.6-7). During the current geologic investigations, the marine sedimentary deposits were further divided into three units, a, b, and c, based on distinct changes in lithology. Unit Tof_a occurs in the eastern part of the plant site area (entirely east of the ISFSI study area) and consists primarily of thick to massively bedded diatomaceous siltstone and tuffaceous sandstone. Unit Tof_b occurs in the central and west-central part of the plant site area, including the entire ISFSI study area and beneath the power block, and consists primarily of medium to thickly bedded dolomite, dolomitic siltstone, dolomitic sandstone, and sandstone. Unit Tof_c occurs in the western part of the plant site area and consists of thin to medium bedded, extensively sheared shale, claystone and siltstone.

Diabase and gabbro sills and dikes intrude the Obispo Formation in the plant site area. These intrusive rocks originally were mapped as a member of the Obispo Formation (Tod) by Hall

(Reference 11), but later were reclassified as a separate volcanic formation (Tvr) by Hall and others (Reference 10), because the rocks intrude several different formations, and are not confined to the Obispo Formation. The nomenclature of Hall and others (Reference 10) has been adopted for this study, and these rocks are mapped as Tertiary volcanic rock (Tvr) in the plant site area. These intrusive rocks are well exposed in the north wall of Diablo Canyon, across from the ISFSI site (Reference 11). The diabase typically is a dark, highly weathered, low-hardness rock. It is altered and weak, has a fine crystalline structure, and weathers spheroidally. Petrographic analysis of hand samples shows the diabase is an altered cataclastic gabbro and diorite. The large diabase sill that intruded between dolomite and sandstone beds in the raw water reservoir area was entirely removed during borrow area excavation (Figures 2.6-10 and 2.6-11). There are no exposures of diabase remaining on the borrow area cutslope and no diabase was encountered in any of the boreholes or trenches excavated at the ISFSI study area. Deeper parts of the original intrusion are still exposed in the roadcut along Tribar Road east of and below the raw water reservoir (Figure 2.6-6).

Quaternary deposits generally cover bedrock within the plant site area (Figure 2.6-7). These unconsolidated sediments are discussed in Section 2.6.1.5.

2.6.1.4.2 ISFSI Study Area Stratigraphy

The ISFSI is sited on folded and faulted marine strata of unit Tof_b of the Obispo Formation (Figures 2.6-7 and 2.6-8). Unit Tof_b in the ISFSI study area has undergone a complex history of deposition, alteration, and deformation. Understanding the complexity of the geology and the various geologic processes giving rise to the current geologic conditions at the site is important for interpreting the stratigraphy and structural geology at the site. Based on analysis of surface and subsurface data, supplemented by petrographic analyses of rock lithology, mineralogy, and depositional history, the following events produced the current lithology and stratigraphic character of bedrock at the site (Figures 2.6-13 and 2.6-14). A detailed description of each of these processes is presented in Reference 2, Attachment 16.

1. Original marine deposition, including vertical and lateral facies changes within the dolomite and sandstone sequence

2. Burial and lithification, followed by diagenesis and dolomitization

3. Localized addition of petroliferous fluids

4. Diabase intrusion, hydrothermal alteration, and associated deformation

5. Tectonic deformation (folding and faulting)

6. Surface erosion and weathering (both chemical and mechanical)

7. Borrow excavation and stress unloading

Across the ISFSI site, unit Tof_b is significantly influenced by a lateral and vertical facies change from dolomite to sandstone. In the ISFSI site area, therefore, unit Tof_b has been further divided into a dolomite unit (Tof_{b-1}) and a sandstone unit (Tof_{b-2}). Figure 2.6-15 provides a generalized stratigraphic column illustrating the distribution of rock types within these two subunits. Unit Tof_{b-1} consists primarily of dolomite, dolomitic siltstone, fine-grained dolomitic sandstone, and limestone. Unit Tof_{b-2} consists primarily of fine- to medium-grained dolomitic sandstone and sandstone. Thin clay beds also are present in both units. The dolomite appears to be a diagenetic product of alteration from a limestone and/or calcareous siltstone and very fine sandstone parent rock. Primary deposition of limestone ($CaCO_3$) or calcareous siltstone occurred in a shallow to moderately deep marine environment. Following burial and lithification, the replacement of calcium by magnesium (dolomitization) during diagenesis of the limestone or siltstone formed dolomite ($CaMg(CO_3)_2$).

The contact between the dolomite and sandstone (units Tof_{b-1} and Tof_{b-2}) marks a facies change from a deep marine dolomite sequence to a sandstone turbidite sequence. The contact varies from sharp to gradational, and bedding from one unit locally interfingers with bedding of the other unit. For purposes of mapping, the contact was arbitrarily defined as the first occurrence (proceeding down-section) of medium- to coarse-grained dolomitic sandstone below the dolomite. Surface and subsurface geologic data were used to construct 12 cross sections across the site and transport route (Reference 2, Attachment 16). The interfingering nature of the dolomite/sandstone contact beneath the ISFSI study area is illustrated on cross sections A-A', B-B''', D-D', F-F', I-I', and L-L' (Figures 2.6-10, 2.6-11, 2.6-16, 2.6-17, 2.6-18, and 2.6-19, respectively). Some of the thin, interfingering beds provide direct evidence for the lateral continuity and geometry (attitude) of bedding within the hillslope (for example, between boring 01-F and 00BA-1 on section I-I').

Analysis of the cross sections shows that the facies contact between the dolomite and sandstone (units Tof_{b-1} and Tof_{b-2}) generally extends from northwest to southeast across the ISFSI study area, with sandstone of unit Tof_{b-2} primarily in the north and northeast part of the area, and dolomite of unit Tof_{b-1} primarily in the south and southwest part of the area. The three-dimensional distribution of the facies contact is well illustrated by comparing cross sections B-B''' and I-I' (Figures 2.6-11–and 2.6-18). This distribution of the two units reflects a cyclic transgressive/regressive/transgressive marine sequence during the Miocene.

The division of unit Tof_b into two subunits also allows for a detailed interpretation of the geologic structure (folds and faults) in the ISFSI study area. This understanding provides the basis for evaluating the distribution of rock types in the area, and for selecting appropriate rock properties for foundation design and slope stability analyses at the ISFSI, as discussed in Sections 2.6.1.7, 2.6.1.8, 2.6.4.2, and 2.6.5.

2.6.1.4.2.1 Dolomite (Unit Tof_{b-1})

The slope above the ISFSI, including most of the borrow area excavation slope, is underlain by dolomite (Figure 2.6-8). The dolomite is exposed as scattered outcrops across the excavated slope, along the unpaved tower access road (Reference 3, Data Report A), in the upper part of most borings in the ISFSI study area (Reference 3, Data Report B), and in most exploratory trenches (Reference 3, Data Report D). The dolomite consists predominately of tan to yellowish-brown, competent, well-bedded dolomite, with subordinate dolomitic siltstone to fine-grained dolomitic sandstone, and limestone (Figure 2.6-20). Petrographic analyses of hand and core samples from, and adjacent to, the ISFSI study area show that the rock consists primarily of clayey dolomite, altered clayey carbonate and altered calcareous claystone, with lesser amounts of clayey fossiliferous, bioclastic and brecciated limestone, fossiliferous dolomite, and friable sandstone and siltstone (Reference 3, Data Report J, Tables J-1 and J-2). As described in the petrographic analysis, the carbonate component of these rocks is primarily dolomite; thus the general term dolomite and dolomitic sandstone is used to describe the rock.

The dolomite crops out on the excavated borrow area slope as flat to slightly undulating rock surfaces. The rock is moderately hard to hard, and typically medium strong to brittle, with locally well defined bedding that ranges between several inches to 10 ft thick in surface exposures and boreholes. Bedding planes are laterally continuous for several tens of feet, as observed in outcrops, and may extend for hundreds of feet based on the interpreted marine depositional environment. The bedding planes are generally tight and bonded. Unbonded bedding parting surfaces are rare and generally limited to less than several tens of feet, based on outcrop exposures.

2.6.1.4.2.2 Sandstone (Unit Tof_{b-2})

Sandstone of unit Tof_{b-2} generally underlies the ISFSI study area below about elevation 330 ft (Figure 2.6-8). Typically, the rocks in this subunit are well-cemented, hard sandstone and dolomitic sandstone, and lesser dolomite beds.

The well-cemented sandstone encountered in the borings and trenches is tan to gray, moderately to thickly bedded, and competent (Figure 2.6-21). The rock is well sorted, fine- to coarse-grained, and is typically well cemented with dolomite. Petrographic analyses show that the sandstone is altered, and that its composition varies from arkosic to arenitic, with individual grains consisting of quartz, feldspar, dolomite, and volcanic rock fragments (Reference 3, Data Report J). The rock is of low to medium hardness, is moderately to well cemented, and is medium strong. The matrix of some samples contains a significant percentage of carbonate and calcareous silt to clay matrix (probably from alteration). Petrographic analyses show that the carbonate is primarily dolomite. Thus, these rocks are referred to as sandstone and dolomitic sandstone. Bedding in places is well defined, and bedding plane contacts are tight and well bonded. Similar to the dolomite beds, unbonded bedding surfaces within the sandstone are rare and generally limited to less than several tens of feet, based on limited outcrop exposure.

2.6.1.4.2.3 Friable Bedrock

Distinct zones of friable bedrock are present within the generally more cemented sandstone and dolomite (Figures 2.6-8, 2.6-15, and 2.6-22). In some cases, the friable bedrock appears to reflect the original deposit, with no subsequent dolomitization. In other cases, the friable bedrock appears to be related to subsequent chemical weathering or hydrothermal alteration. The friable beds within units Tof_{b-1} and Tof_{b-2} have been designated with the subscript (a). Unit Tof_{b-1a} consists primarily of altered or weathered dolomite or dolomitic siltstone that has a block-in-matrix friable consistency, or simply a silt and clay matrix with friable consistency. The friable rock is of low hardness and is very weak to weak. Unit Tof_{b-2a} consists primarily of friable sandstone, is of low hardness, and is very weak to weak. In many cases, the friable sandstone is the original sandstone that has been chemically weathered or altered to a clayey sand (plagioclase and lithics altered to clay). In other cases, the friable sandstone simply lacks dolomite cementation and retains its original friable nature.

The vertical thickness of the friable rock encountered in borings ranges from less than 1 ft to 32 ft. The friable zones extend laterally for tens of feet in trench exposures, and up to about 200 ft were assumed to correlate between borings (Reference 2, Attachment 16). As illustrated on cross section I-I' (Figure 2.6-18), the zones of friable rock are more common, and possibly more laterally continuous, in the sandstone than in the dolomite.

2.6.1.4.2.4 Clay Beds

Clay beds are present within both the sandstone and dolomite units. Clay beds were observed in several trenches (Figures 2.6-23 and 2.6-24) and in many of the borings (Figures 2.6-25 and 2.6-26). Because clay beds are potential layers of weakness in the hillslope above the ISFSI site, they were investigated in detail, (Reference 2, Attachment 16). The clay beds generally are bedding-parallel, and commonly range in thickness from thin partings (less than 1/16 inch thick) to beds 2 to 4 inches thick; the maximum thickness encountered was about 8.5 inches. The clay beds are yellow-brown, orange-brown, and dark brown, sandy and silty, and stiff to hard. Petrographic analyses show that the clay contains marine microfossils and small rock inclusions; the rock inclusions are angular pieces of dolomite that are matrix-supported, and have no preferred orientation or shear fabric (Reference 3, Data Report K). In the trenches, the clay beds locally have slickensides and polished surfaces. The clay beds typically are overconsolidated (due to original burial), as supported by laboratory test data (Reference 3, Data Report G), and, where thick, have a blocky structure.

The clay beds encountered in the borings were recorded on the boring logs (Reference 3, Data Report B). In addition, in most of the borings, the clay beds also were documented in situ by a borehole televiewer. The televiewer logs show that the clay beds generally are in tight contact with the bounding rock, and are bedding-parallel (Reference 3, Data Report E). The clay beds range from massive having no preferred shear fabric, to laminated having clear shear fabric. The shear fabric is interpreted to be the result of tectonic shearing during folding and flexural slip of the bedding surfaces. The shear fabric does not reflect gravitational sliding, because features indicative of sliding, such as disarticulation of the rock mass, tensional fissures, and geomorphic expression of a landslide on pre-construction aerial photographs, are not present.

Clay Beds in Dolomite

Clay beds are more common, thicker, and more laterally continuous in the dolomite (unit Tof_{b-1}). Examination of the continuity of clay beds within and between adjacent trenches, roadcuts, and borings provided data on the lateral continuity (persistence) of the clay beds (Reference 2, Attachment 16). Individual clay beds exposed in the trenches and roadcuts appear to be persistent over distances of between tens of feet to more than 160 ft, extending beyond the length of the exposures. The exposed clay beds are wavy and have significant variations in thickness along the bed. Thinner clay beds (less than about 1/4 inch thick) typically contain areas where asperities on the surfaces of the bounding adjacent hard rock project through or into the thin clay. The bedding surfaces are all irregular and undulating, with the height (amplitude) of the undulation greater than the thickness of the clay beds, such that the clay beds likely will have rock-to-rock contact locally during potential sliding, producing an overall increase in the average shear strength of the clay bed surface. A correlation of clay beds within the slope above the ISFSI site is shown on cross section I-I' (Figure 2.6-18). These correlations indicate that at least some clay beds extend over several hundred feet into the hillslope. However, some beds clearly do not correlate: for example, the clay beds exposed in trenches T-14 and T-15 are not found in nearby boring 01-I.

Clay Beds in Sandstone

Clay beds are less common, generally thinner, and less laterally continuous in the sandstone (unit Tof_{b-2}). Clay beds observed in the sandstone generally are less than 1/4 inch thick. These thinner clay beds are difficult to correlate laterally between borings and, at least locally, are less than 50 to 100 ft in lateral extent. For example, as shown on cross sections B-B''' and I-I' (Figures 2.6-11 and 2.6-18), clay beds were not encountered in boring 01-B, but were encountered in borings 01-A and 01-H, 50 to 100 ft away.

Clay Moisture Content

The clay beds encountered in the borings and trench excavations in both the dolomite and sandstone were moist. Clay beds uncovered in the trenches dried out after exposure during the dry season, and became hard and desiccated. When wetted during the rainy season, the clay in the trenches became soft and sticky (Reference 3, Data Report D, Trench T-11). Possible local perched water tables, as observed in boring 01-F and evident elsewhere in the plant site area (Section 2.5, Subsurface Hydrology), also may soften the upper portions of the clay beds during the rainy season in the ISFSI study area.

Clay Composition

X-ray diffraction analyses (Reference 3, Data Report K) show that the clay-size fraction of the clay beds consists of three primary minerals: kaolinite (a clay), ganophyllite (a zeolite), and sepiolite (a clay). The silt-size fraction of the sample consists primarily of rock and mineral fragments of quartz, dolomite/ankerite, and calcite. Petrographic examination of the clay (Reference 3, Data Report K) shows a clay matrix having matrix-supported angular rock fragments and no shear fabric. Included rock fragments have evidence of secondary dolomitization of original calcite (limestone), and localized post-depositional contact alteration. Some samples contain microfossils (benthic foraminifera). The ganophyllite minerals appear to be expansive, as evidenced by swelling of one sample (X-1 from trench T-14A) after thin-section mounting. Sample X-2 also had a significant percentage of ganophyllite, and a high plasticity index (PI) of 63 (Reference 3, Data Reports K and G).

The presence of microfossils confirms the clay is depositional in origin, and was not formed by alteration or weathering of a lithified host rock. The clay is interpreted to reflect pelagic deposition in a marine environment.

2.6.1.4.2.5 Diabase (Tvr)

Diabase is exposed in the roadcut along Tribar Road and probably underlies the eastern portion of the raw water reservoir area. The diabase is part of the Miocene diabase intrusive complex in Diablo Canyon near the switchyards (Reference 10). A large diabase body was removed during grading for the raw water reservoir pad and the borrow cut area. This body of diabase likely was continuous with the diabase exposed along Tribar Road. Currently, no diabase is exposed on the borrow cut slope, and diabase was not encountered in any of the borings or trenches in the ISFSI study area. The diabase exposed along Tribar Road has been altered to a friable rock, and is soft to dense and easily picked apart; it is judged to be similar in engineering properties to the friable sandstone and friable dolomite found in the ISFSI study area. Though diabase was not encountered elsewhere in the ISFSI study area during field investigations, it is possible that other small dikes or sills of diabase may be encountered during excavation for the ISFSI pads or cutslope.

2.6.1.5 Geomorphology and Quaternary Geology

The geomorphology and Quaternary geology of the plant site area is dominated by a flight of coastal marine terraces, deep fluvial incision along Diablo Creek, and deposition of alluvial and colluvial fans at the base of hillslopes. Quaternary deposits cover bedrock across most of the power plant property, except in the ISFSI study area, where extensive borrow excavation in the 1970s removed the Quaternary deposits. These deposits accumulated in distinctive geomorphic landforms that include coastal marine terrace platforms, debris and colluvial fans at the base of hills and swales, landslides on hillslopes and sea cliffs, and alluvium along the floor of Diablo Canyon. The distribution of Quaternary deposits and landforms are shown on Figures 2.6-7 and 2.6-8.

2.6.1.5.1 Marine Terraces

Several marine terraces form broad coastal platforms within the western part of the power plant property (Figure 2.6-7). The power plant and associated support facilities and buildings are constructed on these terraces (Figure 2.6-2). Discontinuous remnants of older and higher terraces also are present locally across the ISFSI study area. Each of these marine terraces consists of a relatively flat, wave-cut bedrock platform, a thin layer of marine sand and cobble sediments, and surficial deposits of colluvium, alluvium, and eolian sediments. The "staircase" of bedrock platforms resulted from a combination of regional uplift, sea level fluctuations, and wave erosion.

The locations and elevations of marine terraces along the coast from Avila Beach to Montaña de Oro and Morro Bay, including the area of the power plant, were initially characterized during studies for PG&E's Long Term Seismic Program (LTSP Final Report). Several terraces were mapped in more detail for the ISFSI studies, and the location of the inner edge (or shoreline angle) of the terraces was estimated (Figure 2.6-7). Well-developed, wave-cut bedrock platforms and their associated terraces exist in the plant site area at elevations of about 30 to 35 ft (Q_1 terrace), 100 to 105 ft (Q_2 terrace), and 140 to 150 ft (Q_3 terrace), and form relatively level bedrock surfaces under the surficial Quaternary deposits along the coast. The platforms slope gently seaward at angles from 2 degrees to 3 degrees, and are bordered landward by steep (50 degrees to 60 degrees, LTSP Final Report) former sea cliffs that are now largely covered by thick surficial deposits. A sequence of Pleistocene to Holocene colluvial fans covers the landward portion of the coastal terraces. These deposits consist of crudely bedded clay, clayey gravel, and sandy clay, and have distinct paleosol and carbonate horizons. The lower, Pleistocene fan deposits are very stiff and partly consolidated; they have highly weathered clasts, carbonate horizons, and an oxidized appearance. The upper, Holocene deposits are unconsolidated and have a higher organic contact; they do not have argillic or carbonate horizons.

Near the ISFSI site, discontinuous remnants of a higher marine terrace are present. The terrace has an approximate shoreline angle elevation of 290 ft (Q_5 terrace) (Figure 2.6-7). The terrace deposits consist of a basal layer of marine sand and gravel overlain by colluvial sandy clay and clayey gravel. This terrace may be coeval with an estuarine deposit of black clay having interfingering white shell hash that crops out beneath the edge of the 500-kV switchyard fill (Figure 2.6-7). The clay appears to have been deposited in an estuarine environment by an ancient marine embayment into Diablo Canyon. Most of the Q_5 terrace, however, has been eroded by incision along Diablo Creek, or is buried by younger stream terrace and landslide deposits, or switchyard and road fills.

The thickness of the terrace deposits (depth to bedrock) varies greatly, from less than 10 ft to greater than 80 ft. Extensive grading for the DCPP and related facilities and parking areas has substantially modified the morphology and thickness of terrace deposits in some locations. The current thickness of terrace deposits, therefore, is locally dependent on site-specific grading activities.

2.6.1.5.2 Inland Quaternary Deposits

Diablo Creek has carved a deep channel into bedrock, causing oversteepening of the slopes along the canyon walls. Some thin, narrow, channel deposits, and one locally preserved stream terrace veneered by colluvial deposits, are present in the canyon. The rate and extent of erosion, however, generally has been dominant over sedimentation in the canyon, and alluvial deposits are relatively thin and of limited extent. Substantial reaches along the lower part of the creek were artificially filled, channeled, and altered during development of the power plant and related facilities, particularly around the 230-kV and 500-kV switchyards, which are constructed on large fill pads across the bottom of the canyon.

Slopes in the Irish Hills are extensively modified by mass wasting processes, including landslides, debris flows, creep, gully and stream erosion, and sheet wash. Extensive grading to form level platforms for the power plant and related facilities along the back edge of the coastal terraces has greatly modified the lower portions of most slopes in the plant site area. Large, deep-seated landslide complexes are present on the slopes of Diablo Canyon south of the 230-kV and 500-kV switchyards (Figure 2.6-7). These features consist of large (exceeding 100 acres), deep-seated, coalescing, bedrock landslides. The dip of bedrock strata in the vicinity of these large slides is downslope, suggesting the failure planes for these slides probably occurred within the bedrock along clay beds and bedding contacts. Some slides may have occurred at the contact between bedrock and overlying weathered bedrock and colluvium, or along contacts between Obispo Formation bedrock and relatively weaker diabase.

The large landslide complexes have been considerably modified by erosion, and fluvial terraces and possible remnants of the Q_5 marine terrace appear to have been cut into the toes of some of the slides. These conditions suggest they are old features that likely formed prior to the Pleistocene-Holocene transition, during a wetter climate. These large slide complexes, therefore, appear to have a stable configuration under the present climatic conditions, which have persisted during the Holocene (past 10,000 years or so).

Debris-flow scars and deposits are found along some of the steeper slopes (Figure 2.6-7). The debris flows originate where colluvium collects in topographic swales or gullies on the upper and middle slopes. Debris flows usually are triggered by periods of severe weather that allow development of perched groundwater within hillside colluvial deposits. Following initial failure, the saturated mass flows rapidly down drainage channels, commonly scouring the bottom of the channel and increasing in volume as it travels downslope. The flow stops and leaves a deposit of poorly sorted debris at a point where the slope angle decreases. Debris fans formed by accumulation of successive debris flows are present at the mouths of the larger canyons and gullies in the area (Figure 2.6-7).

2.6.1.6 Structure

2.6.1.6.1 Regional Structure

Bedrock structure in the plant site region is dominated by the northwest-trending Pismo syncline (Figure 2.6-4), which forms the core of the Irish Hills (References 10 and 11). The regional bedrock structure and tectonic setting are described in the DCPP FSAR Update, Section 2.5.1.1, and LTSP Final Report, Chapter 2, and are summarized in Section 2.6.2 of this report. The following sections describe the structural setting of the ISFSI study area, including the distribution of bedrock folds, faults, and joints in the area.

2.6.1.6.2 ISFSI Study Area Structure

Bedrock in the ISFSI study area has been deformed by tectonic processes and possibly by the intrusion of diabase. The detailed stratigraphic framework described above provides the basis for analyzing the geologic structure in the site area.

Geologic structures in the ISFSI study area include folds, faults, and joints and fractures. The distribution and geometry of these structures is important for evaluating rock mass conditions and slope stability because (1) folds in the bedrock produce the inclination of bedding that is important for evaluating the potential for out-of-slope, bedding-plane slope failures; and (2) faults and, to a lesser extent, joints in the bedrock produce laterally continuous rock discontinuities along which potential rock failures may detach in the proposed cutslopes.

The distribution and geometry of folds and faults in the bedrock were evaluated through detailed surface geologic mapping, trenches, and borings (References 2 and 3). Data from these studies were integrated to produce geologic maps (Figures 2.6-6, 2.6-7, and 2.6-8) and geologic cross sections (for example, Figures 2.6-10, 2.6-11, and 2.6-16 through 2.6-19). The cross sections were prepared at various orientations to evaluate the three-dimensional distribution of structures. Bedding attitudes were obtained from surface mapping (including roadcut and trench exposures) and from boreholes (based on visual inspection of rock core integrated with oriented televiewer data). These bedding attitudes were used to constrain the distribution of bedrock lithologies and geometry of bedding shown on the cross sections.

2.6.1.6.2.1 Folds

Similar to the power plant, the ISFSI is located on the southwestern limb of the regional Pismo syncline (Figure 2.6-4). As shown on the geologic maps (Figures 2.6-6, 2.6-7, and 2.6-8) and cross sections (Figures 2.6-10, 2.6-11, and 2.6-16 through 2.6-19), bedrock in the ISFSI study area is deformed into a small, northwest-trending syncline and anticline along the western limb of the larger regional Pismo syncline. On the ridge southeast of the ISFSI study area, nearly continuous outcrops of resistant beds expose the small anticline and an en echelon syncline (Figures 2.6-6, 2.6-7, and 2.6-17). These folds are relatively tight and sharp-crested, have steep limbs, and plunge to the northwest.

Within the ISFSI study area, the northwest-plunging anticline appears to be the northwestward continuation of the anticline that is exposed in the ridge top at the Skyview Road overlook area (Figure 2.6-1). The anticline varies from a tight chevron fold southeast of the ISFSI study area, to a very broad-crested open fold across the central part of the area. The northwestward shallowing of dips along the anticlinal trend appears to reflect a flattening of fold limbs up-section. In the ISFSI study area, the broad crest of the fold is disrupted by a series of fold-parallel, minor faults (Figure 2.6-11). The minor faults displace the fold axis, as well as produce local drag folding, which tends to disrupt and complicate the fold geometry. The axis of this broad-crested anticline is approximately located on the geologic map (Figure 2.6-8).

The en echelon syncline at the ridge crest along Skyview Road projects to the northwest along the southwestern margin of the ISFSI study area. From the southeast to the northwest, the syncline changes into a northwest-trending monocline, and then back into a syncline (Figures 2.6-6 and 2.6-7). In the ISFSI study area, the syncline opens into a broad, gently northwest plunging (generally less than 15 degrees) fold with gently sloping limbs (generally less than 20 degrees). Bedding generally dips downslope to the northwest in the upper part of the slope above the ISFSI site, and perpendicular to the slope to the southwest and west in the lower part of the slope. Small undulations in the bedding reflect the transition from a tight syncline to a relatively flat monocline, or "shoulder," and then back to a broad, northwest-plunging syncline. These localized interruptions to the northwestern plunge of the fold may be caused by the diabase intrusion and localized doming associated with the intrusion (compare diagrams C and D on Figure 2.6-13).

As discussed above and shown on cross sections B-B''', D-D', and F-F' (Figures 2.6-11, 2.6-16, and 2.6-17), the western limb of the small syncline varies from steeply dipping (approximately 70 degrees northwest) across the southern part of the plant site area, to gently dipping (approximately 30 degrees northwest) beneath the power block. This change in the dip of the syncline across the plant site area mirrors the change in dip described above across the ISFSI study area. Based on the geometry of the syncline, bedrock beneath the power block consists of sandstone (unit Tof_{b-2}), underlain by dolomite (unit Tof_{b-1}) (Figure 2.6-11). The power block is located on the same stratigraphic sequence exposed in the ISFSI study area; however, the sequence is approximately 400 ft lower in the stratigraphic section. As shown on cross section B-B''' (Figure 2.6-11), boreholes drilled during foundation exploration for the power block encountered calcareous siltstone having abundant foraminifera. This description of the rock is very similar to the dolomite of unit Tof_{b-1}; thus, the lower contact between units Tof_{b-1} and Tof_{b-2} is interpreted to be beneath the power block area.

Folding occurred during growth of the northwest-trending, regional Pismo syncline in the Pliocene to early Quaternary (LTSP Final Report). The smaller folds at and near the ISFSI study area are parasitic secondary folds along the southwestern limb of the larger Pismo syncline. Because of their structural association with the Pismo syncline, the folding in the area is interpreted to have occurred during the Pliocene to early Quaternary (Figure 2.6-8). Some localized fold deformation also may have accompanied the earlier Miocene diabase intrusions.

2.6.1.6.2.2 Faults

Numerous minor, bedrock faults occur within the ISFSI study area (Figures 2.6-27 and 2.6-28). Based on displaced lithologic and bedding contacts, most of the faults have vertical separations of a few inches to a few feet. At least five faults show vertical separation of several tens of feet. Slickensides and mullions on the fault surfaces generally show strike-slip to oblique strike-slip displacement.

The faults trend generally northwest, subparallel to the local fold axes (Figure 2.6-29). They dip steeply to near-vertical, generally 70 to 90 degrees, both northeast and southwest. They consist of interconnecting and anastomosing strands, in zones up to 5 ft wide. The faults have documented lengths of tens of feet to a few hundred feet, and are spaced from several tens of feet to hundreds of feet apart across the ISFSI study area, based on trench exposures and surface geologic mapping.

The fault surfaces within bedrock vary from tightly bonded or cemented rock/rock surfaces, to relatively soft slickensided clay/rock and clay film contacts. Individual faults are narrow, ranging in width from less than an inch to about 2 ft. Fault zones contain broken and slickensided rock, intermixed clay and rock, and locally soft, sheared, clayey gouge. The thickness of fault gouge and breccia is variable along the faults.

Cross section B-B''' (Figure 2.6-11) illustrates the subsurface stratigraphy and structure beneath the ISFSI pads. As shown on the map (Figure 2.6-8) and cross section, five minor faults clearly juxtapose dolomite (Tof_{b-1}) against sandstone (Tof_{b-2}), and truncate individual friable beds. Vertical separation across individual faults ranges from about 10 ft to greater than 50 ft, based on displacements of friable beds and the contact between units Tof_{b-1} and Tof_{b-2}. Total vertical separation across the entire fault zone exceeds 50 ft; cumulative displacement is down on the northeast. As described previously, the contact between dolomite and sandstone (units Tof_{b-1} and Tof_{b-2}) beneath the pads is based on the first occurrence of medium to coarse-grained sandstone, and there is no evidence of significant facies interfingering between the two units beneath the pads that would obscure the amount of displacement. Therefore, the interpretation of vertical separation of bedrock along the faults is given a relatively high degree of confidence.

Subhorizontal slickensides indicate that the minor faults in the ISFSI study area have predominantly strike-slip displacement (Figure 2.6-30). Using a typical range of a 10-degree to 20-degree rake on the slickensides and the vertical separation, total fault displacement is estimated to be several tens to several hundreds of feet. The faults trend subparallel to the axis of the Pismo syncline, and trend approximately 35 to 55 degrees more westward than the offshore Hosgri fault zone (Figure 2.6-29).

The faults in the ISFSI study area may be continuous with several other minor faults having similar characteristics exposed along strike in dolomite in the Diablo Creek roadcut about

800 ft to the north (Figures 2.6-6, 2.6-7, and 2.6-30). Given this correlation and the presence of several hundred feet of strike-slip displacement, the faults may be at least several thousand feet long. Interpretation of pre-borrow excavation aerial photography shows that the faults are not geomorphically expressed in the ISFSI study area (Figure 2.6-31) and there is no evidence of displaced Quaternary deposits along the fault traces.

In the analysis of slope stability (Section 2.6.5), the faults are assumed to form high-angle parting surfaces along the lateral margins of potential rock slides, rock wedges, and topple blocks. Fault-bounded structural blocks are shown on Figure 2.6-8, and on cross section B-B''' (Figure 2.6-11). The age and noncapability of the faults are discussed in Section 2.6.3.

2.6.1.6.2.3 Bedrock Discontinuities

Extensive data on bedrock discontinuities were collected from the borings and trenches within the ISFSI study area to assess their orientation, intensity, and spatial variability (Reference 3, Data Report F). The discontinuity data were used in the failure analysis of the ISFSI cutslopes (Section 2.6.5). Bedrock discontinuities include joints, faults, bedding, and fractures of unknown origin. These discontinuities, in particular joints, are pervasive throughout bedrock in the ISFSI study area (Figure 2.6-20). Steeply dipping faults and joint sets are the dominant discontinuities, giving the rock mass a subvertical fabric. Random and poorly developed low-angle joints also occur subparallel to bedding. The fault discontinuities are described in Section 2.6.1.6.2.2. Joint discontinuities are described below.

Joint contacts vary from tight to partially tight to slightly open; joint surfaces are slightly smooth to rough, and have thin iron oxide or manganese coatings (Reference 3, Data Report H). Joint lengths in trenches and outcrops typically range from a few feet to about 20 ft, and typical joint spacings range from about 6 inches to 4 ft, with an observed maximum spacing of about 14 ft (Reference 3, Data Report F, Table F-6). The intersections of various joints, faults, and bedding divide the bedrock into blocks generally 2 ft to 3 ft in dimension, up to a maximum of about 14 ft. Rock blocks formed by intersecting joints larger than those described above generally are keyed into the rock mass by intact rock bridges or asperity interlocking. The largest expected "free" block in the rock mass is, therefore, estimated to be on the order of about 14 ft in maximum dimension.

Both the well-cemented sandstone and the dolomite contain numerous joints. The jointing typically is confined to individual beds or groups of beds, giving the bedrock a blocky appearance in outcrop. Joints are less well developed and less common in the friable sandstone and friable dolomite. Linear zones of discoloration in the friable rock may represent former joints and small faults, but these zones are partially recemented, and not as frequent or obvious as joints in the harder rock.

The character of joints also differs between the upper, dilated zone of bedrock (generally within the upper 4 ft in the ISFSI study area, but conservatively estimated to extend to a maximum of 20 ft deep, particularly toward the edges of the old borrow cut where the amount of rock removed in 1971 is minimal) and the underlying zone of "tight" bedrock. Joints are generally tight to open in the upper zone. In the lower zone, the joints and other structures are tight and, in places, bonded and healed. This is well demonstrated in the borehole optical televiewer logs (Reference 3, Data Report E), which show the joints are typically tight and/or partly bonded throughout the borings. In both zones, the joints are locally clay-filled, and commonly contain thin fillings of clay, calcite, dolomite, and locally, gypsum. Joints and fractures in the borings are very closely to widely spaced (less than 1/16-inch to 3-ft spacing), with local crushed areas between joints.

In general, the joints group into two broad sets: a west- to west-northwest-striking set, and a north-northwest-striking set. In some trenches, fractures from both sets are present, whereas some show a scatter in orientation within a general northwest-southeast orientation. The variation in orientation and density of the joints with both strata and location across the ISFSI study area shows that the joints are limited in continuity.

The general northwest-southeast-trending character of the joints in the ISFSI study area is consistent with both the overall northwest-trending regional structural grain. Local variations in discontinuity orientations and intensity are attributed to rheological differences between dolomite and sandstone and their friable zones, as well as to proximity to the minor faults that cut across the area.

2.6.1.7 Stratigraphy and Structure of the ISFSI Pads Foundation

Figure 2.6-32 illustrates the expected bedrock conditions that will be encountered in the foundation excavation for the ISFSI pads at the assumed pad subgrade elevation of 302 ft (Reference 2, Attachment 16). The pads will be founded primarily on dolomitic sandstone of unit Tof_{b-2} and dolomite of unit Tof_{b-1}. Dolomitic sandstone generally underlies most of the site; dolomite underlies the eastern end of the site. The proposed cutslopes above the site are generally underlain by dolomitic sandstone in the western and central parts of the cut, and by dolomite in the upper and eastern parts of the cut.

Locally, friable sandstone (Tof_{b-2a}) and friable dolomite (Tof_{b-1a}) underlie the foundation of the ISFSI pads and the proposed cutslopes (Figure 2.6-32). Because the zones are highly variable in thickness and continuity, their actual distribution likely will vary from that shown on Figure 2.6-32. In particular, a large body of friable dolomite underlies the southeastern portion of the proposed cutslope. Other smaller occurrences of friable sandstone and dolomite probably will be encountered in the excavation. These friable rocks locally have dense, soil-like properties; thus, specific analyses were performed to assess the foundation properties and slope stability of these friable rock zones (Reference 3, Data Report I). Small zones of friable diabase may be found in the excavation, as discussed in Section 2.6.1.4.2.5. This rock has properties similar to the friable sandstone.

In two places beneath the foundation of the ISFSI pads, clay beds within dolomite and sandstone are expected to daylight or occur within 5 ft of the base of the foundation

(Figure 2.6-32). Additional clay beds may be exposed in the foundation of the pads. Although available geologic data do not document the presence of clay beds that will daylight in the ISFSI cutslope, some may be encountered when the cuts are made.

In addition, a zone of minor noncapable faults trends northwest across the central and eastern part of the ISFSI pads (Figures 2.6-8 and 2.6-11) (Section 2.6.3). The faults have vertical separations of 10 ft to 30 ft, and locally juxtapose different bedrock units.

2.6.1.8 Stratigraphy and Structure of the CTF Foundation

The CTF site lies about 100 ft directly northwest of the northwest corner of the ISFSI site (Figure 2.6-8). The CTF site is on the same west limb of the small anticline that underlies the ISFSI site (Figure 2.6-8, Section 2.6.1.6.2.1). Borings 00BA-3 and 01-CTF-A show the CTF will be founded on sandstone (unit Tof_{b-2}) and friable sandstone (unit Tof_{b-2a}), similar to the rock at the ISFSI site (Figures 2.6-8 and 2.6-32). The CTF site is located along the northwestern projection of the small bedrock faults at the ISFSI site, and similar faults and joints are expected to be encountered in the excavation for the CTF. Although no clay beds were encountered in borings 00BA-3 and 01-CTF-A, clay beds may underlie the site at deeper elevations (Reference 2, Attachment 16). The dip of the bedrock at the CTF site appears to be near-horizontal. In the cutslope west of the CTF site, bedrock dips moderately to the northeast, into the slope (Figure 2.6-7).

2.6.1.9 Stratigraphy and Structure of the Transport Route

The transport route begins at the power block and ends at the ISFSI. The route will follow existing paved Plant View, Shore Cliff, and Reservoir roads (Figure 2.6-1), except where routed north of the intersection of Shore Cliff and Reservoir roads to avoid an existing landslide at Patton Cove. The lower two-thirds of the route traverses thick surficial deposits, including marine terrace, debris-flow, and colluvial deposits of varying thicknesses (Reference 2, Attachment 16). These surficial deposits overlie two units of the Obispo Formation bedrock: unit Tof_b sandstone and dolomite, and unit Tof_c thinly to thickly bedded claystone, siltstone, and shale. The upper third of the route is on engineered fill, directly above dolomite and sandstone bedrock (units Tof_{b-1} and Tof_{b-2}) of the Obispo Formation (Figure 2.6-7). Locally, the road is on a cut-and-fill bench cut into the bedrock.

In the geologic description below, approximate stations have been assigned to assist in defining distances between locations, starting from the power block and ending at the ISFSI (Figure 2.6-7). Although not surveyed, this informal stationing is standard engineering format to represent the distance, in feet, from the beginning of the route outside the power block to the station location (for example, 21+00 is 2,100 ft from the beginning). The specific conditions along the route are discussed below.

<u>Station 00+00 (south side of power block) to 20+00 (near Reservoir Road)</u>: The transport route generally follows Plant View Road and Shore Cliff Road. The route starts at the power

block and crosses flat, graded topography on the lower coastal marine terrace (Q_2) (Figure 2.6-3). Behind the power block, the route is founded on sandstone (Tof_b) of the Obispo Formation. From there to near Reservoir Road, the transport route is founded on surficial deposits 10 to 40 ft thick, and engineered fill in excavations made during construction of the power plant. The surficial deposits consist primarily of debris-flow and colluvial deposits that overlie the marine bedrock terrace platform (Figures 2.6-7 and 2.6-16). These deposits range in age from middle Pleistocene to Holocene, and consist of overconsolidated to normally consolidated clayey sand and gravelly clay. The deposits contain some carbonate cementation and paleosols, and typically are stiff to very stiff (medium dense to dense). Bedrock below the marine terrace platform consists of east-dipping sandstone (Tof_b) from station 00+00 to about 07+00, and steeply dipping claystone and shale (Tof_c) from about 07+00 to 20+00. Because of the thickness of the overburden, bedrock structure will have no effect on the foundation stability of the road.

Station 20+00 to 34+00 (near Shore Cliff Road to Hillside Road): From station 20+00 to 26+00, the transport route will be on a new road north of the intersection of Shore Cliff Road and Reservoir Road to avoid an existing landslide at Patton Cove (Section 2.6.1.12.1.1; Figures 2.6-6, 2.6-7, and 2.6-19). A 5- to 50-ft-thick prism of engineered fill will be placed to achieve elevation from the lower part of the marine terrace to the upper part of the marine terrace as the road U-turns uphill. The engineered fill will overlie overconsolidated to normally consolidated Pleistocene debris-flow and colluvial deposits 20 to 80 ft thick that cover the marine bedrock platform (Q_2), which in turn overlie steeply dipping claystone and shale of unit Tof_c below the marine platform.

Along Reservoir Road, the route follows the higher part of this terrace, generally over the marine platforms Q_2 and Q_3. The surficial deposits consist of debris-flow and colluvial deposits up to 80 ft thick along the base of the ridge behind parking lot 8 (Figure 2.6-19). Bedrock below the marine terrace is claystone and shale (Tofc) from station 26+00 to 29+50, and sandstone (Tof_b) from station 29+50 to 34+00.

Station 34+00 (Reservoir Road at Hillside Road) to 49+00 (along Reservoir Road): The route follows Reservoir Road to the raw water reservoir area. The road traverses the west flank of the ridge on an engineered cut-and-fill bench constructed over unit Tof_b dolomite and sandstone, and thin colluvium and debris-flow fan deposits. Bedding, as exposed in the roadcut, dips 30 to 50 degrees into the hillslope, away from the road. Engineered fill on sandstone and dolomite underlies the inboard edge of the road, and a wedge of engineered fill over colluvium generally underlies the outboard edge of the road (Figures 2.6-7, 2.6-11, and 2.6-19).

Bedrock joints exposed in this part of the route are similar to those at the ISFSI site. Joints are generally of low lateral persistence, confined to individual beds, and are tight to open. Joint-bounded blocks are typically well keyed into the slope, with the exception of a 1- to 3-

foot-thick outer dilated zone. No large unstable blocks or adverse structures prone to large-scale sliding were observed.

Station 49+00 (along Reservoir Road) to 53+50 (ISFSI pads): The route leaves the existing Reservoir Road and crosses the power plant overview parking area. The route will be placed on new engineered fill up to 5 ft thick that will overlie thin engineered fill (up to 4 ft thick) that was placed over sandstone and friable sandstone (Tof_{b-2} and Tof_{b-2a}), the same rock types that underlie the ISFSI pads and CTF site.

Bedrock structures beneath this part of the route are inferred to be joints and small faults, similar to those exposed at the ISFSI site (Figure 2.6-8). The faults would trend generally northwest, and dip steeply northeast and southeast, to vertical. The primary joint sets are near-vertical (Section 2.6.1.6.2.3). This part of the road is on flat topography, and bedrock structure will have no effect on the foundation stability of the road.

2.6.1.10 Comparison of Power Block and ISFSI Bedrock

Bedrock beneath the ISFSI was compared to bedrock beneath the power block based on stratigraphic position, lithology, and shear wave velocity. Based on these three independent lines of evidence, the bedrock beneath the ISFSI and the power block is interpreted to be part of the same stratigraphic sequence, and to have similar bedrock properties and lithology.

Stratigraphic Position

Cross section B-B''' illustrates the stratigraphic correlation of bedrock between the ISFSI site and the power block site (Figure 2.6-11). As shown on the cross section, the power block and ISFSI are located on the same continuous, stratigraphic sequence of sandstone and dolomite of unit Tof_b of the Obispo Formation. As mentioned previously, the sequence at the power block is approximately 400 ft lower in the stratigraphic section.

The bedrock of the same continuous, stratigraphic sequence as that beneath the power block is exposed directly along strike in roadcuts along Reservoir Road (Figure 2.6-2). The bedrock exposed in the roadcut consists of dolomite, dolomitic siltstone, and dolomitic sandstone of unit Tof_{b-1}.

Lithology

As described in the DCPP FSAR Update, Section 2.5.1.2.5.6, p. 2.5-42, Figures 2.5-9 and 2.5-10) bedrock beneath the power block consists predominantly of sandstone, with subordinate thin- to thick-bedded slightly calcareous siltstone (for examples, see boring descriptions on Figures 2.6-11 and 2.6-19). The rocks are described as thin-bedded to platy and massive, hard to moderately soft and "slightly punky," but firm. These lithologic descriptions are similar to those for the rocks at the ISFSI site, and the rocks are interpreted to be the same lithologies.

The "calcareous siltstone" described in the DCPP FSAR Update is probably dolomite or dolomitic siltstone comparable to unit Tof_{b-1}. For example, based on the geologic descriptions of the rocks, the "siltstone" and "sandstone" encountered in 1977 in power block boring DDH-D is interpreted to be the dolomite and dolomitic sandstone of unit Tof_{b-1} observed at the ISFSI site.

Boring logs from the hillslope between the power block and the ISFSI site, included in the DCPP FSAR Update (Figures 2.5-22 to 2.5-27; Appendix 2.5C, plates A-1 to A-19), describe bedrock as tan and gray silty sandstone and tuffaceous sandstone (Figures 2.6-11 and 2.6-19). These rocks are moderately hard and moderately strong. The rock strata underlying this slope dip into the hillside and correlate with the sandstone and dolomite strata exposed on the west flank of the ridge (and west limb of the syncline) that are exposed in roadcuts along Reservoir Road south of the ISFSI site (Figures 2.6-6, 2.6-7, and 2.6-20) and in the deeper part of the borings at the ISFSI site.

Shear Wave Velocity

Shear wave velocity data from the power block site and the ISFSI site are summarized on Figures 2.6-33 and 2.6-34. Velocity data in Figure 2.6-35 are from borehole surveys at the ISFSI site (Reference 3, Data Report C), and comparative velocities at the power block site are from the DCPP FSAR Update. As evident from the figures, shear-wave velocities from surface refraction and borehole geophysical surveys at the ISFSI site are within the same range as those obtained at the power block site. The velocity profiles at both sites are consistent with a classification of "rock" for purposes of characterizing ground-motions (Reference 12).

2.6.1.11 Groundwater

Refer to Section 2.5, Subsurface Hydrology.

2.6.1.12 Landslides

2.6.1.12.1 Landslide Potential in the Plant Site Area

Slopes in the Irish Hills are subjected to mass-wasting processes, including landslides, debris flows, creep, gully and stream erosion, and sheet wash (Reference 9). Extensive grading in the plant site area to create level platforms for structures along Diablo Canyon and the coastal terraces has modified the lower portions of most of the slopes near the plant site.

Debris-flow scars and deposits occur on, and at the base of, slopes in the plant site area. The debris flows initiate where colluvium collects in topographic swales or gullies, and are usually triggered by periods of severe weather. Debris-flow fans, caused by the accumulation of successive debris flows, form at the mouths of the larger canyons and gullies in the area. Several typical gullies that have colluvium-filled swales, debris-flow chutes, and debris-flow fans at the bottom of the chutes are found on the slope above parking lots 7 and 8, south of the power plant (Figures 2.6-5 and 2.6-7).

During landslide investigations in 1997, PG&E identified a large, (exceeding 100 acres) ancient landslide complex on the slopes of Diablo Canyon, directly east of the 230- and 550-kV switchyards (Reference 9) (Figure 2.6-7). The dip of the bedrock in the vicinity of these large slides is downslope, contributing to slope instability (Reference 9, Figure 21). This structure suggests the failure planes for these slides are probably within the bedrock along bedding contacts, clay beds, and possibly along the intrusive contacts between Obispo Formation bedrock and the altered diabase.

The large landslide complex is subdued, and has been considerably modified by erosion. Thin stream-terrace deposits and remnants of the Q_5 430,000-year-old marine terrace at elevation 290 ±5 ft appear to have been cut into the toes of some of the slides. These relations indicate the landslides are old, and likely formed in a wetter climate during the middle to late Pleistocene. The landslides appear to be stable under the present climatic conditions. There is no geomorphic evidence of activity in the Holocene (past 10,000 years or so). Additionally, the 500-kV switchyard embankment fill in the canyon provides a partial buttress to the toe of the old landslide deposit, and serves to help stabilize the landslide. The switchyard shows evidence of no post-construction slope movement. The complex lies entirely east of the ISFSI, and does not encroach, undermine, or otherwise affect the ISFSI.

Patton Cove Landslide

The Patton Cove landslide (Figure 2.6-36) is a deep-seated rotational slump located at a small cove adjacent to Shore Cliff Road along the coast, about one-half mile east of the power plant (Figures 2.6-6, 2.6-7, and 2.6-17) (Reference 9, p. 78-83). Shore Cliff Road was constructed on engineered fill benched into marine-terrace and debris-flow fan deposits directly east of the slide. Cracks within Shore Cliff Road suggest that the landslide may be encroaching headward beneath the road. The landslide is approximately 125 ft long, 400 ft wide, and 50 ft deep. The slide occupies nearly the full height of the bluff face, which is inclined about 1.3:1 (H:V).

Slide movement was first documented in 1970 by Harding Lawson Associates (HLA) (Reference 13). In 1970, the head scarp of the slide was approximately 15 ft south of the toe of the fill that supports Shore Cliff Road. In the 31 years since slide movement was first documented, the slide mass has been episodically reactivated by heavy rains and continued wave erosion at the toe of the slide along the base of the sea cliff.

Renewed activity of the landslide in the winter of 1996/1997 coincided with development of numerous en echelon cracks in the asphalt roadway and walkway along Shore Cliff Road. In the winter of 1999/2000, a water line separated beneath the paved roadway in the vicinity of the cracks. Comparison of pre- and post-construction topographic maps shows that the locations of these cracks coincide approximately with the contact between the road fill wedge and the underlying colluvium, suggesting that deformation in this area may be caused by fill settlement or creep. However, the arcuate pattern of the cracks and proximity to the Patton Cove landslide suggest that incipient landsliding is encroaching into the roadway. The cracks also are located in the general area of a crescent-shaped marine terrace riser mapped prior to road construction (DCPP FSAR Update, Figure 2.5-8). The mapped terrace riser is more likely a subdued landslide headscarp.

An inclinometer was installed on the road shoulder closest to the slide in November 2000 to monitor the depth and rate of future movements. The inclinometer has recorded small movements near the contact between the base of the fill and the underlying colluvium and debris-flow deposits.

To avoid the potential hazard of the landslide and unstable fill, the transport route will be constructed north of the existing road, where the Patton Cove slide will pose no hazard (Section 2.6.1.12.3). The closest approach of the transport route will be about 100 ft north of the cracks at the intersection of Shore Cliff and Reservoir roads.

2.6.1.12.2 Landslide Potential at the ISFSI and CTF Sites

Detailed investigation of landslides in the plant site area (Reference 9) shows there are no existing deep-seated landslides or shallow slope failures at the ISFSI and CTF sites. Field mapping and interpretation of 1968 aerial photography (Figure 2.6-31) during the ISFSI site investigations confirmed the absence of deep-seated bedrock slides or shallow slope failures at the site.

Excavation of the existing slope at the ISFSI site was completed in 1971. No stability problems were encountered during excavation using bulldozers and scrapers, and the slope has been stable, with minimal surface erosion, since 1971. Prior to excavation of the slope, Harding Miller Lawson (HML) (Reference 8) described a shallow landslide in weathered bedrock (Figure 2.6-10) along a "shale seam" in their exploratory trench A (Reference 8, Plate D-3). This feature was less than 15 ft deep, and was removed entirely, along with underlying intact bedrock, to a depth of about 75 ft during excavation of the slope. Zones of "fractured, decomposed, and locally brecciated sandstone, siltstone, and shale" and "breccia and clay zones" described in HML trench A are interpreted to be friable dolomite zones and steep faults.

The Harding Miller Lawson landslide is apparent on 1968 black-and-white aerial photography, and is expressed by a subtle, arcuate headscarp, hummocky landscape, and locally thicker vegetation, probably reflecting high soil moisture within the slide debris (Figure 2.6-31). The slide was located along a slight swale in colluvial soils and possibly weathered bedrock that mantled the slope prior to excavation. The slide mass appears to have moved northeast along the axis of the swale, and not directly downslope. Because bedding is interpreted to dip to the northwest in this area, the landslide probably was not a bedrock-controlled failure. There is no evidence of deep-seated bedrock landslides on the 1968 aerial photographs; the ISFSI study area appears as a stable, resistant bedrock ridge in the photos.

Because surficial soils were removed from the ISFSI site area during past grading, there is no potential for surficial slides to adversely affect the site. There is no evidence of bedrock landslides below the ISFSI site or along the southern margin of Diablo Canyon near the raw water reservoir. Reservoir facilities (including the water treatment plant) and paved areas between the ISFSI and CTF sites and Diablo Canyon show no evidence of sliding or distress. Because the 290-foot Q_5 marine terrace is preserved locally across the ISFSI study area, it is apparent that no deep-seated bedrock slides have occurred since formation of the 430,000-year-old terrace, and the ridge is interpreted to be stable. Some shallow debris-flow failures and slumps were identified in surficial soil on the outermost 3 ft to 4 ft of weathered rock in the steep (45 to 65 degrees) slope below the raw water reservoir (Figure 2.6-7). These failures are shallow, and do not pose a stability hazard to the ISFSI or CTF sites, which are set more than 180 ft back from the top of the slope.

2.6.1.12.3 Landslide Potential Along the Transport Route

The transport route is located 100 ft north of the headscarp of the active Patton Cove landslide (Figure 2.6-7). Based on detailed mapping, borings, and an inclinometer, the landslide headscarp is defined by a series of cracks at the intersection of Shore Cliff and Reservoir Roads. A cross section through the landslide is shown in Figure 2.6-17. The geometry and depth of the slide plane indicate further headward encroachment of the landslide toward the transport route is not likely.

Where the transport route follows Reservoir Road at the base of the bedrock hillslope north from near Hillside Road, there are no bedrock landslides. Sandstone beds in the hillslope above the road dip obliquely into the slope at about 30 to 50 degrees (Figures 2.6-7, 2.6-11, and 2.6-19). These beds extend continuously across much of the hillside, providing direct evidence of the absence of bedrock slope failures (Figure 2.6-5). Small faults and joints in the rock mass do not appear to adversely affect potential slope stability, and the existing roadcut and natural slopes have no evidence of any slope failures.

Kinematic analyses of the bedding and fractures along the road were performed where the road borders the bedrock slope (Section 2.6.5.4.1). Two portions of the route were analyzed: a northern part from approximately station 43+00 to 49+00 (Figure 2.6-37), and a northwesterly stretch from approximately station 35+00 to 42+00 (Figure 2.6-38). The rock mass is stable against significant wedge or rock block failures; however, the analysis indicates that rock topple failure from the cutslope into the road is possible. Field evaluations indicate such failures would be localized and limited to small blocks. The existing drainage ditches on the inboard edge of the road would catch these small topple blocks.

Several colluvial or debris-flow swales are present above the transport route along Reservoir Road (Figures 2.6-5 and 2.6-7). These swales have been the source of past debris flows that primarily have built the large fans on the marine terraces over the past tens of thousands of years. Additional debris flows could develop within these swales during sever weather events, similar to those described elsewhere in the Irish Hills following the 1997 storms (Reference

9). Holocene debris-flow fan deposits extend to just below the road alignment, indicating that future debris flows could cross the road. However, large graded benches for an abandoned leach field system are present above a portion of the Reservoir Road, and concrete ditches and culverts are present in swale axes. These existing facilities will catch and divert much of the debris from future debris flows above the road. However, two debris-flow chutes are present above the road northwest of Hillside Road; this part of Reservoir Road is not protected from these potential debris flows. Based on the thickness of the colluvium in the swales (5 to 10 ft), and the slope profile, the maximum depth of debris on the road following severe weather is estimated to be less than 3 ft, which easily could be removed after the event.

2.6.1.13 Seismicity

A detailed analysis of the earthquake activity in south-central coastal California was presented in the LTSP Final Report. The report included the historical earthquake record in the region since 1800, instrumental locations from 1900 through May 1988, and selected focal mechanisms from 1952 to 1988. From October 1987 through May 1988, the earthquake catalog incorporated data recorded by the PG&E Central Coast Seismic Network (CCSN). This station network has operated continuously since then to monitor earthquake activity in the region.

The seismicity in the region is illustrated in two frames on Figure 2.6-39: (a) historical earthquakes of magnitude 5 and greater since 1830, and (b) instrumentally recorded seismicity of all magnitudes from 1973 through September 1987. Epicentral patterns of the microearthquakes (Figure 2.6-39) show that most of activity within the region occurs to the north, beneath the Santa Lucia Range and north of San Simeon, and in the southern onshore and offshore region south of Point Sal. Earthquakes in the southern offshore region extend westward to the Santa Lucia Bank area. Within about 15 miles of the ISFSI, small, scattered earthquakes occur between the Los Osos fault and faults of the Southwest Boundary fault zone (including the Irish Hills subblock (Section 2.6.1.3), in the nearshore region within Estero Bay, and along the Hosgri fault zone. Focal mechanisms along the Hosgri fault zone show right-slip displacement along nearly vertical fault planes (LTSP Final Report, Chapter 2, Figures 2-30 and 2-36).

McLaren and Savage (Reference 14) updated the earthquake record and present well-determined hypocenters and focal mechanisms for earthquakes recorded from October 1987 through January 1997 by the CCSN and by the U.S. Geological Survey, from north of San Simeon to the southern region near Point Arguello (Figure 2.6-40). No significant earthquakes occurred during this time period, and no significant change in the frequency of earthquake activity was observed. The largest event recorded was the local (Richter) magnitude 5.1 (duration magnitude 4.7) Ragged Point earthquake on 17 September 1991 northwest of San Simeon (Figure 2.6-40 inset). The focal mechanism of this event is oblique thrust, typical of nearby recorded earthquakes. Earthquake data since January 1997 also do not show any significant change in the frequency or epicentral patterns of seismic activity in the region.

The seismicity data presented in Reference 14 is consistent with the LTSP observations and conclusions (LTSP Final Report). Specifically:

- Epicentral patterns of earthquakes have not changed. As shown in Figure 2.6-40, microearthquakes continue to occur to the north, along a northwest trend to San Simeon, east of the Hosgri fault zone, and in the southern offshore region.

- Selected seismicity cross sections A-A' through D-D' along the Hosgri fault zone (Figure 2.6-41) show that onshore and nearshore hypocenters extend to about 12-kilometers depth, consistent with the seismogenic depth range reported for the region (LTSP Final Report). Seismicity cross section B-B', across the Hosgri fault zone, shows the Hosgri fault zone is vertical to steeply dipping. The earthquakes projected onto cross sections C-C' and D-D' are evenly distributed in depth.

- Focal mechanisms along the Hosgri fault zone (Figure 2.6-42) are primarily strike slip, consistent with the LTSP conclusion that the Hosgri is a northwest-trending, vertical, strike-slip fault (LTSP Final Report). Mechanisms from events within the Los Osos/Santa Maria domain show oblique slip and reverse fault motion, consistent with the geology.

- The location of the 1991 Ragged Point earthquake in the San Simeon region, as well as its size and focal mechanism, are consistent with previous earthquakes in the region.

2.6.2 VIBRATORY GROUND MOTIONS

2.6.2.1 Approach

10 CFR 72.102(f) states the following "The...DE for use in the design of structures must be determined as follows:

(1) For sites that have been evaluated under the criteria of Appendix A of 10 CFR 100, the DE must be equivalent to the safe shutdown earthquake (SSE) for a nuclear power plant."

Thus, DCPP ground motions are considered to be the seismic licensing basis, in accordance with 10 CFR 72.102(f), for the evaluation ISFSI design ground motions. Seismic analyses for the ISFSI used ground motions that meet or exceed the DCPP ground motions.

Vibratory ground motions were considered in the design and analyses (Section 8.2.1) of (1) the ISFSI pads, (2) the CTF, including the reinforced concrete support structure and structural steel, (3) the ISFSI casks and cask anchorage, (4) ISFSI pad sliding and cutslope stability, (5) transport route slope stability, and (6) transporter stability.

The approach used for developing the ground motion characteristics to be used for design and analysis of the ISFSI SSCs consisted of the following.

- Use the DCPP ground motions (Section 2.6.2.2) as the basis for developing the ISFSI design ground motions, in accordance with 10 CFR 72.102(f).

- Compare the earthquake source and distance and ISFSI site conditions with those at the DCPP to confirm the applicability of the DCPP ground motions to the ISFSI site.

- Because ISFSI pad sliding and cutslope stability, transport route slope stability, and transporter stability may be affected by longer-period ground motions than those characterized by the DCPP ground motions, develop appropriate response spectra for the analysis of these elements, conservatively taking into account the additional influence of near-fault effects, such as fault rupture directivity and fling, that have been recorded in recent large earthquakes.

- Develop, as necessary, spectra-compatible time histories for use in analyses and design.

2.6.2.2 DCPP Licensing-Basis Ground Motions

The basis for the DCPP design ground motions is discussed in the DCPP FSAR Update, Sections 2.5.2.9, 2.5.2.10, and 3.7.1. There are three design ground motions for the DCPP: the design earthquake (DE), DCPP FSAR Update, Figures 2.5-20 and 2.5-21; the double design earthquake (DDE), DCPP FSAR Update, Section 3.7.1.1; Reference 5; and the Hosgri earthquake (HE), DCPP FSAR Update, Figures 2.5-29 through 2.5-32, which was incorporated into the DCPP seismic design basis as part of the seismic reevaluation of applicable existing structures by PG&E, and is now required as part of the licensing basis at the plant.

As discussed in the DCPP FSAR Update, the seismic qualification basis for the plant is the original design earthquakes (DE and DDE), plus the HE evaluation, along with their respective analytical methods, acceptance criteria, and initial conditions. Future additions and modifications to the plant are to be designed and constructed in accordance with these seismic design bases. In addition, as discussed in the DCPP FSAR Update, certain future plant additions and modifications are to be checked against the insights and knowledge gained from the Long Term Seismic Program (LTSP) to verify that the plant's "high-confidence-of-low-probability-of-failure" (HCLPF) values remain acceptable (Reference 5). As part of the Long Term Seismic Program, response spectra were developed for verification of the adequacy of seismic margins of certain plant structures, systems, and components (LTSP Final Report). The DE, DDE, HE, and LTSP spectra are defined for periods up to 1.0 second, 1.0 second, 0.8 second, and 2.0 seconds, respectively.

2.6.2.3 Comparison of Power Block and ISFSI Sites

The Diablo Canyon ISFSI site is located in the plant site area of the licensed DCPP; therefore, the applicability of the DCPP ground motions to the ISFSI site was evaluated by comparing the ground-motion response characteristics of the ISFSI site with those of the plant site, and by comparing the distance from the controlling seismic source to the plant with the distance from the controlling source to the ISFSI.

As described in Section 2.6.1.4.2 and shown in Figures 2.6-6 and 2.6-11, the power block and the ISFSI are sited on bedrock that is part of the same, continuous, thick sequence of sandstone and dolomite beds of unit b of the Obispo Formation. In the classification of site conditions used for purposes of ground-motion estimation, both of these sites are in the "rock" classification (Reference 12).

Shear-wave velocity profiles from both sites are compared in Figure 2.6-35. As these comparisons indicate, shear-wave velocities from surface refraction and borehole geophysical surveys at the ISFSI site are within the same range as those obtained at the power block site. The velocity profiles at both sites are consistent with the "rock" classification for purposes of ground-motion estimation (Reference 12).

The earthquake potential of the significant seismic sources in the region was characterized during development of the DCPP FSAR Update and the Long Term Seismic Program (LTSP Final Report). The Hosgri fault zone, at a distance of 4.5 kilometers, was assessed to be the controlling seismic source for the DCPP (DCPP FSAR Update, Sections 2.5.2.9 and 2.5.2.10; LTSP Final Report, Chapters 3 and 4). The ISFSI is approximately 800 ft to 1,200 ft east of the power block, and is thus only slightly farther from the Hosgri fault zone (Figure 2.6-4).

Therefore, because both sites are classified as rock, and because within the rock classification they have similar ranges of shear-wave velocities, and the distance to the controlling seismic source is essentially the same, the DCPP ground motions are judged to be applicable to ISFSI design.

2.6.2.4 Spectra for ISFSI Pads, Casks and Cask Anchorage, and CTF

The DE, DDE, HE, and LTSP spectra (Figures 2.6-43 and 2.6-44; the DE is one-half the DDE and is not shown) are applicable to the analysis of the pads, casks and cask anchorage, and CTF (Section 8.2.1.2).

For cask anchorage design, the design spectra were defined by the HE spectrum for periods up to 0.8 second, and the LTSP spectrum for periods up to 2.0 seconds. New three-component, spectrum-compatible time histories were developed for the HE and LTSP by modifying recorded ground motions using the spectral matching procedure described by Silva and Lee (Reference 15). The recorded time histories used in the spectral matching were selected based on their similarity to the DDE, HE and LTSP earthquakes. The NRC Standard Review Plan spectral matching criteria (Section 3.7.1, NUREG-0800) were followed for 4-percent, 5-percent, and 7-damping; however, the NUREG requirement for a minimum value for the power spectral density (PSD) based on an NRC Regulatory Guide 1.60 spectral shape is not applicable to the spectral shapes of the HE or LTSP. The objective of the minimum PSD requirement was met by requiring the spectrum of each time history to be less than 30 percent above and 10 percent below the target spectrum. This ensures that no Fourier amplitudes are deficient in energy for the frequency range of interest.

2.6.2.5 ISFSI Long-Period Earthquake (ILP) Spectra and Time Histories For Pad Sliding, Slope Stability, and Transporter Stability Analyses

Because ISFSI pad sliding and cutslope stability, transport route slope stability, and transporter stability may be affected by longer-period ground motions than those characterized by the DCPP ground motions, PG&E has developed longer-period spectra and associated time histories for the analysis of pad sliding, slope stability, and transporter stability. These are referred to as the ISFSI long period (ILP) ground motions (Figures 2.6-45 and 2.6-46). The ILP spectra represent 84th percentile horizontal and vertical spectra, at damping values of 2 percent, 4 percent, 5 percent, and 7 percent, that extend out to a period of 10 seconds.

New information has become available from analytical studies of near-fault strong-motion recordings of large earthquakes in the past decade to evaluate the influence of near-fault effects, such as fault rupture directivity and tectonic deformation (fling), especially on ground motions in the longer-period range. PG&E has incorporated the influence of rupture directivity and fling in the ILP spectra and time histories used for the analyses of pad sliding, slope stability, and transporter stability.

Development of the ILP horizontal spectra (Figure 2.6-46) incorporated the following assumptions and considerations:

- Although the LTSP (LTSP Final Report) considered alternative styles of faulting for the Hosgri fault zone, the weight of the evidence favored strike-slip, and subsequent earthquake data and geologic and geophysical data interpretations (References 14 and 16) indicate the style of faulting is strike slip. Therefore, ground-motion characteristics appropriate for strike-slip earthquakes were used.

- The effect of directivity was analyzed for the case in which rupture begins at the southern end of the Hosgri fault zone, progresses 70 kilometers to the northwest where it passes at a closest distance of 4.5 kilometers from the plant site, and continues an additional 40 kilometers to the northwest end of the Hosgri fault zone. This assumption is conservative, because this rupture scenario has the greatest directivity effects at the site.

- The ILP horizontal spectrum at 5-percent damping at periods less than 2.0 seconds envelopes the DDE, HE, and LTSP spectra.

- The spectrum based on the Abrahamson and Silva (Reference 16) attenuation relation is consistent with the envelope of the DDE, HE, and LTSP spectra at 2 seconds, and has the same slope-with-period as the Sadigh (Reference 17) and

Idriss (References 18, 19, and 20) attenuation relations, so it was used to extrapolate the envelope spectrum to 10 seconds. This spectrum is the 84th percentile horizontal spectrum.

- The 5-percent-damped horizontal spectra were increased to assure they envelope the Hosgri spectra at 4-percent and 7-percent damping ratios. Scaling factors for computing spectra at damping values other than 5 percent are from Abrahamson and Silva (Reference 16).

- Abrahamson's (Reference 21) and Somerville and others' (Reference 22) models were used to scale the average horizontal spectrum, to compute the fault-normal and fault-parallel ground-motion components, incorporating directivity effects.

- The fault-normal component was increased in the period range of 0.5 second to 3.0 seconds to account for possible directivity effects for earthquakes having magnitudes less than 7.2 at periods near 1 second.

- Because fling can occur on the fault-parallel component for strike-slip faults, a model was developed to compute the 84th percentile ground motion due to tectonic fling deformation at the ISFSI accompanying fault displacement on the Hosgri fault zone in a magnitude 7.2 earthquake. The fling arrival time was selected, and the fling and the transient fault-parallel ground motion were combined so as to produce constructive interference of the fling and the *S*-waves, resulting in a conservative fault-parallel ground motion.

Development of the ILP vertical spectra (Figure 2.6-46) incorporated the following assumptions and considerations:

- The ILP vertical spectrum at 5-percent damping at periods less than 2 seconds is defined by the envelope of the DDE, HE, and LTSP (Reference 5) spectra.

- Current empirical attenuation relations (References 16, 17, and 23) were used to estimate the vertical-to-average-horizontal ratio for periods greater than 2 seconds; the value of two-thirds is conservative. The envelope vertical spectrum at 5-percent damping at periods less than 2 seconds was extended to a period of 10 seconds using two-thirds the average horizontal spectrum.

- The 5-percent-damped vertical spectra were increased to assure they envelop the Hosgri spectra at 4 percent and 7 percent damping ratios. Scaling factors for computing spectra at damping values other than 5 percent are from Abrahamson and Silva (Reference 16).

Five sets of spectrum-compatible acceleration time histories were developed to match the ILP ground motions spectra. The recordings in the table below were selected because they are from strike-slip earthquakes of magnitude 6.7 or greater, recorded at distances less than 15 kilometers from the fault, and contain a range of characteristics of near-fault ground motions.

Earthquake	Magnitude	Recording	Distance (km)	Site Type
1992 Landers	7.3	Lucerne	1.1	Rock
1999 Kocaeli	7.4	Yarimca	8.3	Soil
1989 Loma Prieta	6.9	LGCP	6.1	Rock
1940 Imperial Valley	7.0	El Centro #9	8.3	Soil
1989 Loma Prieta	6.9	Saratoga	13.0	Soil

The NRC Standard Review Plan spectral matching criteria (Section 7.1, NUREG-0800) recommends 75 frequencies for spectral matching. Augmented frequency sampling at 104 frequencies was used to account for the broader frequency range being considered for the ISFSI analyses. The interpolation of the response spectral values was done using linear interpolation of log spectral acceleration and log period. The NRC requirement permits not more than 5 of the 75 frequencies to fall below the target spectrum, and no point to fall below 0.9 times the target spectrum. This requirement was adhered to with the 104 frequencies.

The time histories were matched to the target spectra at 5-percent damping. The mean response spectrum of the five sets must envelop the target to meet the criteria of SRP 3.7.1. This criterion was applied to the damping values of 2 percent, 4 percent, 5 percent, and 7 percent.

The fault-parallel time histories were modified to include the effects of fling.

2.6.2.6 Transport Route and Transporter Design-Basis Ground Motions

As discussed in Section 2.6.1.9 and shown in Figures 2.6-6 and 2.6-7, the transport route is underlain by Obispo Formation bedrock consisting of unit b dolomite and sandstone (the same bedrock as at the power block and ISFSI sites), and unit c claystone and shale. Varying thicknesses of dense soil deposits overlie the bedrock.

Because the transport route is about the same distance from the Hosgri fault zone as the DCPP and the ISFSI sites, the ILP spectra are appropriate for use along the transport route where the route is constructed on bedrock. Approximately one-third of the route will be constructed on bedrock, and this portion was analyzed using the ILP ground motions (Section 8.2.1.2.1).

Where the transport route crosses surficial deposits over bedrock (approximately two-thirds of the route), the effect of the soil response was considered. To account for soil response, dynamic response analyses were performed at selected locations along the route. The analyses indicate that peak ground accelerations at certain points along the surface of the transport route can be 1.5 to 2.0 times the amplitude of the peak bedrock acceleration, due primarily to the effect of amplification through the colluvial soils overlying the rock.

The exposure time of the transporter to potential ILP ground motions is estimated to be very short as it traverses the transport route to the ISFSI site, as discussed in Section 8.2.1.2.1. An evaluation of the impact of a seismic event occurring during cask transport also is discussed in Section 8.2.1.2.1.

2.6.3 SURFACE FAULTING

Potentially active faults at Diablo Canyon and in the surrounding region were identified and characterized in the DCPP FSAR Update, Section 2.5.3, the LTSP Final Report, Chapter 2, and the LTSP Addendum (Reference 7, Chapter 2). Together, these documents provide a comprehensive evaluation of the seismotectonic setting and location of capable faults in the plant site region, and document the absence of capable faults beneath the power block and in the plant site area. These studies used detailed mapping of Quaternary marine terraces and paleoseismic trenching to document the absence of middle to late Pleistocene faulting in the plant site area, including the ISFSI study area (LTSP Final Report, p. 2-38, Plates 10 and 12). Hence, there are no capable faults at the ISFSI site.

Several minor bedrock faults were encountered in trenches at the ISFSI site during site characterization studies (described in Section 2.6.1.6.2.2). These faults are similar to minor faults that are commonly observed throughout the Miocene Obispo and Monterey formations in the Irish Hills (DCPP FSAR Update, Section 2.5.1; References 9 and 11). Similar minor bedrock faults encountered beneath the power block strike generally northwest to west, dip 45 degrees to 85 degrees, and have displacements of up to several tens of feet (DCPP FSAR Update, Section 2.5.1.2.5.6, Figure 2.5-14).

The faults at the ISFSI site (Figure 2.6-8) are near-vertical (dip generally 70 to 90 degrees) and trend northwest, subparallel to the regional structural trend of the Pismo syncline (Figure 2.6-29). As described in Section 2.6.1.6.2.2, individual faults have vertical separation of a few tens of feet or less; cumulative vertical separation across the fault zone is greater than 50 ft, down on the northeast (Figure 2.6-11). Subhorizontal slickensides on the fault plane indicate a significant component of oblique strike slip, so total displacement is hundreds of feet. Detailed site investigations, including mapping and trench excavations, show that the individual faults generally extend across the ISFSI site and at least across the lower slope above the ISFSI.

The faults do not align with any significant bedrock fault in the plant site area (Figures 2.6-4 and 2.6-6), nor do the faults have major stratigraphic displacement. The origin of the faults may be related to one or more of three possible causes, all prior to 1 million years ago.

The faults most likely formed during a period of regional transtensional deformation during the Miocene, when normal and strike-slip faulting occurred in the region. This most directly explains the observed normal-oblique slip on the fault zone. A transition to transpressional deformation occurred during the late Miocene to Pliocene, and is well expressed in the offshore Santa Maria Basin and along the Hosgri fault zone (LTSP Final Report). The minor bedrock faults at the ISFSI site were subsequently rotated during the growth of the Pismo Syncline, although the faults occur near the flat-lying crest of a small parasitic anticline and, thus, have not been rotated significantly. Given this origin, the faults formed during the Miocene, contemporaneous with the transtensional formation of Miocene basins along the south-central coast of California, prior to 5 million years ago.

Alternatively, the minor faults may be secondary faults related to growth of the regional Pismo syncline (Figure 2.6-4), as concluded for the small bedrock faults at the power block (DCPP FSAR Update, p. 2.5-49, -50). As shown on Figure 2.6-29, the faults trend subparallel to the axis of the Pismo syncline, and are located near the crest of a small anticline on the southwestern limb of the syncline. The apparent oblique displacements observed on the faults may be related to bending-moment normal faults and right shear along the axial plane of the small anticline that formed in the Pliocene to early Quaternary. The zone of minor faulting may have used the area of diabase intrusion as an area of crustal weakness to accommodate tensional stresses along the axial plane of the anticline. As described in the DCPP FSAR Update, pages 2.5-14, -33, -34, and in the LTSP reports (LTSP Final Report, p. 2-34 to -38; and Reference 7, p. 2-10), growth of the Pismo syncline and related folds ceased prior to 500,000 years to 1,000,000 years ago. Thus, the observed minor faults also ceased activity prior to 500,000 years to 1,000,000 years ago.

A third alternative explanation for origin of the minor bedrock faults is that they are related to intrusion of the diabase into the Obispo Formation. Diabase is present locally in the ISFSI study area. Forceful intrusion, or magmatic stoping of the diabase may have produced faulting in response to stresses induced by the magma intrusion in the adjacent host rock. Hydrothermal alteration is extensive in the diabase. The friable sandstone and dolomite in the ISFSI study area are spatially associated with the zone of faulting (Figures 2.6-8 and 2.6-11), indicating the faults may have acted as a conduit for hydrothermal solutions. Assuming the hydrothermal fluids were associated with the diabase intrusion, the minor faults predate, or are contemporaneous with, intrusion of the diabase. Diabase intrusion into the Obispo Formation occurred in the middle Miocene (References 10 and 11), indicating the faulting would have occurred prior to or contemporaneous with the diabase intrusion in the middle Miocene, more than 10 million years ago. The faulting may have originated by transtensional regional deformation, as described above, then subsequently was modified by diabase intrusion.

In addition to their probable origin related to transtensional deformation in the Miocene (or to growth of the Pismo syncline in the Pliocene to early Quaternary, or to intrusion of the diabase in the middle Miocene), several additional lines of evidence indicate the minor faults are not capable and do not present a surface faulting hazard at the site:

- As described in the LTSP Final Report, pages 2-37 to -39, Plates 10 and 12), the Quaternary marine terrace sequence in the plant site vicinity is not deformed, providing direct stratigraphic and geomorphic evidence demonstrating the absence of capable faulting. The minor faults observed at the ISFSI site project northwest across, but do not visibly displace, any of the lower marine terrace platforms, within a limit of resolution of ±5 ft, indicating the absence of deformation in the past 120,000 years. Assuming the displacement does not die out at the coast, this resolution is enough to recognize the greater-than-50-ft of vertical separation on the faults at the ISFSI site.

- As described in the DCPP FSAR Update, (p. 2.5-35 to -50, Figures 2.5-13 to 2.5-16), similar northwest-trending minor faults were mapped in bedrock in the power block area. Detailed trenching investigations of these faults and mapping of the power block excavation provided direct observation that they do not displace and, hence, are older than the late Pleistocene (120,000 years old) marine terrace deposits. By analogy, the minor faults at the ISFSI site also would be older than late Pleistocene.

- Interpretation of aerial photographs taken before the 1971 excavation of the ISFSI site area (former borrow area) and construction of the raw water reservoir (Figure 2.6-31), shows there are no geomorphic features in the ISFSI study area (tonal lineaments, drainage anomalies, scarps) indicative of displacement of the minor faults prior to grading. The landscape in the ISFSI study area is interpreted to have formed in the middle to late Quaternary, about 430,000 years ago, based on the preserved remnants of marine terraces in the surrounding site area.

Based on these lines of evidence, the minor faults observed in bedrock at the ISFSI site are not capable; hence, there is no potential for surface faulting at the ISFSI site.

2.6.4 STABILITY OF SUBSURFACE MATERIALS

2.6.4.1 Scope

An extensive program of field investigations, in situ testing, and laboratory testing was conducted to define the static and dynamic characteristics of the soil and rock materials. The scope of the program is summarized in Table 2.6-1. A detailed discussion of the test procedures and results is presented in Reference 3, Data Reports B, C, F, G, H, and I, and Reference 9. The results are summarized below.

2.6.4.2 Subsurface Characteristics

The geology at the subgrade of the foundation of the ISFSI pads (elevation about 302 ft, 8 ft below the pad grade) is shown in Figure 2.6-32. The subsurface beneath the ISFSI pads consists of dolomite (Tof_{b-1}), sandstone (Tof_{b-2}), friable dolomite (Tof_{b-1a}), and friable sandstone (Tof_{b-2a}) (Section 2.6.1.7). The bedrock contains minor faults and joints

(Section 2.6.1.6.2). The groundwater table is near elevation 100 ft, about 200 ft below the foundation elevation. Clay beds of limited extent occur at a few locations under the ISFSI pads, below the surface of the cutslope, and in the existing slope above the pads (Section 2.6.1.7).

The geology at the CTF foundation grade is shown in Figure 2.6-32. At this grade (elevation about 286 ft), the bedrock consists of sandstone and friable sandstone (Section 2.6.1.8). At the site, the sandstone may have a few minor faults and joints, similar to those described in Section 2.6.1.6.2. Because the rocks are the same, the static and dynamic engineering properties of the rock at the foundation of the CTF were selected to be the same as those at the ISFSI pads.

The transport route traverses thick surficial deposits along nearly two-thirds of its route, including a new 500-foot-long section of thick, engineered fill near Patton Cove. It is constructed on engineered fill placed on dolomite and sandstone for the rest of its length (Section 2.6.1.9).

The detailed geologic characteristics of these rock units are described in Section 2.6.1.4.2.

2.6.4.3 Parameters for Engineering Analysis

2.6.4.3.1 ISFSI and CTF Sites

The static and dynamic engineering properties for use in foundation analyses of the rock at the ISFSI and CTF sites are as follows:

Density: A density of 140 pounds per cubic ft (pcf) was chosen as appropriate for foundation analyses (Reference 3, Data Report I).

Strength: A friction angle for the rock mass of 50 degrees was chosen as appropriate for foundation analyses. This friction angle is consistent with that used in the slope stability analyses (Section 2.6.5.1.2.3).

Poisson's ratio: A representative value of Poisson's ratio of 0.22 for dolomite and sandstone was selected as appropriate for analyses. A representative value of 0.23 was selected for friable rock. These values were derived from seismic velocity measurements in the bedrock below the footprint of the pads, and laboratory-based measurements on samples of bedrock from beneath the pads (Reference 2, Attachment 16; Reference 3, Data Report I).

Young's modulus: Representative values of Young's modulus of between 1.34 times 10^6 psi (mean) and 2.0 times 10^6 psi (84^{th} percentile upper bound) for dolomite and sandstone were selected as appropriate for analyses. A representative value of 0.2 times 10^6 psi was selected for friable rock. These values were derived from seismic velocity measurements in the bedrock below the footprint of the pads, and laboratory-based measurements on samples of bedrock from beneath the pads (Reference 2, Attachment 16; Reference 3, Data Report I).

2.6.4.3.2 Slopes

Static and dynamic engineering properties of soils and rock at the ISFSI site for use in slope stability analyses are as follows:

Rock Strength: A friction angle of 50 degrees for the rock mass was selected for stability analyses of the hillslope above the ISFSI pads. A range of friction angles between 16 degrees and 46 degrees for rock discontinuities was selected for stability analyses of the cutslopes behind the ISFSI pads. Further discussion of rock strength parameters is provided in Sections 2.6.5.1.2.3 and 2.6.5.2.2.3.

Clay Bed Strength and Unit Weight: The following parameters were defined for clay:

- unit weight, 115 pcf (Reference 3, Data Report G)
- shear strength, drained, $c' = 0$ psf; $\phi' = 22$ degrees
- shear strength, undrained, lower of $c = 800$ psf and $\phi = 15$ degrees or $\phi = 29$ degrees.

Further discussion of clay strength parameters is provided in Section 2.6.5.1.2.3.

Shear wave velocities: Representative values of shear wave velocities were selected for stability analyses (Section 2.6.5.1.3.2). These values were based on suspension geophysical surveys in boreholes beneath the footprint of the pads, as well as on data summarized in the Addendum to the LTSP Final Report (Reference 7, Chapter 5, Response to Question 19).

Dynamic shear modulus and damping values: Relationships of the dynamic shear modulus and damping values with increasing shear strain were selected for stability analyses (Section 2.6.5.1.3.2), based, in part, on literature review and dynamic tests of DCPP rock core samples performed in 1977 and 1988 (Reference 2, Attachment 21).

Additional considerations for the selection of rock and clay properties for specific static and dynamic stability analyses, and the calculation of seismically induced displacements are presented in Section 2.6.5.1.3.

2.6.4.3.3 Transport Route

As described earlier, the transport route generally follows existing Plant View, Shore Cliff, and Reservoir roads (Figure 2.6-7). The specifications for the construction of these roads required all fills to be compacted to 90-percent relative density, and the upper 2.5 ft to be compacted to 95-percent relative density. Fills on slopes were benched and keyed a minimum of 6 ft into the hillside (Reference 24). Based on these requirements, the road base and subgrade material are expected to be at least as capable for transporter loads and earthquake ground motions as the underlying rock and soil.

The new section of the transport route near Patton Cove will be constructed on engineered fill, as will a section of the route near the CTF (Figure 2.6-7). These fills and the overlying road subgrade also will be constructed to the same specifications as the existing roads (Reference 24). Both new roadway sections will support the imposed loads.

Where the transport route follows Plant View, Shore Cliff and Reservoir roads to Hillside Road, the alignment is founded on marine terrace deposits overlain by dense colluvial deposits. The remaining portions of the route, on Reservoir Road (beyond station 34+00), are founded on cuts made in the dolomite and sandstone. The static and dynamic engineering properties of the rock and soil deposits underlying the transport route are summarized in Reference 9, Tables 1 and 2.

2.6.4.4 Static Stability

The ISFSI pads will be founded on dolomite, sandstone, friable dolomite, and friable sandstone (Figure 2.6-32). The CTF will be founded on sandstone and friable sandstone (Figure 2.6-32). This bedrock will support the proposed facilities without deformation or instability. The borrow excavation removed between 75 ft and 100 ft of rock from the ISFSI and CTF sites. As a result, the existing rock is overconsolidated, and facility loads are likely to be much less than the former overburden loading on the rock (calculated to be about 10,000 to 14,000 psf). The overconsolidated state of the rock mass in the foundation precludes any settlement, including differential settlement between rock types, under the planned loading conditions.

As discussed in the DCPP FSAR Update, Section 2.5.4, there are no mines or oil wells in the plant site area. The two makeup-water wells draw water from fractured bedrock that is fed groundwater from the shallow alluvium along Diablo Creek (Section 2.5). No subsidence has been observed, nor is any expected, near these wells, which are approximately 2,500 ft east of the ISFSI.

Similarly, there is no evidence of solution features or cavities within the dolomite and sandstone strata, or in the friable dolomite and friable sandstone, beneath the ISFSI, or in the plant site area. Hence, there is no potential for karst-related subsidence or settlement at the ISFSI or CTF sites.

There is no potential for differential settlement across the different rock units (sandstone, dolomite, friable sandstone, friable dolomite) at the ISFSI, because the rock is well consolidated, joints and fractures are tight, and the friable rocks have almost no joints. Although no piping voids in the friable rocks are expected beneath the ISFSI pads, very small voids (a few inches across) are possible, as found in the friable dolomite in one of the trenches (Reference 3, Data Report D, trench T-20A. The foundation will be below the dilated zone for the borrow area cutslope (observed to be at about 4 ft in the trenches), and the rock mass is expected to be tight, with no open fractures. The rock mass is also overconsolidated, having had 100 ft of rock overburden removed from the location of the borrow area in the vicinity of the ISFSI for construction of the raw water reservoir and the 230-kV and 500-kV switchyards (Figure 2.6-10).

There is no potential for displacement on the faults at the sites, because the faults are not capable (Section 2.6.3). No differential displacement or settlement is expected during potential ground shaking.

2.6.4.5 Dynamic Stability

The ISFSI is located entirely within bedrock. There are no loose, saturated deposits of sandy soil beneath the pads or CTF site, and the groundwater table is near elevation 100 ft, about 200 ft below the foundation level. Therefore, there is no potential for liquefaction at either site.

The CTF foundation will be embedded into rock at least 20 ft below grade, as shown on Figure 2.6-32. This precludes the development of unstable foundation blocks under static or dynamic loading conditions.

Because the transport route subgrade will be on engineered fill on rock and well-consolidated surficial deposits, no liquefaction or other stability problems are expected.

2.6.4.6 Potential for Construction Problems

No significant construction-related problems are anticipated for preparation of the ISFSI and CTF foundations subgrade. The permanent groundwater table is about 200 ft below the planned foundation elevations (Section 2.5), and groundwater is not expected to rise to within the zone of foundation influence. The rock mass is generally tight, and does not have significant voids or soft zones that would require grouting or dental work, with the possible exception of small piping voids related to the friable dolomite. The fractures are tight or filled, and are tightly confined by the surrounding competent rock. The prepared foundation pads will be level, and will be a considerable distance from descending slopes, thus precluding development of unstable blocks or foundation loads into slopes.

2.6.5 SLOPE STABILITY

The ISFSI is located on the lower portion of a hillslope that has been modified by excavation for borrow materials during the construction of the DCPP. Construction of the ISFSI pads, the CTF, and portions of the transport route will include cutslopes and fills. The purpose of this section is to examine the stability of the hillslope and the cuts and fills. For each slope, the static and seismic stability were analyzed, and the potential seismically induced displacements were estimated.

The analyses, which are summarized on Table 2.6-2, show that the hillslope and the cutslopes above the ISFSI are generally stable under modeled seismic inputs, slope geometries, and material properties. The seismically induced displacements of the rock mass above the ISFSI, estimated using very conservative assumptions, are small. Under the modeled seismic loads, small rock wedges appear to be susceptible to movement in the cutslopes around the pads. These potential hazards will be mitigated by setbacks in slope design, rock anchors, and debris fences, as discussed in Section 4.2.1.1.9.1. The slopes along the transport route and below the CTF are stable.

For each slope analysis, the objectives and scope of the stability analysis are defined, and the analysis methods are described. The slope geometry and selection of material properties are then given. Finally, the results of the analyses for the hillslope above the ISFSI, the ISFSI cutslopes, the slope below the CTF, and slopes along the transport route are presented.

2.6.5.1 Stability of the Hillslope above the ISFSI

A critical section of the hillslope above the ISFSI was analyzed to examine the static and dynamic stability of the jointed rock mass along postulated slide surfaces. Analyses also were conducted to estimate potential seismically induced displacements due to the vibratory ground motions derived in Section 2.6.2. In addition, an analysis was conducted to evaluate the conservatism of the analysis parameters and examine the geologic data to estimate past displacements due to earthquakes.

2.6.5.1.1 Geometry and Structure of Rock Mass Slide Models

Cross section I-I' (Figure 2.6-18) parallels the most likely direction of potential slope failure, and illustrates the geometry of bedding in the ISFSI study area for analysis of slope stability. The cross section shows apparent dips, and the facies variation and interfingering of beds between the dolomite and sandstone (units Tof_{b-1} and Tof_{b-2}) beneath the slope. The clay beds, where orientation and extent are critical to this evaluation of slope stability, have been correlated based on stratigraphic position, projection of known bedding attitudes, and superposition of sandstone and dolomite beds (clay beds have not been allowed to cross cut dolomite or sandstone beds, but have been allowed to cross facies changes). These clay beds, as drawn, are a conservative interpretation of their lateral continuity for the analysis of the stability of the slope.

Individual clay beds that are, in places, thick (more than about 0.5-inch thick) in the dolomite, may continue up to several hundred feet. Thinner clay beds are less laterally continuous. On cross section I-I' (Figure 2.6-18), clay beds are not shown to extend continuously through the slope, but are terminated at set distances from exposures in boreholes, trenches, or outcrops, reflecting the estimates of possible lateral continuity. Because of the generally limited lateral continuity of the clay beds, potential large surfaces (greater than several hundred feet in maximum dimension) likely would require sliding on several clay beds, and stepping between beds on joints and in places through rock in a "staircase" profile. Stepping between basal clay failure surfaces would probably be localized where the individual clay beds are stratigraphically close and are thin and pinch out. Other likely locations for stair-stepping failure or structural boundaries for possible rockslide margins are at changes in structural orientation (transitions from monocline to syncline), and along the lateral margins of the slide. These limit the size of potential rock masses. Faults at the site are subparallel to the potential down-slope motion, and impart a strong near-vertical fabric in the rock mass. It is likely that lateral margins for potential larger rockslides would develop, at least partially, along these faults.

Based on the above considerations, three rock mass slide models, comprising ten potential slide surfaces, were defined for cross section I-I' of the hillslope:

Model 1. A shallow slide mass model (Figure 2.6-47) involving sliding rock masses along shallow clay beds encountered in trench T-14A and boring 01-I. It toes out at the upper part of the tower access road.

Model 2. A medium-depth slide mass model (Figure 2.6-48) involving sliding rock masses along clay beds encountered at depths of between about 25 ft and 175 ft in borings 01-F, 00BA-1, and 01-I, and trench T-11D. It toes out on the slope between the ISFSI and below the tower access road.

Model 3. A deep slide mass model (Figure 2.6-49) involving sliding along deep clay beds encountered in borings 01-H, 01-F, 00BA-1, and 01-I at depths of between about 50 ft and 200 ft. It toes out behind or below the proposed ISFSI cutslope and pads.

Model 1 has been segmented into two possible geometries, labeled 1a and 1b on Figure 2.6-47. These two modeled slide blocks daylight at a clay bed encountered in trench T-14A (model 1a), or along the projected dip of a clay bed encountered in boring 01-I. The failure headscarp/tension break-up zone extends upward from the inferred maximum upslope extent of the clay bed in trench T-14A (model 1a), or from the inferred likely uphill extent of a clay bed encountered in boring 01-I.

Model 2 has been segmented into three subblocks: 2a, 2b, and 2c (Figure 2.6-48). The three blocks daylight along a clay bed encountered in trench T-11D (2a and 2b), or along the dip projection of a clay bed encountered in boring 00BA-1 (2b). Model 2a breaks up near trench T-14A at the location of a major structural discontinuity for potential slide blocks; the transition between the monocline and syncline where the bedding geometry (strike and dip) changes. Models 2b and 2c break up from the basal failure planes in a "stair-stepping" manner between clay beds, and have a common headscarp that daylights about 50 ft above the brow of the 1971 borrow cut excavation. The geometry of the headscarp break-up zone is inferred to be controlled by the uphill limit of clay beds encountered in the borings, and dominant steep joint fabric in the rock mass.

Model 3 has been segmented into three subblocks: 3a, 3b, and 3c. The three blocks daylight in the ISFSI pads cutslope, or at the base of the cutslope (Figure 2.6-49). All three modeled blocks have basal slide surfaces along clay beds encountered in borings 01-F, or 00BA-1 and 01-I. Models 3a and 3b break up with headscarp/tension zones at the location of the structural change in bedding geometry described for model 2a (3a and 3b), or about 75 ft above the top of the borrow cut (3c) at an inferred maximum uphill extent of clay beds encountered in boring 01-I. Model 3 has been further segmented into 3c-1, which daylights beyond the ISFSI pads, and 3c-2, which daylights at the base of the first cutslope bench.

For all models, the toe daylight geometry reflects the propensity for failure planes to break out along bedding planes and along the projection of clay beds. In contrast, the geometry of the headscarp/tension failure was inferred to be controlled by the dominant steep (greater than 70 degrees) joint/fault fabric in the rock mass.

2.6.5.1.2 Static Stability Analysis

2.6.5.1.2.1 Method

The static stability analysis of the hillslope was conducted using the computer program UTEXAS3 (Reference 25). Spencer's method, a method of slices that satisfies force and moment equilibria, was used in the analysis.

2.6.5.1.2.2 Assumptions

The following assumptions were made:

- The clay beds are saturated. This assumption is reasonable, because during the rainy season, rainfall would infiltrate the slope through the fractured rock and perch temporarily on the clay beds, and would saturate at least the upper part of the clay.

- There is little water in the slope. This assumption is reasonable, because the groundwater table is about 200 ft below the ISFSI site, and the rock is fractured and well-drained. There are no springs from perched water tables near the ISFSI slope.

- The lateral margins of the potential slide masses have no strength. This is conservative, because the margins of a potential failure wedge would, in part, follow discontinuous joints, small faults, and, in part, break through rock. Friction between rock surfaces and by asperity overriding, or shearing along the lateral slide margins would provide some resistance to sliding.

- The upper 20 ft of the rock mass forming the head of a potential sliding mass has been modeled as a tension crack, that is, the zone has been given no strength. This assumption is conservative, because the dilated zone is only about 4 ft deep (Reference 2, Attachment 16).

- The head of the slide below the tension crack would break irregularly along joints and clay beds and through some rock. The strength assigned to this rock mass is discussed below.

- The orientation, continuity, and extent of the clay beds is assumed to be as shown on cross section I-I'. This is reasonable, because the extent of the clay beds and their dip is based on extensive geologic data from the ISFSI study area.

- The strength of the clay (discussed below) is assumed to apply along the entire length of a clay bed, as shown on cross section I-I'. This is conservative, because the clay beds are commonly thin and irregularly bedded, providing rock contact through the beds, thereby increasing the strength.

2.6.5.1.2.3 Material Properties

Drained and undrained clay-bed strength parameters were developed from the results of strength and index testing performed on clay-bed samples collected from borings and trenches excavated at the site. Strength tests consisted of consolidated-undrained triaxial compression tests (CU) with pore pressure measurements, drained and undrained monotonic direct-shear tests, and undrained cyclic direct-shear tests (Reference 3, Data Report G). Atterberg limits tests were conducted on the clay-bed samples to measure their liquid limits (LL) and plasticity indices (PI). Drained strength parameters were developed from the results of the CU triaxial and drained monotonic direct-shear tests, and from published empirical correlations with Atterberg limits. Drained strength was taken as the post-peak strength (defined as strength at the maximum displacement) from the drained direct-shear tests, and the lower of either the stress at 5 percent axial strain or the post-peak strength for the CU tests. Undrained strength parameters were developed from the results of the CU triaxial, undrained monotonic and cyclic direct-shear, and Atterberg limits tests. As with the drained strength parameters, the undrained strength was taken as post-peak strength from the monotonic direct-shear tests, and the lower of either the stress at 5 percent axial strain or the post-peak strength for the CU tests.

Undrained strength parameters $c = 800$ psf and $\phi = 15$ degrees were determined from analysis of the undrained strength data (Figure 2.6-50). Similarly, $c' = 0$ psf, and $\phi' = 22$ degrees were selected based on analysis of the drained strength data (Figure 2.6-51). Because the overburden pressure under the original ground surface is higher than the consolidation pressure used in most of the laboratory strength tests, overconsolidation effects are likely present in the laboratory test results. This effect was conservatively removed at low confining pressures by estimating corresponding undrained shear strengths for a maximum overconsolidation ratio (OCR) of 3.0 and determining an equivalent friction angle, as shown in Figure 2.6-50, of 29 degrees (with no cohesion). Accordingly, undrained strength parameters were selected as the lower of $\phi = 29$ degrees and $\phi = 15$ degrees (Figure 2.6-50).

Two different empirical methods were used to develop in situ rock mass strength envelopes for the dolomite and sandstone (units Tof_{b-1} and Tof_{b-2}): Barton and Choubey (Reference 26), and Hoek and Brown (Reference 27).

The Barton-Choubey method estimates the in situ shear strength of naturally occurring rock discontinuities (joints, bedding planes, faults) in relatively hard rock on the basis of field and laboratory measurements of discontinuity properties. Shear strength envelopes for discontinuity surfaces within the shallow rock mass at the ISFSI site were used in the stability analyses of surficial rock mass sliding, wedge, and topple slope failures in the proposed cutslope above the ISFSI, and frictional sliding along shallow rock discontinuities below the foundation of the ISFSI pads. The range of strength envelopes for dolomite (Tof_{b-1}) and sandstone (Tof_{b-2}) discontinuities calculated using the Barton-Choubey method are plotted in Figure 2.6-52, using the derived stress-strain data.

The Hoek-Brown method is an empirically based approach that develops nonlinear shear-strength envelopes for a rock mass, and accounts for the strength influence of discontinuities (joints, bedding planes, faults), mineralogy and cementation, rock origin (for example, sedimentary or igneous), and weathering. The resulting rock-mass shear-strength envelopes were used for evaluation of the ISFSI pads and CTF foundation properties, and for stability analyses of potential bedrock failures within jointed confined rock at the ISFSI site. The Hoek-Brown method is for rock masses having similar surface characteristics, in which there is a sufficient density of intersecting discontinuities such that isotropic behavior involving failure along multiple discontinuities can be assumed. The method is not for use when failure is anticipated to occur largely through intact rock blocks, or along discrete, weak, continuous failure planes (such as weak bedding interfaces). The structure (or failure) geometry must be relatively large with respect to individual block size. The rock mass conditions and relative size differences between rock blocks, potential deep-seated masses, and the ISFSI and CTF foundations for which the Hoek-Brown criterion is being applied are appropriate and meet these rock-mass requirements. Strength envelopes for dolomite and sandstone calculated using the Hoek-Brown method are plotted in Figures 2.6-53 and 2.6-54, using the derived stress-strain data.

A strength envelope having a friction angle, ø, of 50 degrees and cohesion, c, of zero was selected for the portion of the rock mass consisting of dolomite (unit Tof_{b-1}) and sandstone (Tof_{b-2}) below the dilated zone (Figures 2.6-53 and 2.6-54). This envelope is lower than (but approximately parallel to) the envelopes for either dolomite or sandstone derived from the empirical Hoek-Brown method, and is more nearly equal to the post-peak strength envelope for the friable sandstone derived from laboratory tests of nonjointed rock blocks. The interpreted post-peak strength envelope for the friable rocks has a friction angle, ø, of 51.2 degrees and cohesion, c, of zero (Figure 2.6-55). Accordingly, a ø of 50 degrees was also selected for the friable rocks.

2.6.5.1.2.4 Results

The static factors of safety computed using UTEXAS3 (Reference 25) for the ten slide surfaces analyzed are shown in Table 2.6-3 (Reference 2, Attachment 19). The table shows that, in all cases, the computed factor of safety varies between 1.62 and 2.86. It is, therefore, concluded that the hillslope is stable.

2.6.5.1.3 Seismically Induced Displacements

2.6.5.1.3.1 Method

The selected slide surfaces were analyzed to estimate the potential for earthquake-induced displacements by using the concept of yield acceleration proposed by Newmark (Reference 28) and modified by Makdisi and Seed (Reference 29). The procedure used to estimate permanent displacements involved the following steps:

- A yield acceleration, k_y, at which a potential sliding surface would develop a factor of safety of unity, was estimated using limit-equilibrium, pseudostatic slope-stability methods. The yield acceleration depends on the slope geometry, the phreatic surface conditions, the undrained shear strength of the slope material, and the location of the potential sliding surface.

- Computations were made using UTEXAS3 (Reference 25) to identify sliding masses having the lowest yield accelerations. A two-stage approach was used that consisted of first calculating the normal stresses on the failure plane under pre-earthquake (static) loading conditions using drained strength properties. For each slice, the normal effective stress on the failure plane was then used to calculate the undrained strength on the failure plane. In the second stage of the analysis, horizontal seismic coefficients were applied to the potential sliding mass, and the stability analysis was repeated using the undrained strengths calculated at the end of the first stage. The yield acceleration was calculated by incrementally increasing the horizontal seismic coefficient until the factor of safety equaled unity.

  The material properties used for the UTEXAS3 analysis (unit weights and shear strength) were the same as those for the static stability calculations. Drained rock strengths were used for both stages of the yield acceleration analysis. Drained clay strengths were used for the first stage and a bilinear undrained strength envelope was used for the clay beds in the second stage of the analysis.

- The seismic coefficient time history (and the maximum seismic coefficient, k_{max}) induced within a potential sliding mass was estimated using two-dimensional, dynamic finite-element methods. The seismic coefficient is the ratio of the force induced by an earthquake in a sliding block to the total mass of that block. Alternatively, the seismic coefficient time history can be obtained directly by averaging acceleration values from several finite-element nodes within the sliding block at each time interval, as long as variations in the accelerations between nodes are not substantial.

- Earthquake-induced seismic coefficient time histories (and their peak values, k_{max}) for the potential sliding surfaces were computed using the two-dimensional, dynamic finite-element analysis program QUAD4M (Reference 30). This is a time-step analysis that incorporates a Rayleigh damping approach, and allows the use of different damping ratios in different elements. The program uses equivalent linear strain-dependent modulus and damping properties, and an iterative procedure to estimate the nonlinear strain-dependent soil and rock properties.

- The QUAD4M program (Reference 30) was used to analyze three slide surfaces (1b, 2c, and 3c) for which the calculated yield acceleration values were the lowest (Table 2.6-3). Because the base of the finite element mesh is at a depth of 300 ft, and because QUAD4M only allows the input motion to be applied at the base, the base motion was first computed by deconvolving the surface ground motion using a one-dimensional wave propagation analysis (SHAKE, Reference 31) to obtain motions at the level of the base of the two-dimensional finite-element model.

- For a specified potential sliding mass, the seismic coefficient time history of that mass was compared with the yield acceleration, k_y. When the seismic coefficient exceeds the yield acceleration, downslope movement will occur along the direction of the assumed failure plane. The movement will decelerate and will stop after the level of the induced acceleration drops below the yield acceleration, and the relative velocity of the sliding mass drops to zero. The accumulated permanent displacement was calculated by double-integrating the increments of the seismic coefficient time history that exceed the yield acceleration.

2.6.5.1.3.2 Material Properties

The material properties needed for the QUAD4M analyses are the unit weight, the shear modulus at low shear strain, G_{max}, and the relationships describing the modulus reduction and damping ratio increase with increasing shear strain (Reference 2, Attachment 20, Figures 7 and 8). The rock mass was modeled as having a unit weight and shear wave velocity that vary with depth, based on field measurements of shear wave velocity and laboratory values for unit weight. The shear wave velocity profile used is shown in Reference 2, Attachment 20, Figure 6.

2.6.5.1.3.3 Seismic Input

The seismic input consisted of the five sets of time histories developed to match the ILP ground-motion spectra (Section 2.6.2.5). Both fault-parallel and fault-normal components were defined for each of the five motions postulated to occur on the Hosgri fault zone at a distance of 4.5 kilometers from the site. Because the strike of the Hosgri fault zone is

36 degrees from the orientation of cross section I-I', the input motions were rotated to the direction of cross section I-I'. For a specified angle of rotation, there will be 10 rotated earthquake motions along I-I', because the fault-normal component will be either positive (to the east) or negative (to the west) and each needs to be considered separately.

2.6.5.1.3.4 Analysis

Acceleration time-histories were calculated for 26 locations within the three selected slide surfaces (1b, 2c, and 3c) (Reference 2, Attachment 21, Figure 2). Average acceleration time histories were computed for each rock mass. Sensitivity studies using a cross section having a slightly different orientation indicated that the calculated peak accelerations are not significantly influenced by orientation or the total height of the hillslope.

Because the slope at the ISFSI site is a rock slope and its seismic response is anticipated to be generally similar to the input rock motions, the earthquake-induced deformation was first estimated using a Newmark-type analysis for a sliding block on a rigid plane (Reference 28). An estimated yield acceleration of 0.20 g (Table 2.6-4) was used to calculate the deformation of the sliding block. The displacement was computed for the negative direction (representing down-slope movement) only. The down-slope permanent displacement of the sliding block was integrated by using rock motions in the positive direction (representing up-slope direction) only. These preliminary displacement estimates were used to help in selecting the ground-motion time histories that provided the largest permanent displacement.

Table 2.6-4 shows the calculated down-slope permanent displacements (for the five sets of rotated rock motions) following the Newmark sliding block approach. The results (for a rotation angle ø = 36 degrees) indicate that, on average, ground-motion sets 1, 3, and 5 provided the largest displacements (2.4 ft to 2.9 ft). A sensitivity analysis was performed to evaluate the effect of the uncertainty in the direction of cross section I-I' (Figure 2.6-18) relative to the fault strike (Figure 2.6-29). For this analysis, ø was varied by ±10 degrees. As shown in Table 2.6-4, for a ø of 46 degrees, ground-motion set 1 (with a negative fault-normal component) and set 5 (with a positive fault-normal component) produced the largest displacements (3.3 ft and 2.8 ft, respectively). This is because the fault-normal components are stronger than the fault-parallel components in most cases, and for a ø of 46 degrees, the I-I' direction is closer to the fault-normal direction. Set 3, when combined with the negative fault-normal component, produced 2.8 ft of displacement; however, when combined with the positive fault-normal component, produced a much smaller displacement than that of set 5. Based on the rigid sliding block analyses, two rotated ground motions: set 1 motions (rotated 46 degrees with a negative fault-normal component) and set 5 motions (rotated 46 degrees with a positive fault-normal component) were used in the two-dimensional finite-element analyses (Reference 2, Attachment 20).

The potential sliding masses and the node points of the computed acceleration time histories were used to develop average-acceleration time histories for each sliding mass. The seismic coefficient time histories were then double integrated to obtain earthquake-induced displacements for any specified yield acceleration. As mentioned before, the integration was made for the ground-motion amplitudes exceeding the yield acceleration in the positive direction only, and the resulting displacement was computed for potential sliding in the down-slope direction. The relationships between calculated displacement and yield acceleration, k_y, for the three potential sliding masses considered are presented in Reference 2, Attachment 21, Figures 5 and 6, for input motion sets 1 and 5, respectively. The normalized relationships between calculated displacement and yield acceleration ration, k_y/k_{max}, for the three potential sliding masses considered are presented on Figures 7 and 8 of Reference 2, Attachment 21, for input motions sets 1 and 5, respectively.

2.6.5.1.3.5 Results

The earthquake-induced down-slope displacements for the potential slip surfaces analyzed are summarized on Table 2.6-5. Computed permanent displacements using ground-motion set 1 as input range from about 3.1 ft, for sliding mass 1b, on the upper slope, to about 1.4 ft, for sliding mass 3c, on the lower slope. Computed displacements using ground-motion set 5 as input were lower, and ranged from 2.4 ft, for sliding mass 1b, to about 0.6 foot, for sliding mass 3c.

Sliding mass 1b (located in the upper portion of the slope) daylights at a horizontal distance of about 400 ft from the toe of the cutslope behind the pads. As mentioned above, the computed displacements for this sliding mass ranged between 2.4 ft and 3.1 ft. Sliding mass 2c (located in the middle of the slope) daylights about 100 ft from the toe of the cutslope. The computed displacements for this sliding mass ranged between 2.5 ft and 3 ft. The computed displacements for sliding mass 3c (located in the lower portion of the slope) ranged between 0.6 ft and 1.4 ft. Two additional potential sliding masses were analyzed in addition to 3c: sliding mass 3c-1, which daylights 70 ft beyond the north edge of the ISFSI pads, and sliding mass 3c-2, which daylights at the first bench on the cutslope behind the pads (Figure 2.6-56). The computed displacements for sliding mass 3c-1 ranged between 0.4 ft and 1.2 ft. For sliding mass 3c-2, the computed displacements ranged between 0.8 ft and 2.0 ft, depending on the input motion used in the analysis. Given the planned mitigation measures for the ISFSI (Section 4.2.1.1.9), none of the potential displacements indicated by any of the rock mass models would impact the ISFSI pads.

2.6.5.1.3.6 Estimating Displacements Based on Geologic Data

Potential slide mass displacement can be estimated by evaluating past performance of the hillslope above the ISFSI site. As described below, the topographic ridge upon which the ISFSI site is located has been stable for the past 500,000 years or more (Reference 2, Attachment 16; LTSP Final Report, p. 2-38). A geologic analysis of slope stability, therefore, provides insights into the minimum shear strength and lateral continuity of the clay beds used in the analysis and, hence, a check on the conservatism of the assumptions used to analyze the stability of the hillslope above the ISFSI site.

Geomorphic and geologic data from mapping and trenching in the ISFSI study area show no evidence of past movements of large rock masses on the slope above the ISFSI (Reference 2, Attachment 16). Analysis of pre-construction aerial photographs shows no features indicative of such landslides: no arcuate scarps, no vegetational lineaments indicative of filled fissures, and no textural differences in the rock exposures or slopes indicative of a broken rock mass at the ISFSI study area. Similarly, the many trenches excavated into the slope, the tower access road cuts, the extensive outcrops exposed by the 1971 borrow cut, and the many borings exposed no tension cracks or fissure fills on the hillslope (Reference 3, Data Reports A, B, and D). Open cracks or soil-filled fissures greater than 1 foot to 2 ft in width would be easily recognized across the slope, given the extensive rock exposure provided by the borrow cut. Therefore, it is reasonable to conclude that any cumulative displacement in the slope greater than 3 ft would have produced features that would be evident in rock slope. The absence of this evidence places a maximum threshold of 3 ft on the amount of cumulative slope displacement that could have occurred in the geologic past.

The hillslope at the ISFSI site is older than at least 500,000 years, because remnants of the Q_5 (430,000 years old) marine terrace are cut into the slope west of the ISFSI site (Reference 2, Attachment 16; LTSP Final Report, p. 2-18). Preservation of the terrace documents that the slope has had minimal erosion (a few tens of feet) since that time. Moreover, gradual reduction of the ridge by erosion at the ISFSI site would not destroy deep tension cracks or deep disruption of the rock mass; these features would be preserved as filled fractures and fissures, even as the slope is lowered.

The topographic ridge upon which the ISFSI site is located is presumed to have experienced strong ground shaking from numerous earthquakes on the Hosgri fault zone during the past several hundred thousand years. Studies for the LTSP (LTSP Final Report) estimated a recurrence interval of 11,350 years for a magnitude 7.2 earthquake on the Hosgri fault zone. Assuming that deep cracks from rock mass movements during the past 400,000 years would have been preserved, approximately 35 to 40 large earthquakes have occurred during the past 400,000 years without causing significant (greater than 3 ft) cumulative slope displacement. .

2.6.5.1.3.7 Assessment of Conservatism in Displacement Estimates

Because a major portion of the rock mass slide surfaces analyzed is along clay beds, an approximate analysis of the slope at its pre-borrow excavation configuration was conducted to assess the degree of conservatism associated with the assumptions used in the analysis, in particular, the lateral continuity and shear strength of the clay beds. The calculation consisted of extending the potential slide surfaces 1a and 1b (located in the upper part of the slope) to the pre-excavated ground surface, and varying the undrained strength of the clay bed until a yield acceleration corresponding to a displacement of 4 inches was calculated. Ground-motion sets 1 and 5, multiplied by 1.6 and rotated through the same angle as in the previous analysis (ϕ = 46 degrees) were used. Several combinations of the undrained strength parameters c and ϕ were considered in the analysis. The results indicate that the calculated undrained clay bed shear strength is significantly greater than the undrained shear-strength parameters developed from laboratory test data. It is reasonable to conclude, therefore, that the clay bed strength properties used in the analyses are conservative (that is, the clay beds are thin, with rock-to-rock contact through some of the length of the bed that increases the strength), and that the clay beds are more limited in lateral extent than was assumed in analysis.

2.6.5.2 Stability of Cutslopes

Construction of the ISFSI will involve preparing cutslopes along the southwestern, southeastern, and northeastern margins of the site (Figure 2.6-32). The stability of these cutslopes was evaluated using kinematic, pseudostatic, and dynamic analyses.

2.6.5.2.1 Kinematic Analysis

Three potential failure modes were identified for analysis of the cutslopes along the margins of the ISFSI site (Reference 2, Attachment 17):

- planar sliding on a single discontinuity
- wedge sliding on the intersection of two discontinuities
- toppling of blocks

2.6.5.2.1.1 Method

Kinematic analyses, based on the collected fracture data, were performed for each of the three ISFSI site cutslopes: east cutslope (northeast), back cutslope (southeast), and west cutslope (southwest), proposed to be excavated at an inclination of 70 degrees. Discontinuity data from the trenches and outcrops in the area of each cutslope (Reference 3, Data Report F) were applied in the analysis (Figures 2.6-57, 2.6-58, and 2.6-59). Data from outcrops along Reservoir Road were applied in the analyses of the slope above the road (Figures 2.6-37 and 2.6-38).

Using the Markland procedure (Reference 32), discontinuities were analyzed for three modes of rock block failure. All kinematic analyses used a friction angle (ø) of 28 degrees to represent sliding resistance along dilated joints or discontinuities in the rock mass. This friction angle value represents a conservative estimate for rock friction, and was selected on the basis of laboratory direct-shear test data on borehole core joints, and estimation of in situ shear strength using the Barton-Choubey method (Figure 2.6-52). Discontinuities generally are 2 ft to 4 ft long, and locally up to 14 ft long (Reference 3, Data Report F).

2.6.5.2.1.2 East Cutslope

Kinematic analyses of the east cutslope are shown on Figure 2.6-57. The analysis shows low potential for toppling failure, as only a few random discontinuities plot within this failure envelope. There is a moderate to high potential for planar sliding failure, as numerous discontinuities from discontinuity set 2, as well as some random discontinuities, plot within the planar sliding failure envelope. Potential also exists for wedge sliding along the intersection lines between discontinuity sets 1 and 2, and between sets 2 and 4; though these intersections plot very close to the failure envelope, these lines represent the average orientation of the set and there is a scatter of orientations around this mean. Thus, there is a moderate to high potential for planar sliding, and a moderate to high potential for wedge sliding failures in the east cutslope.

2.6.5.2.1.3 Back Cutslope

Kinematic analyses of the back cutslope are shown on Figure 2.6-58. The analysis shows low potential for toppling failure, as only a few random discontinuities plot within this failure envelope. Planar sliding failure represents a low to moderate potential, as a few discontinuities from sets 1 and 2, as well as a number of random discontinuities, plot within the planar sliding failure envelope. Potential exists for wedge sliding along the intersection line of discontinuity sets 2 and 3, whereas another intersection (1 and 3) plots outside but relatively close to the failure envelope and should be considered a potential hazard, given that these lines represent the average orientation of the set and that there is a scatter of orientations around this mean. Thus, there is a high potential for wedge failure and minor planar sliding failure in the back cutslope.

Reducing the rock friction angle value to a value appropriate to represent the strength of the bedding-parallel clay beds results in a larger failure envelope, and introduces the possibility of planar sliding failures along the clay beds in the back cutslope and in the hill above the ISFSI site. Static and dynamic modeling of potential sliding along clay beds is presented in Sections 2.6.5.1.2 and 2.6.5.1.3.

A portion of the back cutslope will be in friable dolomite. This material does not behave as a jointed rock mass but, rather, behaves as a stiff soil. The potential exists for slumps within this material.

2.6.5.2.1.4 West Cutslope

Analyses of the west cutslope are shown on Figure 2.6-59. The west cutslope shows a high potential for topple failure. The majority of discontinuity set 2, as well as some fractures from set 1, plot within the zone of potential failure for toppling. However, analyses of planar and wedge sliding failures show low and very low potential, respectively, for these modes of failure in the west cutslope, as very few discontinuities (and none belonging to any of the defined sets) fall within the failure envelope for planar sliding, and none of the discontinuity intersections fall within the failure envelope for wedge sliding failure. Thus, the failure mode for the west cutslope is topple failure. A portion of the southwest side of the ISFSI slope will be in a fill prism; therefore, the topple failure mode would not be applicable there.

2.6.5.2.1.5 Results

None of the three potential failure modes described above pose a threat to the ISFSI, because potential displacements will be mitigated using conventional methods and appropriate setback distances from the toe of cutslopes, as discussed in Section 4.2.1.1.9.

2.6.5.2.2 Pseudostatic Analyses of Potential Wedge Slides

A pseudostatic seismic analysis of the wedges identified in the kinematic analysis was conducted to assess cutslope stability under seismic loads.

2.6.5.2.2.1 Geometry and Dimensions of Wedge Blocks

The size of potential wedge block failures in the ISFSI cutslope (Figure 2.6-32) will be controlled, in part, by the spacing, continuity, and shear strength of discontinuities in the rock mass. Both the dolomite (unit Tof_{b-1}) and sandstone (unit Tof_{b-2}) bedrock at the site are jointed and faulted. Joints and faults in friable dolomite and friable sandstone are less well developed and do not control the mechanical behavior of this rock; rather, strength of the friable rock is controlled primarily by the cementation properties of the rock.

The orientation of the joint sets varies somewhat across the site; however, field measurements of the discontinuities (Reference 3, Data Report F) document two primary, steeply dipping, joint sets: a west- to northwest-striking set, and a north-northwest- to north-striking set. The joints are continuous for about 1 foot to about 14 ft, and commonly die out or terminate at subhorizontal bedding contacts. Field observations from surface exposures and trenches show that the joints commonly are slightly open or dilated in the upper 4 ft, probably due to the stress unloading from the 1971 borrow excavation and surface weathering. Dilation of the joints reduces the shear strength of the discontinuity. To be conservative, the zone of near-surface dilation was assumed to extend to a depth of 20 ft on the ISFSI cutslope.

Joints in the dolomite typically are spaced about 1 ft to 3 ft apart, and divide the rock mass into blocks having an average dimension of 1 foot to 3 ft; typical maximum dimensions are about 14 ft (Reference 3, Data Report F, Table F-6). Twenty ft was conservatively assumed to be the maximum block size in the wedge block stability analysis. This dimension would allow for multiple-block wedges to form in the cutslope.

2.6.5.2.2.2 Method

Kinematic analyses (Section 2.6.5.2.1) show that the proposed east and back cutslopes along the southeast margin of the ISFSI pads have potential for wedge slides. The back cutslope would be the highest, and also has the least stable geometry with respect to rock mass discontinuities. Pseudostatic wedge analyses of these cutslopes were performed to evaluate the potential for shallow wedge slides along joints emerging on the cut faces through the zone of stress-relieved rock (Reference 2, Attachment 18). Analyses were performed using SWEDGE

(Reference 33) a computer program for the analysis of translational slip of surface wedges in rock slopes defined by two intersecting discontinuity (joint, fault, shear, or fracture) planes, a slope face, and an optional tension crack. The program performs analyses using two techniques: probabilistic analyses (probability of failure), and deterministic analyses (factor of safety). For probabilistic analyses, variation or uncertainty in discontinuity orientation and strength values can be accounted for, resulting in safety factor distribution and prediction of failure probability. For deterministic analyses, a factor of safety is calculated for a specified wedge geometry and a set of strength parameters.

Results from the kinematic analysis show that the most critical wedges are formed by intersections between steeply dipping, northwest-trending faults and joints that intersect at a high oblique angle. These fault/joint intersections plunge steeply to the northwest, and some could daylight on the proposed back cut. These wedge geometries were specifically modeled in the SWEDGE analyses. Planar sliding along low-angle clay beds is addressed in Section 2.6.5.1.3.

Probabilistic analyses were performed to evaluate the overall susceptibility of the slope to wedge failure, and to evaluate the sensitivity of failure to variations in material strength, geometry, and water conditions. Twenty-six separate model runs were performed using the probabilistic approach. Each probabilistic model run included 1,000 Monte Carlo iterations of input parameter variations to generate a probability distribution. After completing the probabilistic analyses, deterministic analyses were performed for the most critical modeled conditions in terms of probability of failure, and size and weight of wedge. Sixteen separate deterministic models were run that included variations in slope height and inclination, wedge geometry (with and without tension cracks), and degree of water saturation.

2.6.5.2.2.3 Rock Wedge Strength Parameters

Strength values derived from the Barton-Choubey method (Reference 26) (Figure 2.6-52) were used for the analyses of potential shallow rock wedge failures of rock blocks along existing discontinuities within the stress-relieved outermost rock zone directly behind the cutslope face. Cohesion was neglected. The friction angles selected and used in the probabilistic analyses ranged from 16 degrees (clay-coated faults) to 46 degrees (clay-free joints), and from about 26 degrees to 31 degrees, respectively, for the deterministic analyses.

2.6.5.2.2.4 Assumptions

The following assumptions and parameters were used for the pseudostatic analysis:

- Three 70-degree cutslope geometrics were analyzed for the back cutslope: a 20.5-ft-high cutslope, a 31.8-ft-high cutslope, and 52.3-ft-high cutslope. The 20.5-ft-high cutslope models potential failures from base of cut to the intermediate bench

(Figure 2.6-60). The 31.8-ft-high cutslope models potential failures from the intermediate bench to top of cut. The 52.3-ft-high cutslope models potential failures from base of cut to top of cut, at an "average" inclination of about 47 degrees.

- Each slope was evaluated with and without tension cracks, for example, in the case of the back cutslope, tension cracks were located at distances of 1.6 ft and 23 ft back from the crest of the slope. These distances are reasonable for a slope model, because the fractures at the ISFSI site have spacings of up to several feet, and the cutslope bench is 25 ft wide. One set of tension cracks (at 23 ft) specifically models the potential for tension cracks to develop along a backfilled trench for a drainage pipe at the back of the intermediate bench.

- Analyses were performed for each cutslope configuration using (1) a horizontal (out-of-slope) pseudostatic seismic coefficient of 0.5 g, and (2) dry and partially saturated rock mass (water levels at one-half the height of the slope). The value of 0.5 g was derived using the procedure described by Ashford and Sitar (Reference 34), and is approximately two-thirds of the peak horizontal acceleration of 0.83 g from the LTSP spectra shown in Figure 2.6-43. This level of reduction has been shown to be appropriate for pseudostatic analyses of slopes (Reference 35).

2.6.5.2.2.5 Results

The results of the pseudostatic probabilistic SWEDGE analysis for the back cutslope and the east cutslope are presented in Tables 2.6-6 and 2.6-7, respectively. Results of the deterministic analyses for these cutslopes are presented in Table 2.6-8. The probabilistic analyses show that rock wedges in the modeled cutslopes (Figure 2.6-60) have a low probability of failure in a dry condition. The probability of failure increases significantly with partial saturation of the slope and the addition of seismic force. The largest predicted wedge, with a factor of safety less than 1.0, weighs 4,475 kips and has an estimated face area of 2,649 square ft (Table 2.6-6).

Deterministic analyses were performed to calculate support forces required to restrain the wedges and achieve a factor of safety of 1.3 under seismic loading conditions (Table 2.6-8). The calculated total support force to stabilize the largest predicted wedge to a factor of safety of 1.3 is 1,881 kips. For an assumed anchor spacing of 5 ft by 5 ft, this force translates to 32 kips per anchor (Table 2.6-8). The design of slope reinforcement to prevent wedges from displacing is described in Section 4.2.1.1.9.

2.6.5.3 Slope Stability at CTF Site

In a previous submittal examining the stability of the slope behind DCPP Unit 1 (Reference 9, p. 30-36), it was shown that displacements along the interface between colluvial and terrace deposits within the underlying bedrock would be limited. The results of this analysis also indicate that the farthest extent of these estimated displacements is at the uppermost edge of the colluvium/bedrock interface, which is more than 100 ft west of the CTF (Figure 2.6-7), and similar to the relationship shown in cross sections B-B''' and L-L' (Figures 2.6-11 and 2.6-19). Therefore, slope-related displacements at the CTF site are estimated to be nil.

2.6.5.4 Slope Stability Along the Transport Route

2.6.5.4.1 Static Stability

As discussed in Section 2.6.1.12.3, the Patton Cove landslide is more than 100 ft from the transport route, and it is not likely to encroach headward to where it would affect the route.

Small debris flows (up to 3 ft deep on the road) could impact the roadway as they issue from the swales on the steep slopes above the road (Section 2.6.1.12.3). These debris flows occur infrequently during or shortly following severe rainstorms (Reference 7), and are relatively easy to clear from the road.

Kinematic analyses of the stability of the slope above the transport route are shown on Figures 2.6-37 and 2.6-38. (Reference 2, Attachment 17, Figures 7 and 8). The north-trending slope (station 43+00 to 46+00) shows moderate potential for toppling failure, as a large portion of set 1 plots within this failure envelope. There is low potential of planar sliding failure, and very low potential for wedge sliding failure. Due to the very low inclination of the northwest-trending slope (station 35+00 to 43+00), this slope shows low potential for all three failure modes. Thus, the only potentially significant failure mode is for small topple failures along the transport route cutslopes.

2.6.5.4.2 Dynamic Stability and Displacements

Stability analyses using the ILP ground motions (Section 2.6.2.5) were performed on the hillslope behind Unit 2 using cross section L-L' (Figure 2.6-19). Borings drilled during investigations for the power block along the slope provided data for modeling the slope. The results of these analyses indicate the bedrock slope and the transport route that crosses it are expected to undergo only minor displacements of about 1.0 ft or less during the possible occurrence of the ILP ground motions (Reference 2, Attachment 25).

An additional location, shown on cross section D-D' (Figure 2.6-16), along the transport route also was modeled, and the responses to the ILP ground-motions were assessed in a similar manner. Results from this analysis show that this location also is expected to undergo only minor displacements of about 1.0 ft or less. Other locations along this road cut are expected to perform similarly.

2.6.6 REFERENCES

1. PG&E Letter DIL-01-006 to the NRC, Submittal of Seismic Hazards Review Board Final Report, December 21, 2001.

2. PG&E Letter DIL-01-004 to the NRC, Submittal of Non-Proprietary Calculation Packages, December 21, 2001.

3. PG&E Letter DIL-01-005 to the NRC, Submittal of Geologic Data Reports, December 21, 2001.

4. PG&E, Units 1 and 2 Diablo Canyon Power Plant, Final Safety Analysis Report Update, Revision 14, November 2001.

5. USNRC, Supplement Number 34 to NUREG-0675, Safety Evaluation Report for Diablo Canyon Power Plant, Units 1 and 2, June 1991.

6. PG&E, Final Report of the Diablo Canyon Long Term Seismic Program, 1988.

7. PG&E, Addendum to the 1988 Final Report of the Diablo Canyon Long Term Seismic Program, 1991.

8. PG&E, Assessment of Slope Stability Near the Diablo Canyon Power Plant (Response to NRC Request of January 31, 1997), 1997.

9. Harding Miller Lawson Associates, Soil Investigation, Intake and Discharge Lines, Borrow Area, and Switchyards for Unit 1, Diablo Canyon Site, San Luis Obispo County, California, 1968.

10. C. A. Hall, Jr., W. G. Ernst, S. W. Prior, and J. W. Siese, Geologic Map of the San Luis Obispo-San Simeon Region, U.S. Geological Survey Miscellaneous Investigation I-1097, 1979.

11. C. A. Hall, Jr., Geologic Map of the Morro Bay South and Port San Luis Quadrangles, San Luis Obispo County, California, U.S. Geologic Survey Miscellaneous Field Studies Map MF-511, scale 1:24,000, 1973.

12. N. A. Abrahamson, and K. Shedlock, Overview [of Special Issue of SRL on Attenuation Relations], Seismological Research Letters, v. 68, no. 1, p. 9-23, 1997.

13. Harding Lawson Associates, Landslide Investigation, Diablo Canyon Site, San Luis Obispo County, California, 1970.

14. M. K. McLaren, and W. U. Savage (in press), "Seismicity of South-central coastal California", October 1987 through January 1997, accepted for publication in Bull. Seis. Soc. America, 2001.

15. W. J. Silva, and K. Lee, WES RASCAL: Code for Synthesizing Earthquake Ground Motions, State-of-the-Art for Assessing Earthquake Hazards in the United States, Report 24, U. S. Army Waterways Experiment Station, Misc. Paper S-73-1, 1987.

16. K.L. Hanson, W.R. Lettis, J.R. Wesling, K.I. Kelson, and L. Mezger, Quaternary Marine Terraces, South-Central Coastal California: Implications for Crustal Deformation and Coastal Evolution: in Quaternary Coasts of the United States: Marine and Lacustrine system, SEPM Special Publication No. 48, p 323-332, 1992.

17. N. A. Abrahamson, and W. J. Silva, Empirical Response Spectral Attenuation Relations for Shallow Crustal Earthquakes, Seis. Res. Let. Vol 68, p 94-127, 1997.

18. K. Sadigh, C.Y. Chang, J.A. Eagan, F. Makdisi, R.R. Youngs, Attenuation Relationships for Shallow Crustal Earthquakes Based on California Strong Motion Data, Seis. Res. Let., vol. 68, p 180-189, 1997.

19. I. M. Idriss, Selection of Earthquake Ground Motions at Rock Sites, report prepared for the Structural Division, Building and Fire Research Laboratory, National Institute of Standards and Technology, Department of Civil Engineering, University of California, Davis, 1991, included in Idriss (1992).

20. I. M. Idriss, Updated Standard Error Terms, Memo to Phalkun Tan, April 17, 1994.

21. I. M. Idriss, An Overview of Earthquake Ground Motions Pertinent to Seismic Zonation, Proc. Fifth International Conference on Seismic Zonation, vol. III, p 2111-2126, 1995.

22. N. A. Abrahamson, Effects of Directivity on Probabilistic Seismic Hazard Analyses, Earthquake Engineering Research Institute, Proceedings, Sixth International Conference on Seismic Zonation, Palm Springs, California, 2000.

23. P. G. Somerville, N. F. Smith, R. W. Graves, and N. A. Abrahamson, Modification of Empirical Strong Motion Attenuation Relations to Include the Amplitude and Duration Effects of Rupture Directivity, Seismological Research Letters, v. 68, p. 199-222, 1997.

24. K. W. Campbell, Empirical Near-Source Attenuation Relationships for Horizontal and Vertical Components of Peak Ground Acceleration, Peak Velocity and Pesudo Absolute Acceleration Response Spectra, Seis. Res. Let. vol 68, p 154-179, 1997.

25. PG&E, Specification for General Earthwork and Related Work for Unit 1 Diablo Canyon Site for the Pacific Gas and Electric Company, 1968.

26. S. G. Wright, UTEXAS3, A Computer Program for Slope Stability Calculations, Shinoak Software, Austin, Texas, 1991.

27. N. R. Barton, and V. Choubey, The Shear Strength of Rock Joints in Theory and Practice, Rock Mechanics, v. 10, no. 1-2, p. 1-54, 1977.

28. E. Hoek, Rock Engineering Course Notes, Hoek's Corner, University of Toronto, www.rocscience.com/roc/hoek/hoeknotes98.htm, 1998.

29. N. M. Newmark, Effects of Earthquakes on Dams and Embankments, Geotechnique, v. 15, no. 2, p. 139-160, 1965.

30. F. I. Makdisi, and H. B. Seed, Simplified Procedure for Estimating Dam and Embankment Earthquake-Induced Deformations, Journal of the Geotechnical Engineering Division, American Society of Civil Engineers, v. 104, no. GT7, p. 849-867, 1978.

31. M. Hudson, I. M. Idriss, and Beikae, (QUAD4M) User's Manual for a Computer Program to Evaluate the Seismic Response of Soil Structures Using Finite-Element Procedures and Incorporating a Compliant Base, Center for Geotechnical Modeling, University of California, Davis, 1994.

32. P. B. Schnabel, J. Lysmer, and H. B. Seed, SHAKE: A Computer Program for Earthquake Response Analysis of Horizontally Layered Sites, Report EERC 72-12, Earthquake Engineering Research Center, University of California, Berkeley, 1972.

33. R. E. Goodman, Introduction to Rock Mechanics, John Wiley and Sons, second edition, New York, 1989.

34. Rocscience, Inc., SWEDGE, Probabilistic Analyses of the Geometry and Stability of Surface Wedges, version 3.06, 1999.

35. S. A. Ashford, and N. Sitar, Seismic Response of Steep Natural Slopes, Report No. UCD/EERC-94/05, College of Engineering, University of California, Berkeley, 1994.

36. H. B. Seed, G. R. Martin, The Seismic Coefficient in Earth Dam Design, Journal of the Soil Mechanics and Foundations Division, ASCE, v. 92, no. SM2, March 1966.

TABLE 2.1-1

POPULATION TRENDS OF THE STATE OF CALIFORNIA AND OF SAN LUIS OBISPO AND SANTA BARBARA COUNTIES

Year	State of California	San Luis Obispo County	Santa Barbara County	Notes
1940	6,907,387	33,246	70,555	(a)
1950	10,586,233	51,417	98,220	(a)
1960	15,717,204	81,044	168,962	(a)
1970	19,953,134	105,690	264,324	(a)
1980	23,668,562	155,345	298,660	(a)
1990	29,760,021	217,162	369,608	(a)
2000	33,871,648	246,681	399,347	(a)
2005	40,262,400	323,100	467,700	(b)
2025	48,626,052	426,812	603,966	(c)

Notes: (a) U.S. Bureau of the Census
(b) State of California Department of Finance (June 2001)
(c) State of California Department of Finance Data Files (March 16, 2000)

TABLE 2.1-2

GROWTH OF PRINCIPAL COMMUNITIES WITHIN
50 MILES OF ISFSI SITE

Community	Population (1960 Census)	Population (1970 Census)	Population (1980 Census)	Population (1990 Census)	Population 2000 Census
Arroyo Grande	3,291	7,454	10,350	21,992	15,851
Atascadero	5,983	10,290	15,930	27,720	26,411
Grover Beach	5,210	5,939	8,827	11,790	13,067
Guadalupe	2,614	3,145	3,629	6,464	5,659
Lompoc	14,415	25,284	26,267	49,960	41,103
Morro Bay	3,692	7,109	9,064	10,457	10,350
Paso Robles	6,617	7,168	9,163	29,255	24,297
Pismo/Shell Beach	1,762	4,043	5,364	7,474	8,551
San Luis Obispo	20,437	28,036	34,253	56,614	44,174
Santa Maria	20,027	32,749	39,685	60,187	77,423

TABLE 2.1-3

POPULATION CENTERS OF 1,000 OR MORE
WITHIN 50 MILES OF DCPP SITE

Community	County	Distance and Direction From the Site	Population (1970 Census)	Population (1980 Census)	Population (1990 Census)	Population (2000 Census)
Baywood-Los Osos	San Luis Obispo	8 miles N	3,487	10,933	15,290	14,351
Morro Bay	San Luis Obispo	10 miles N	7,109	9,064	12,949	10,350
San Luis Obispo	San Luis Obispo	12 miles ENE	28,036	34,253	51,173	44,174
Pismo Beach	San Luis Obispo	13 miles ESE	4,043	5,364	7,699	8,551
Grover City	San Luis Obispo	14 miles ESE	5,939	8,827	11,656	13,067
Oceano	San Luis Obispo	15 miles ESE	2,564	4,478	6,169	7,260
Arroyo Grande	San Luis Obispo	17 miles ESE	7,454	10,350	14,378	15,851
Cayucos	San Luis Obispo	17 miles N	1,772	2,301	2,960	2,943
Atascadero	San Luis Obispo	21 miles NNE	10,290	15,930	23,138	26,411
Guadalupe	Santa Barbara	23 miles SE	3,145	3,629	5,479	5,659
Nipomo	San Luis Obispo	24 miles ESE	3,642	5,247	7,109	12,626
Cambria	San Luis Obispo	28 miles NNW	1,716	3,061	5,382	6,232
Santa Maria	Santa Barbara	29 miles SE	32,749	39,685	61,284	77,423
Paso Robles	San Luis Obispo	30 miles NNE	7,168	9,163	18,583	24,297
Orcutt	Santa Barbara	33 miles SE	8,500	1,469	----	28,830
Vandenberg	Santa Barbara	35 miles SSE	13,193	13,975	----	11,953
Lompoc	Santa Barbara	45 miles SSE	25,284	26,267	37,649	41,103
		Total	180,793	203,996	280,898	351,081

TABLE 2.1-4

TRANSIENT POPULATION AT RECREATION AREAS WITHIN 50 MILES OF ISFSI SITE

Name	Visitor Days
State Parks [(a)]	
Cayucos State Beach	698,000
Hearst San Simeon State Historical Monument	795,000
Montana de Oro State Park	683,000
Morro Bay State Park	1,129,000
Morro Strand State Beach	129,000
Pismo State Beach	1,297,000
San Simeon State Park	696,000
W. R. Hearst Memorial State Beach	213,000
County and Local Parks [(b)]	
Lake Nacimiento	345,000
San Antonio Reservoir	361,000
Avila Beach	800,000
Cambria	15,000
Cayucos Beach	918,000
Cuesta	67,000
Lopez Recreation Area	379,000
Nipomo	168,000
Oceano	95,000
San Miguel	54,000
Santa Margarita Lake	169,000
Shamel	130,000
Templeton	99,000
Los Alamos Park	45,000
Miguelito Park	36,000
Ocean Park	105,000
Rancho Guadalupe Dunes Park	48,000
Waller	450,000
Atascadero Lake	300,000

Name	Visitor Days
Los Padres National Forest [(c)]	
Agua Escondido	700
American Canyon	800
Balm of Gilead	200
Brookshire Springs	1,600
Buckeye	200
Cerro Alto	15,600
French	200
Frus	700
Hi Mountain	4,800
Horseshoe Springs	1,400
Indians	600
Kerry Canyon	300
La Panza	4,400
Lazy Camp	500
Miranda Pine	2,300
Navajo	2,800
Pine Flat	300
Pine Springs	400
Plowshare Springs	300
Queen Bee	2,200
Stony Creek	1,100
Sulphur Pot	1,000
Upper Lopez	600
Wagon Flat	2,200

(a) California Department of Parks and Recreation (July 1998 through June 1999).
(b) County Park Departments:
Monterey and Santa Barbara Counties (July 1999 through June 2000).
San Luis Obispo County (July 1998 through June 1999).
(c) Los Padres National Forest (July 1971 through June 1972. Current data is no longer compiled).

TABLE 2.6-1

SOIL AND ROCK TEST PROGRAM

Type of Properties	Soil		Rock	
	Tests Conducted	Reference	Tests Conducted	Reference
Basic properties	Classification, identification, unit weight, saturation	Reference 3, Data Report B and Data Report G	Classification, identification, JRC, (mi)	Reference 3, Data Report B and Data Report H
Strength, deformation (static)	Drained, undrained triaxial strength, direct shear	Reference 3 Data Report G	Drained and undrained triaxial strength, unconfined compression, direct shear, Poisson's ratio, Young's modulus	Reference 3 Data Report I
Strength, deformation (dynamic)	Triaxial, drained, undrained strain vs. damping, strain vs. shear modulus	Reference 3 Data Report G		
Field and in situ properties			Field discontinuity, shear wave and compression wave velocity, Poisson's ratio, Young's modulus	Reference 3 Data Report F and Data Report C

TABLE 2.6-2

SUMMARY OF SLOPE STABILITY ANALYSES

SLOPE	TYPE OF ANALYSIS						
	Kinematic	**Static**	**Pseudo-Static**	**Seismic Displacement**	**Displacement Historical/ Back Calculation**	**Results**	**Action**
Hillslope		X	X	X	X	• Stable under static and dynamic conditions • Less than 3 feet seismic displacement	— —
Pad Cutslope	X	X	X	X		• Potential for small wedge slippage under partial saturation and/or seismic loading	Mitigation
CTF Slope	X	X		X		• Stable under static and dynamic conditions	—
Transport Route Slope		X		X		• Stable under static and dynamic conditions • Small seismic displacement (less than 1 foot)	— —

TABLE 2.6-3

FACTORS OF SAFETY AND YIELD ACCELERATIONS COMPUTED FOR POTENTIAL SLIDING MASSES

Slide Mass Analyzed	Static Factor of Safety	Yield Acceleration, k_y (g)
1a	2.55	0.28
1b	1.62	0.20
2a	2.55	0.31
2b	2.16	0.24
2c	2.18	0.19
3a	2.86	0.44
3b	2.70	0.39
3c	2.26	0.25
3c-1	2.38	0.28
3c-2	2.28	0.23

TABLE 2.6-4

DOWN SLOPE DISPLACEMENT CALCULATED BASED ON ROTATED INPUT MOTIONS ALONG CROSS SECTION I-I'
(DISPLACEMENT UNIT: FEET; YIELD ACCELERATION: 0.2 G)

Set No.	Description	Polarity	$K_y = 0.20$		
			$I\text{-}I_{36}$	$I\text{-}I_{46}$	$I\text{-}I_{26}$
Set 1	Lucerne	FN-	2.9	3.3	2.5
		FN+	1.4	1.4	1.5
Set 2a	Yarimca	FN-	2.4	2.8	1.8
		FN+	1.2	1.4	1.1
Set 3	LGPC	FN-	2.5	2.8	2.3
		FN+	1.3	1.2	1.4
Set 5	El Centro	FN-	2.2	2.6	1.8
		FN+	2.4	2.8	2.1
Set 6	Saratoga	FN-	0.9	1.1	0.8
		FN+	0.9	1.0	0.8

TABLE 2.6-5

COMPUTED DOWN-SLOPE DISPLACEMENTS
USING SET 1 AND SET 5 INPUT MOTIONS

Sliding Mass Location	Input Motion	Yield Acceleration, k_y, (g)	Peak Seismic Coefficient, k_{max}, (g)	Down-Slope Displacement (feet)
1b	Set 1	0.20	0.98	3.1
2c	Set 1	0.19	0.89	3.1
3c	Set 1	0.25	0.81	1.4
3c-1	Set 1	0.28	0.80	1.2
3c-2	Set 1	0.23	0.81	2.0
1b	Set 5	0.20	0.75	2.4
2c	Set 5	0.19	0.68	2.3
3c	Set 5	0.25	0.61	0.6
3c-1	Set 5	0.28	0.61	0.4
3c-2	Set 5	0.23	0.62	0.8

TABLE 2.6-6

PSEUDOSTATIC PROBABILISTIC SWEDGE ANALYSES OF ISFSI BACK CUTSLOPE

Run	Cut[1] Height (ft)	Discontinuity[2] A	Discontinuity[2] B	Mean[3] Friction Angle	Tension[4] Crack Distance (ft)	Seismic[5] Force (g)	Water[6] Unit Weight (kips*/ft^3)	Probability of Failure	Factor of Safety	Wedge Weight (kips*)	Wedge Face Area (ft^2)
Back cut P1R	31.8	69/220 (2)	88/12 (3)	26.5 (A/B)	None	None	None	0.036	1.39	40.1	101.8
Back cut P2R	31.8	69/220 (2)	88/12 (3)	26.5 (A/B)	3.3	None	None	0.007	1.39	25.1	101.8
Back cut P3R	31.8	69/220 (2)	88/12 (3)	26.5 (A/B)	None	None	0.031	0.978	0.27	40.1	101.8
Back cut P4R	31.8	69/220 (2)	88/12 (3)	26.5 (A/B)	None	0.50	None	1.0	0.49	40.1	101.8
Back cut P5R	31.8	69/220 (2)	88/12 (3)	26.5 (A/B)	None	0.50	0.031	1.0	0	40.1	101.8
Back cut P6R	31.8	88/12 (3)	24/232 (4)	26.5 (A) 30.5 (B)	None	None	None	0	2.74	11,991.8	1059.9
Back cut P7R	31.8	88/12 (3)	24/232 (4)	26.5 (A) 30.5 (B)	11.5	None	None	0	2.74	915.9	1059.9
Back cut P8R	31.8	88/12 (3)	24/232 (4)	26.5 (A) 30.5 (B)	23.0	None	None	0	2.74	1783.8	1059.9
Back cut P9R	31.8	88/12 (3)	24/232 (4)	26.5 (A) 30.5 (B)	23.0	None	0.031	0	1.44	1783.8	1059.9
Back cut P10R	31.8	88/12 (3)	24/232 (4)	26.5 (A) 30.5 (B)	23.0	0.50	None	0.90	0.92	1783.8	1059.9
Back cut P11R-R	31.8	88/12 (3)	24/232 (4)	26.5 (A) 30.5 (B)	23.0	0.50	0.031	1.0	0.62	1783.8	1059.9
Back cut P12R	31.8	75/12 (3)	75/261 (1)	26.5 (A) 30.5 (B)	None	None	None	1.0	0.43	10.8	77.5
Back cut P13R	31.8	75/12 (3)	75/261 (1)	26.5 (A) 30.5 (B)	None	0.50	0.031	1.0	0	10.8	77.5
Back cut P14R	52.3	88/12 (3)	24/232 (4)	26.5 (A) 30.5 (B)	None	None	None	0	2.74	21,836.2	2649.1
Back cut P15R	52.3	88/12 (3)	24/232 (4)	26.5 (A) 30.5 (B)	11.5	None	None	0	2.74	3243.9	2649.1
Back cut P16R	52.3	88/12 (3)	24/232 (4)	26.5 (A) 30.5 (B)	23.0	None	None	0	2.74	4474.6	2649.1
Back cut P17R	52.3	88/12 (3)	24/232 (4)	26.5 (A) 30.5 (B)	23.0	0.50	0.031	1.0	0.63	4474.6	2649.1
Back cut P18R	20.5	69/220 (2)	88/12 (3)	26.5 (A/B)	4.9	0.50	0.031	1.0	0.42	9.7	42.2
Back cut P19R	20.5	88/12 (3)	24/232 (4)	26.5 (A) 30.5 (B)	4.9	0.50	0.031	1.0	0.71	1,751.6	1,059.9

TABLE 2.6-6

*1 kip = 1000 pounds

[1]Cut height geometry from PG&E/Enercon Drawing PGE-009-SK-001, 9/12/01

[2]Mean dip and dip direction of intersecting joints (set number indicated in parentheses) that were identified by kinematic analyses in Reference 2, Attachment 17, as forming potential wedges. Geometry of discontinuity is defined by the dip/dip direction convention. (Reference 2, Attachment 18, Table 23-1). Numbers in brackets refer to Joint Set identification (Table 23-1).

[3]Mean rock discontinuity friction angle determined by Barton-Choubey method.

[4]Tension crack distance is the distance between the top of the wedge block crest and tension crack location, measured along strike of discontinuity A. Wedges modeled in Runs P6-P11 and P14-P17 consisted of unrealistically long, narrow wedges when tension cracks were not included. Final runs, therefore, include a tension crack at 23 ft behind slope face.

[5]Seismic force recommended for pseudostatic wedge analyses.

[6]Water unit weight of 0.031 kips/ft^3 approximates a condition in which water collects halfway up wedge-bounding discontinuities.

TABLE 2.6-7

PSEUDOSTATIC PROBABILISTIC SWEDGE ANALYSES OF ISFSI EAST CUTSLOPE

Run	Cut Height[1] (ft)	Discontinuity[2] A	Discontinuity[2] B	Mean Friction Angle[3] (ø)	Tension Crack Distances[4] (ft)	Seismic Force[5] (g)	Water Unit Weight[6] (kips/ft^3)*	Probability of Failure	Factor of Safety	Wedge Weight (kips)*	Wedge Face Area (ft^2)
East cut P1	23.3	76/08 (4)	67/239 (2)	35.0 (A) 36.0 (B)	None	None	None	0.20	1.08	33.96	446.0
East cut P2	23.3	76/08 (4)	67/239 (2)	35.0 (A) 36.0 (B)	1.64	None	None	0.12	1.08	33.96	446.0
East cut P3	23.3	76/08 (4)	67/239 (2)	35.0 (A) 36.0 (B)	None	None	0.031	0.31	1.02	33.96	446.0
East cut P4	23.3	76/08 (4)	67/239 (2)	35.0 (A) 36.0 (B)	None	0.50	None	1.0	0.65	33.96	446.0
East cut P5	23.3	76/08 (4)	67/239 (2)	35.0 (A) 36.0 (B)	None	0.50	0.031	1.0	0.54	33.96	446.0
East cut P6	23.3	88/98 (1)	67/239 (2)	36.0 (A) 36.0 (B)	None	None	None	0.97	0.31	23.81	469.8
East cut P7	23.3	88/98 (1)	67/239 (2)	36.0 (A) 36.0 (B)	None	0.50	0.031	0.99	0	23.81	469.8

*1 kip = 1000 pounds

[1]Cut height geometry from PG&E/Enercon drawing, PGE-009-SK-001, 9/12/01.

[2]Mean dip and dip direction of intersecting joints (set number indicated in parentheses) that were identified by kinematic analyses in Reference 2, Attachment 17, as forming potential wedges. Geometry of discontinuity is defined by the dip/dip convention. (Reference 2, Attachment 18, Table 23-1). Numbers in brackets refer to Joint Set identification (Table 23-1).

[3]Mean rock discontinuity friction angle determined by Barton-Choubey method.

[4]Tension crack distance is the distance between the top of the wedge block crest and tension crack location, measured along strike of discontinuity A.

[5]Seismic force recommended for pseudostatic wedge analyses.

[6]Water pressure of 0.031 kips/ft^3 approximates a condition in which water collects halfway up wedge-bounding discontinuities.

TABLE 2.6-8

PSEUDOSTATIC DETERMINISTIC SWEDGE ANALYSES OF ISFSI BACK CUTSLOPE AND EAST CUTSLOPE

Run	Cut[1] Height (ft)	Discontinuity[2] A	Discontinuity[2] B	Mean[3] Friction Angle	Tension[4] Crack Distance (ft)	Seismic[5] Force (g)	Water[6] Unit Weight (kips*/ft^3)	Bolt[7] Force (kips*)	Factor of Safety	Wedge Weight (kips*)	Wedge Face Area (ft^2)	Penetration[8] Anchor Length (ft)	Per Anchor[9] Force (kips*)
Back cut D1RR	31.8	69/220 (2)	88/12 (3)	26.5 (A/B)	None	0.5	0.031	None	0	40.1	101.8		
Back cut D2R	31.8	69/220 (2)	88/12 (3)	26.5 (A/B)	None	0.5	0.031	41.8	1.39	40.1	101.8	6.6	18.6
Back cut D3R	31.8	88/12 (3)	24/232 (4)	26.5 (A) 30.5 (B)	23.0	0.5	0.031	None	0.62	1783.8	1059.9		
Back cut D4R	31.8	88/12 (3)	24/232 (4)	26.5 (A) 30.5 (B)	23.0	0.5	0.031	796.4	1.30	1783.8	1059.9	13.1	33.9
Back cut D5R	52.3	88/12 (3)	24/232 (4)	26.5 (A) 30.5 (B)	23.0	0.5	0.031	None	0.63	4474.6	2649.1		
Back cut D6R	52.3	88/12 (3)	24/232 (4)	26.5 (A) 30.5 (B)	23.0	0.5	0.031	1881.0	1.30	4474.6	2649.1	23.0	32.1
Back cut D7R	20.5	69/220 (2)	88/12 (3)	26.5 (A/B)	4.92	0.5	0.031	-	0.27	10.12	41.94		
Back cut D8R	20.5	69/220 (2)	88/12 (3)	26.5 (A/B)	4.92	0.5	0.031	8.8	1.67	10.12	41.94	3.9	9.4
Back cut D9R	20.5	88/12 (3)	24/232 (4)	26.5 (A) 30.5 (B)	20.0	0.5	0.031	-	0.76	596.2	440.1		
Back cut D10R	20.5	88/12 (3)	24/232 (4)	26.5 (A) 30.5 (B)	20.0	0.5	0.031	189.2	1.31	596.2	440.1	16.4	19.4
East cut D1R	23.3	76/08 (4)	67/239 (2)	35.0 (A) 36.0 (B)	None	None	None	None	1.08	33.96	446.0		
East cut D2R	23.3	76/08 (4)	67/239 (2)	35.0 (A) 36.0 (B)	None	0.5	0.031	None	0.54	33.97	446.0		
East cut D3R	23.3	76/08 (4)	67/239 (2)	35.0 (A) 36.0 (B)	None	0.5	0.031	81.6	1.34	33.98	446.0	3.3	9.0
East cut D4R	23.3	88/98 (1)	67/239 (2)	36.0 (A/B)	None	None	None	None	0.31	23.81	469.8		
East cut D5R	23.3	88/98 (1)	67/239 (2)	36.0 (A/B)	None	0.5	0.031	None	0	23.81	469.8		
East cut D6R	23.3	88/98 (1)	67/239 (2)	36.0 (A/B)	None	0.5	0.032	83.8	1.43	23.81	469.8	3.3	8.4

*1 kip = 1000 pounds

[1]Cut height estimated from PG&E Drawing Fig 4.2-6, Rev. A.

[2]Mean dip and dip direction of intersecting joints (set number indicated in parentheses) that were identified by kinematic analyses in Calculation Package GEO.DCPP.01.22 as forming potential wedge. Geometry of discontinuity is defined by the dip/dip direction convention. Refer to Table 23-1. Numbers in brackets refer to Joint Set identification on Table 23-1 and in GEO.DCPP.01.22.

[3]Mean rock discontinuity friction angle determined by Barton Equation as developed in Calculation Package GEO.DCPP.01.20.

TABLE 2.6-8

[4]Tension crack distance is the distance between the top of the wedge block crest and tension crack location measured along strike of discontinuity A. Wedges modeled in runs D3-D6 were unrealistically long and narrow when tension cracks were not included. Final runs therefore include tension cracks at 23 feet behind the slope face.

[5]Seismic force recommended for pseudostatic wedge analyses as defined in Calculation Package GEO.DCPP.01.05.

[6]Water pressure of 0.031 kips/ft^3 represents approximately a condition with water collecting halfway up wedge-bounding discontinuities.

[7]Total force required to stabilize block to the listed factor of safety.

[8]Length of anchor in meters required to penetrate modeled wedge sliding plane, assuming an anchor inclination of 15° below horizontal, and plunge direction perpendicular to slope face. Additional length is required to provide anchor anchorage and capacity in sound rock behind the failure wedge.

[9]Per anchor force calculated by dividing wedge face area by 50% to account for wedge margins that are not suitable for providing anchor restraint, and then dividing this value by the required anchor force, and assuming one anchor per 22.6 ft^2, which represents an anchor pattern spacing of 5.0 feet.